清華大學机械工程系
Department of Mechanical Engineering, Tsinghua University

自主机器人实验室
AUTOROBOT LABORATORY

Tactile Sensing and Grasping Control for Contact-Rich Manipulation Tasks

Name: Mingxuan Li

Date: 2025.06.16

Department of Mechanical Engineering
Tsinghua University

Self Introduction

Name: Mingxuan Li

Major: Mechanical Engineering, 2st-year master student, Tsinghua University

Research Interests： Tactile Perception & Manipulation, Vision-Based Tactile Sensors

Selected Awards:

- Shortlisted for Tsinghua Prestigious Scholarship (特等奖学金) in 2024
- Excellent Graduates and Outstanding Graduation Thesis, Tsinghua University, 2023
- Comprehensive Outstanding Scholarship in Tsinghua University for several times
- Excellent Oral Presentation, The 734th and 777th Doctoral Academic Forums of Tsinghua University
- 2023 Person of the Year in the Department of Mechanical Engineering, Tsinghua University
- 1st Place in "New Engineering“ National Undergraduate Graduation Thesis Competition
- Best Poster and Excellent Oral Presentation Award, Tsinghua Youth Science and Innovation Forum
- Excellent academic paper, The 16th National Conference on Undergraduate Innovation
- Grand Prize of Outstanding Project of Tsinghua University Student Research Training Program
- “Spark” Innovative Talent Cultivation Program (Top 2% for outstanding research performance)

Overview

1. **Background and Motivation**
2. Contact Modelling
3. Contact Representation
4. Contact Reconstruction
5. Contact-Rich Tasks

Contact-Rich Manipulation

VS

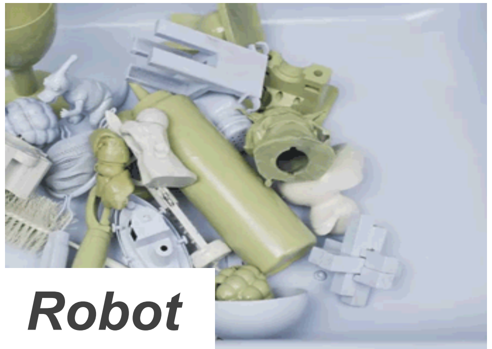

VS

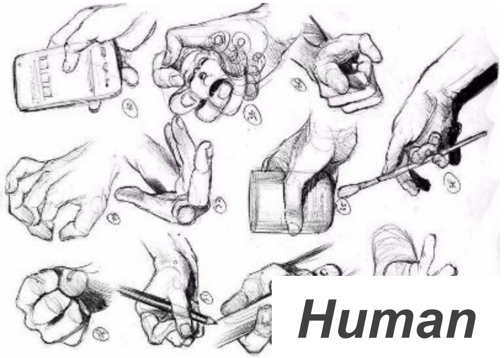

Grasping Reliability

Manipulation Adaptability

Tactile Sensing in Manipulation: Providing valuable **Contact Information**

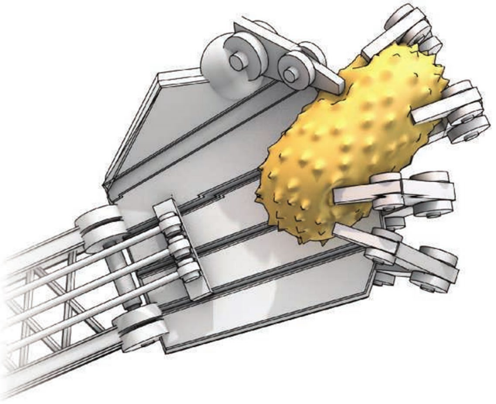

Unknown contact

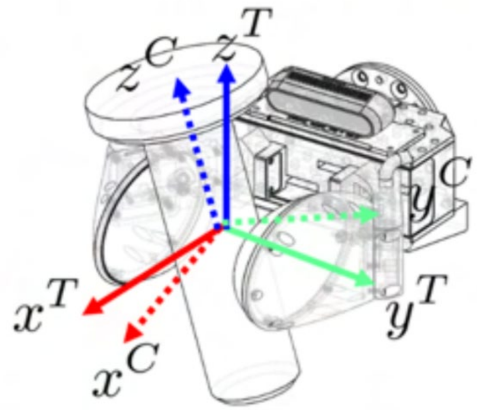

Object pose

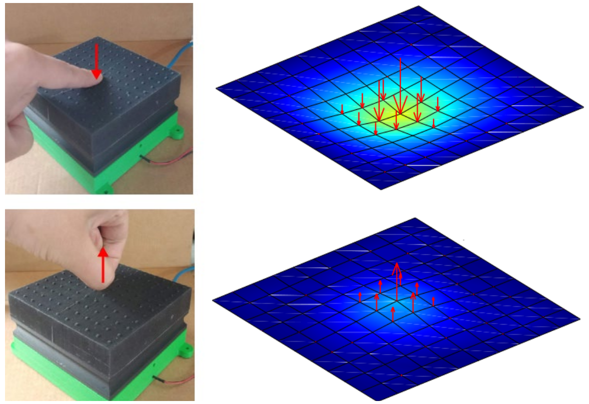

Contact force

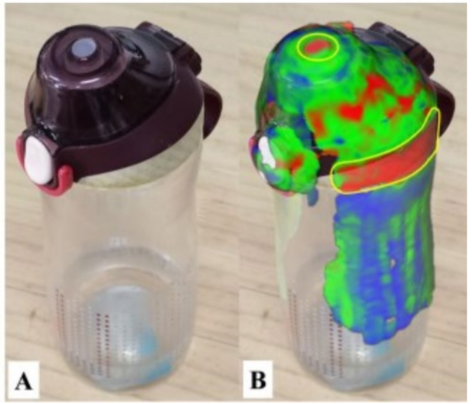

Friction distribution

Difficulties in Tactile Sensing

Representation

Hard to capture uncertainties from unknown objects and force conditions

Reconstruction

Lack of direct methods to measure distributed contact characteristics.

Application

Difficult to translate tactile features into intuitive and convenient contact state indicators.

Science Robotics 2023：

Grasping objects is a **daunting challenge**…To account for uncertainties arising from imperfect object models and dynamics during interaction, we must move beyond single-point contact modeling and **make substantial progress in fundamental theory**.

Reviewing Tactile Sensing in Robot Contact

- **Transmission of tactile information in VBVS:**

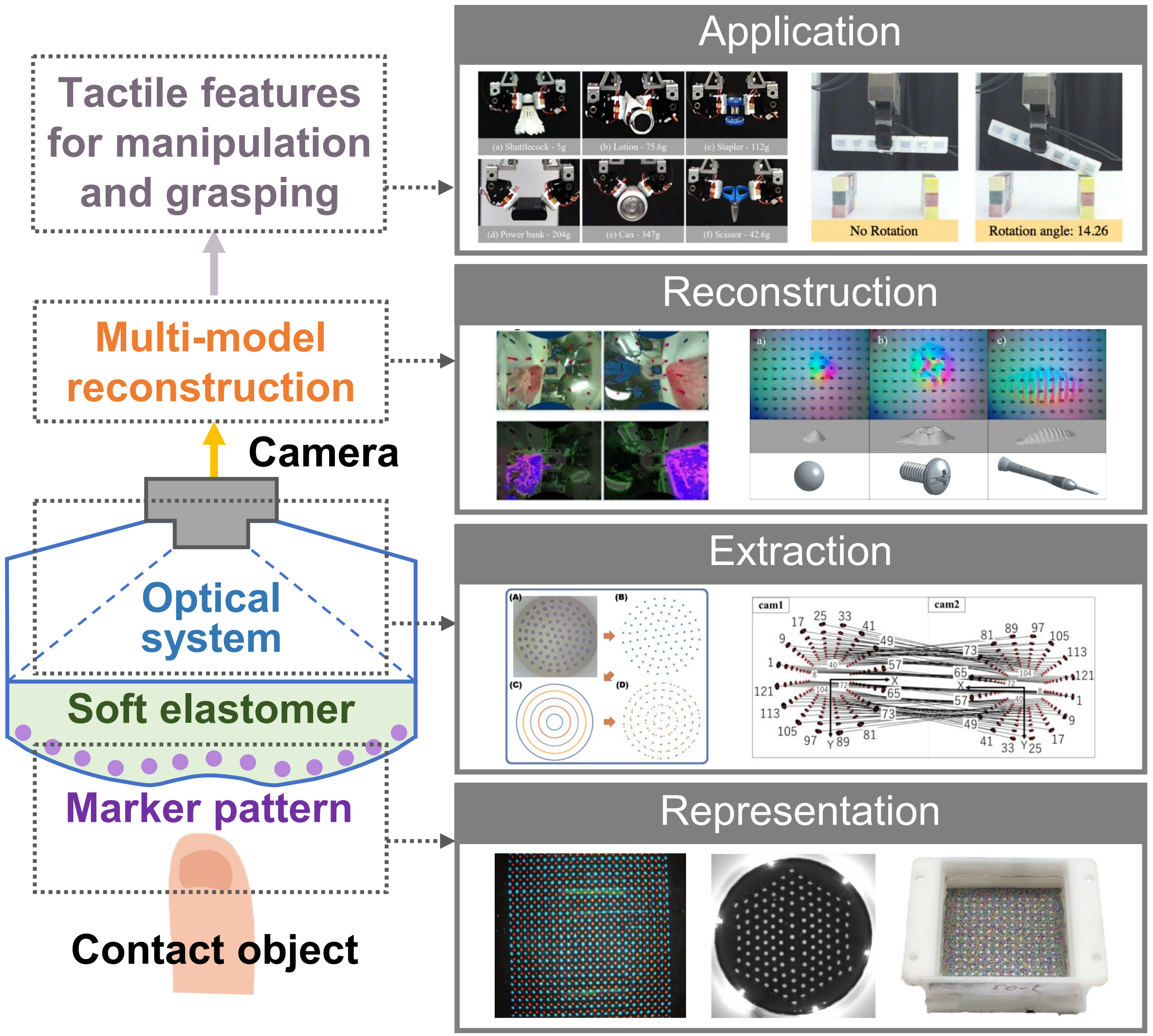

how to better utilize contact information?

How to better obtain contact information?

Overview

1. Background and Motivation
2. **Contact Modelling**
3. Contact Representation
4. Contact Reconstruction
5. Contact-Rich Tasks

Requirement of Contact Modelling

Contact Modelling

Friction Characteristics

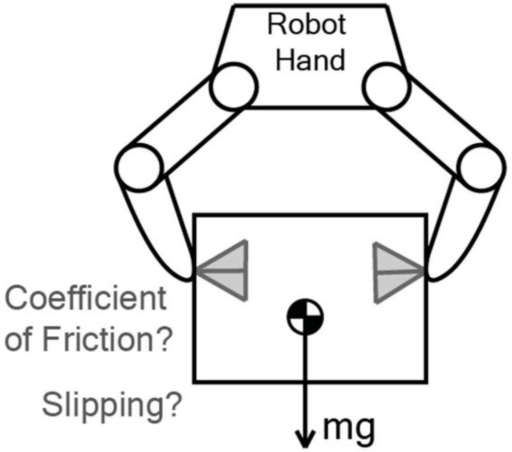

Material Properties

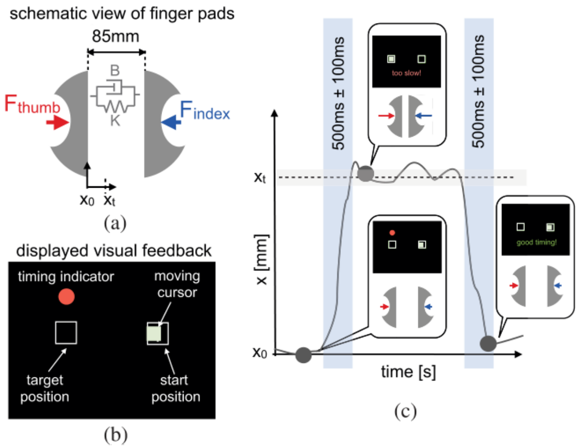

Grasp Evaluation

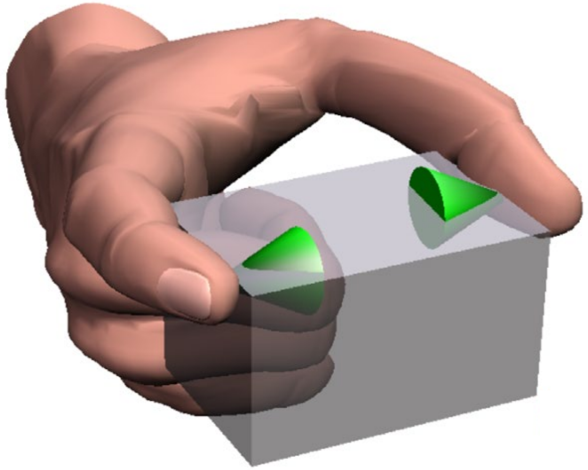

Friction Characteristics (1)

- **Incipient Slip:**

Stick region   Slip region

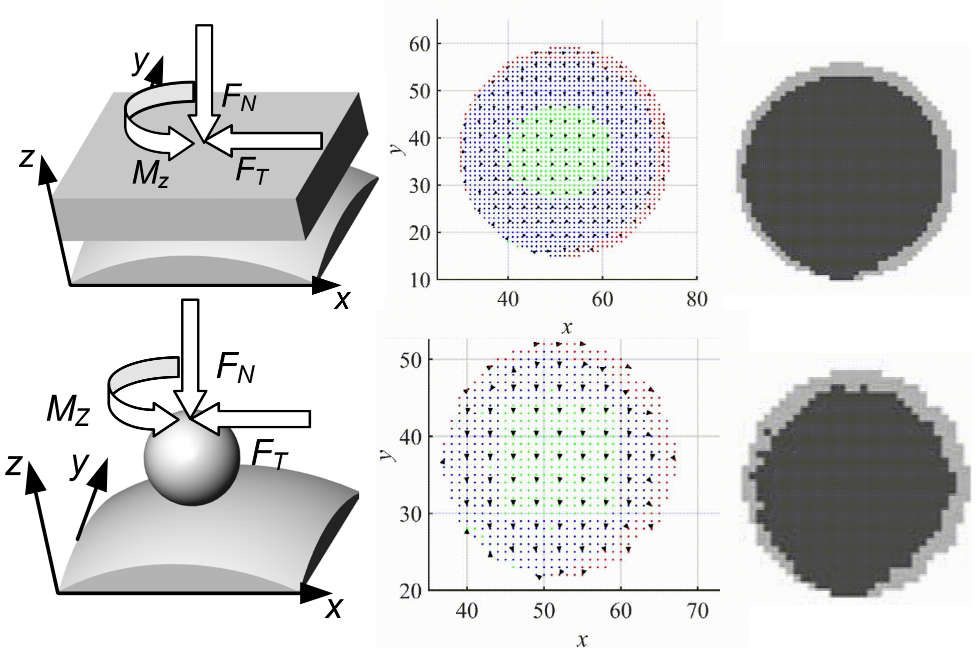

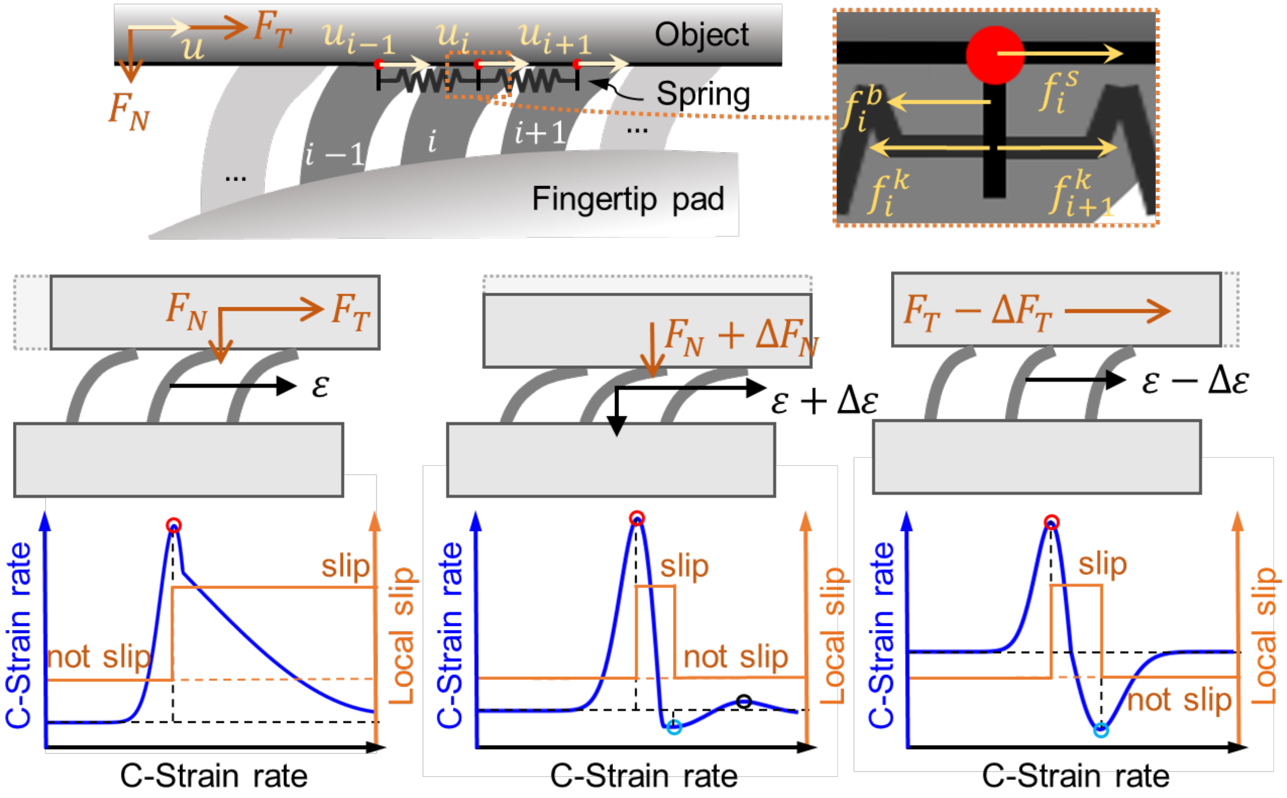

✓ **Temporal characteristics:** The relationship between the strain state and the local slip state

✓ **Spatial characteristics:** The distribution of local slip states and the incipient slip degree

[1] Mingxuan. Li *et al.*, in revision to *IEEE TRO*

Friction Characteristics (2)

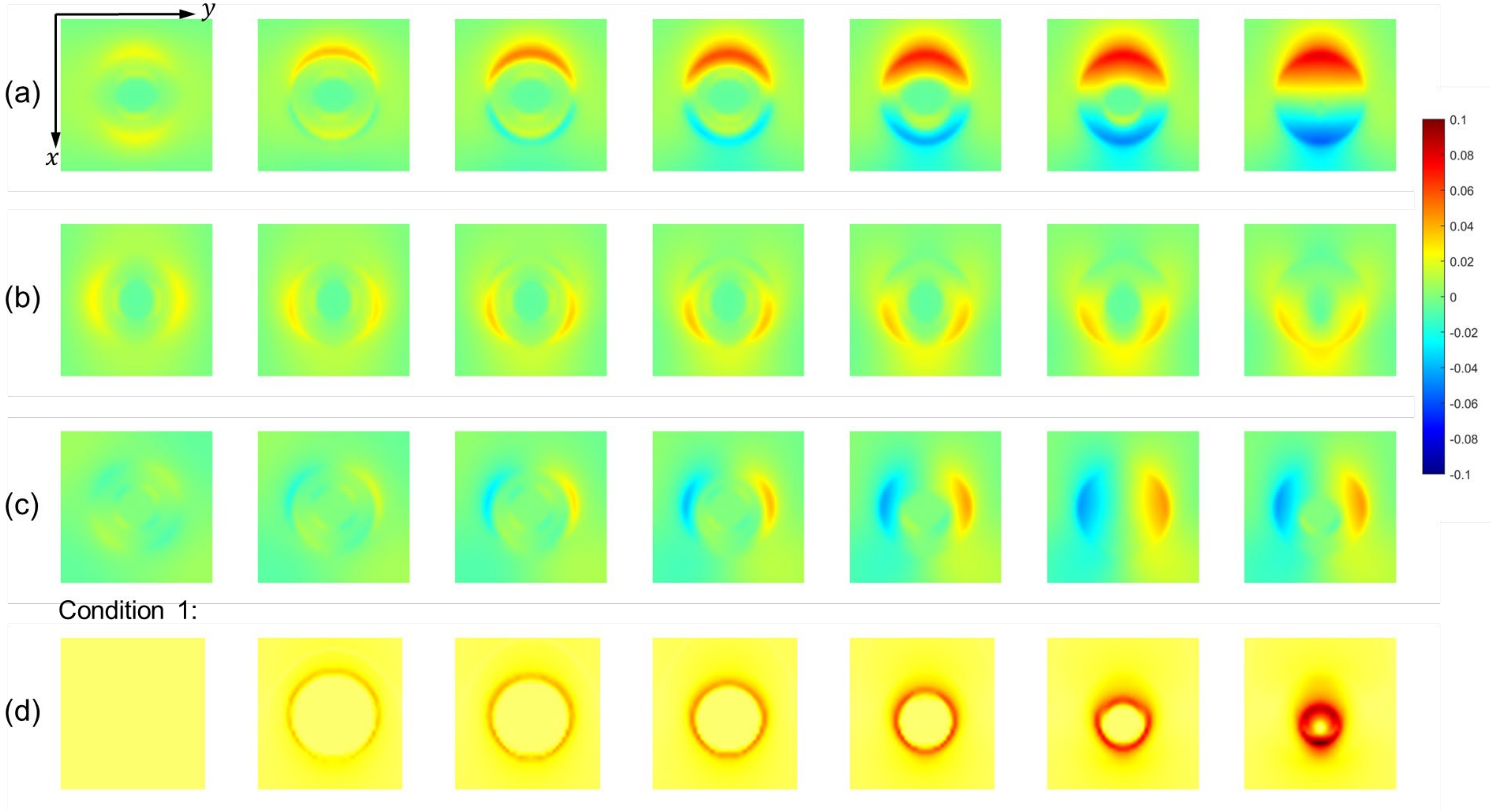

[1] Mingxuan. Li *et al.*, in revision to *IEEE TRO*

Friction Characteristics (3)

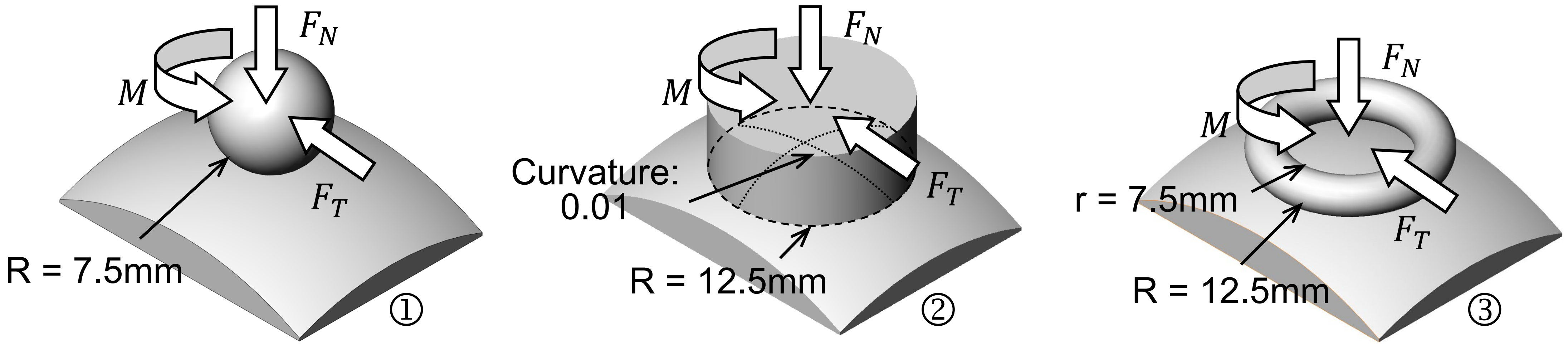

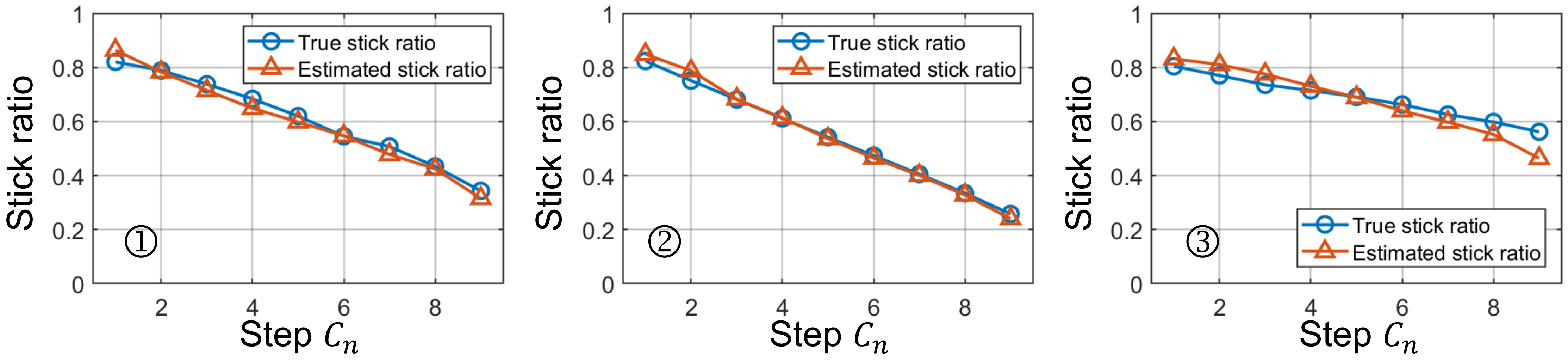

[1] Mingxuan. Li *et al.*, in revision to *IEEE TRO*

Friction Characteristics (4)

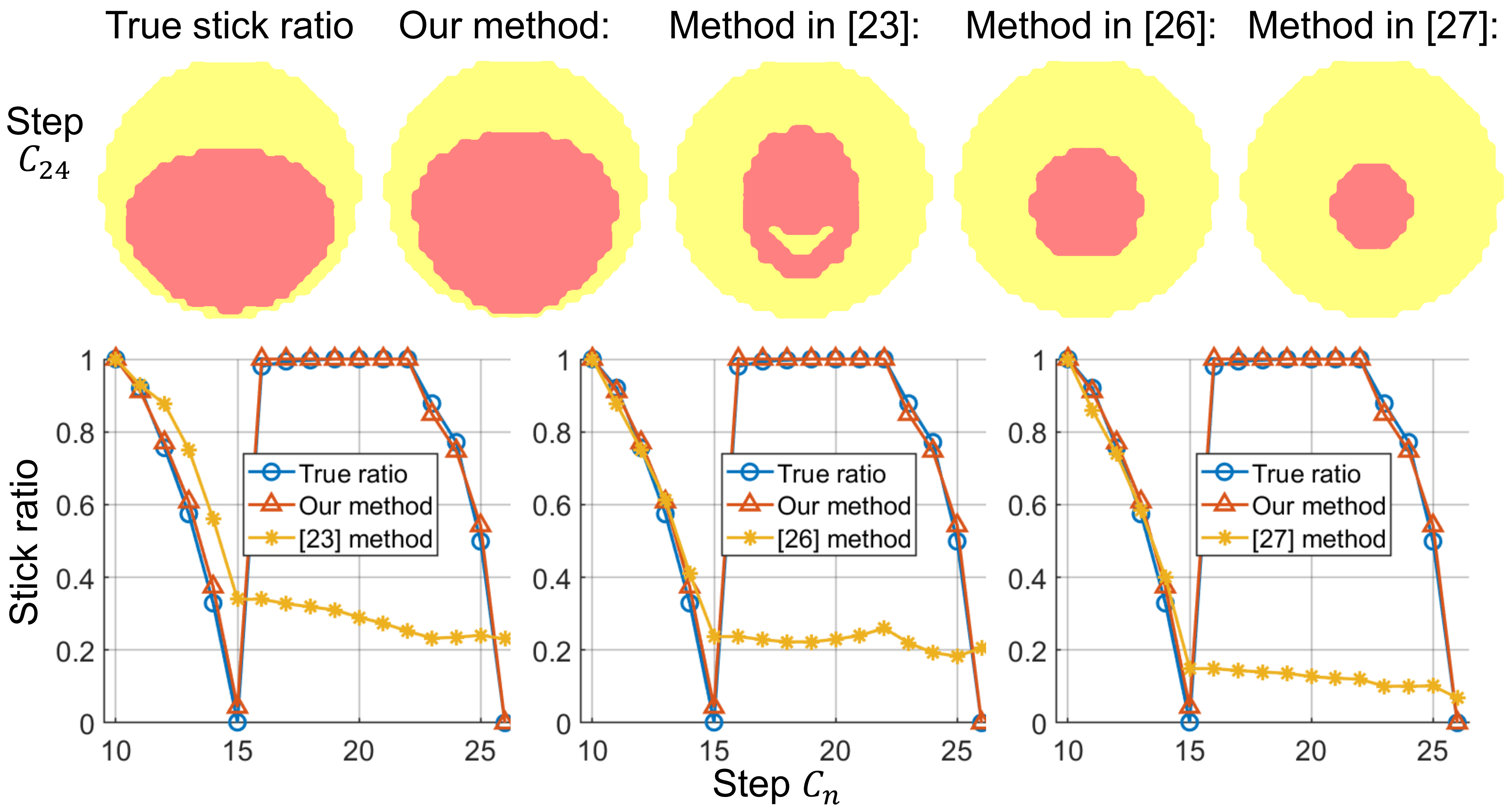

[1] Mingxuan. Li *et al.*, in revision to *IEEE TRO*

Material Properties (1)

- **Observations**:
- Humans utilize the viscoelasticity of fingertips to enhance grasping stability.
- Viscoelastic contact improves grasp stability by increasing energy consumption.

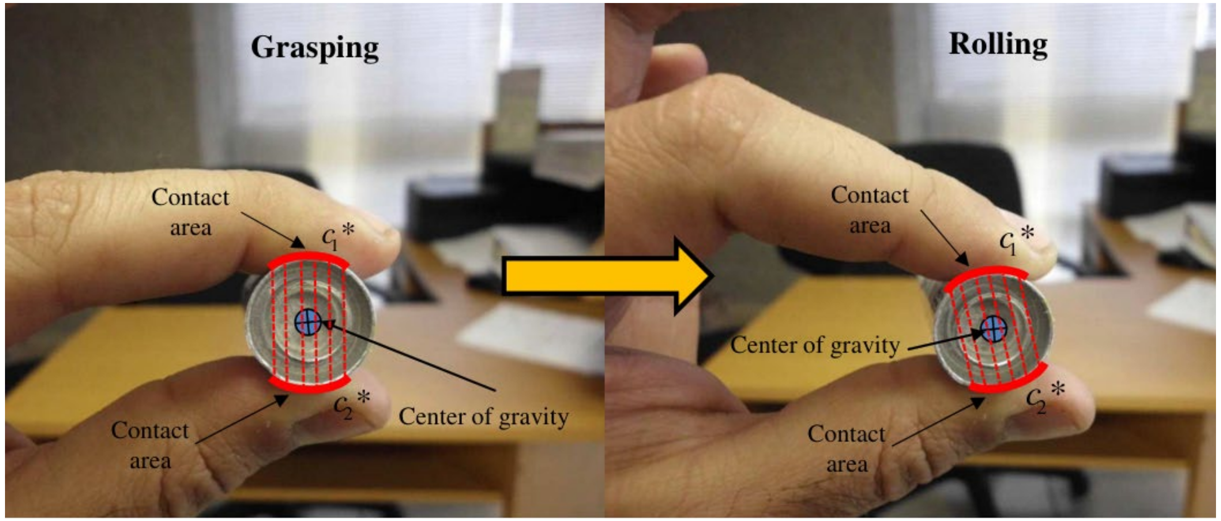

Utilizing viscoelastic deformations

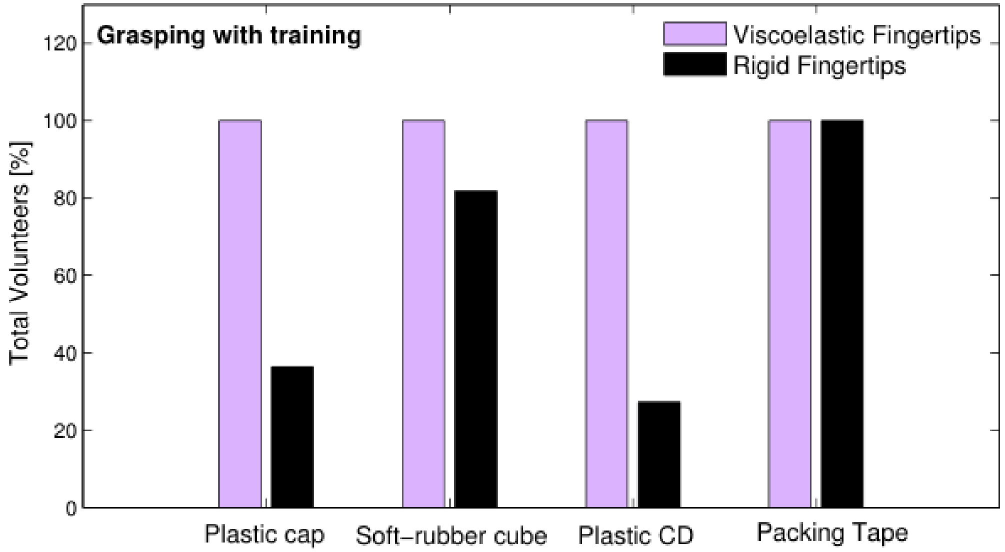

Human-in-the-loop telemanipulation

Motivation: Study the influence of material properties (viscoelasticity) on robot contact and grasp stability

[2] Mingxuan. Li *et al.*, submitted to *IEEE TASE*, Jun. 2025

Material Properties (2)

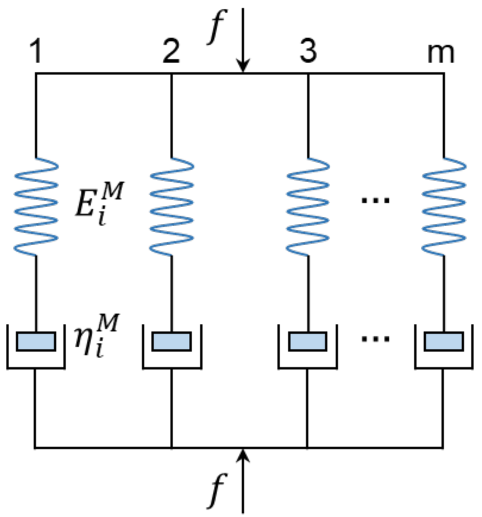

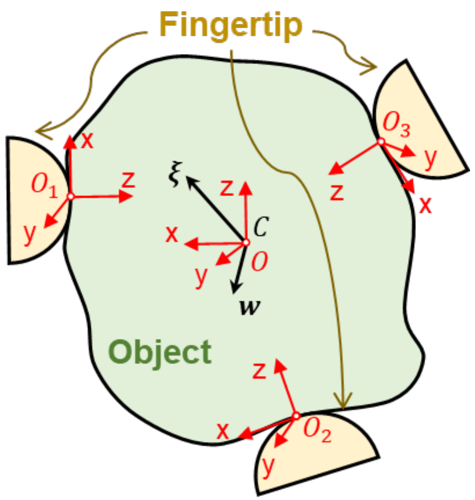

- **Grasping Stiffness Metrics：**

G1: The geometric mean of singular values in stiffness matrix (**overall stability**)

$$G_1(t) = \sqrt[n]{\prod_{i=1}^{n} \sigma_i(t)}$$

G2: The minimum singular value in stiffness matrix (**lower bound of stability**)

$$G_2(t) = \sigma_{min}(t)$$

G3: The ratio of the minimum singular value to the maximum singular value in the stiffness matrix (**equilibrium of stability**)

$$G_3(t) = \frac{\sigma_{min}(t)}{\sigma_{max}(t)}$$

[2] Mingxuan. Li *et al.*, submitted to *IEEE TASE*, Jun. 2025

Material Properties (3)

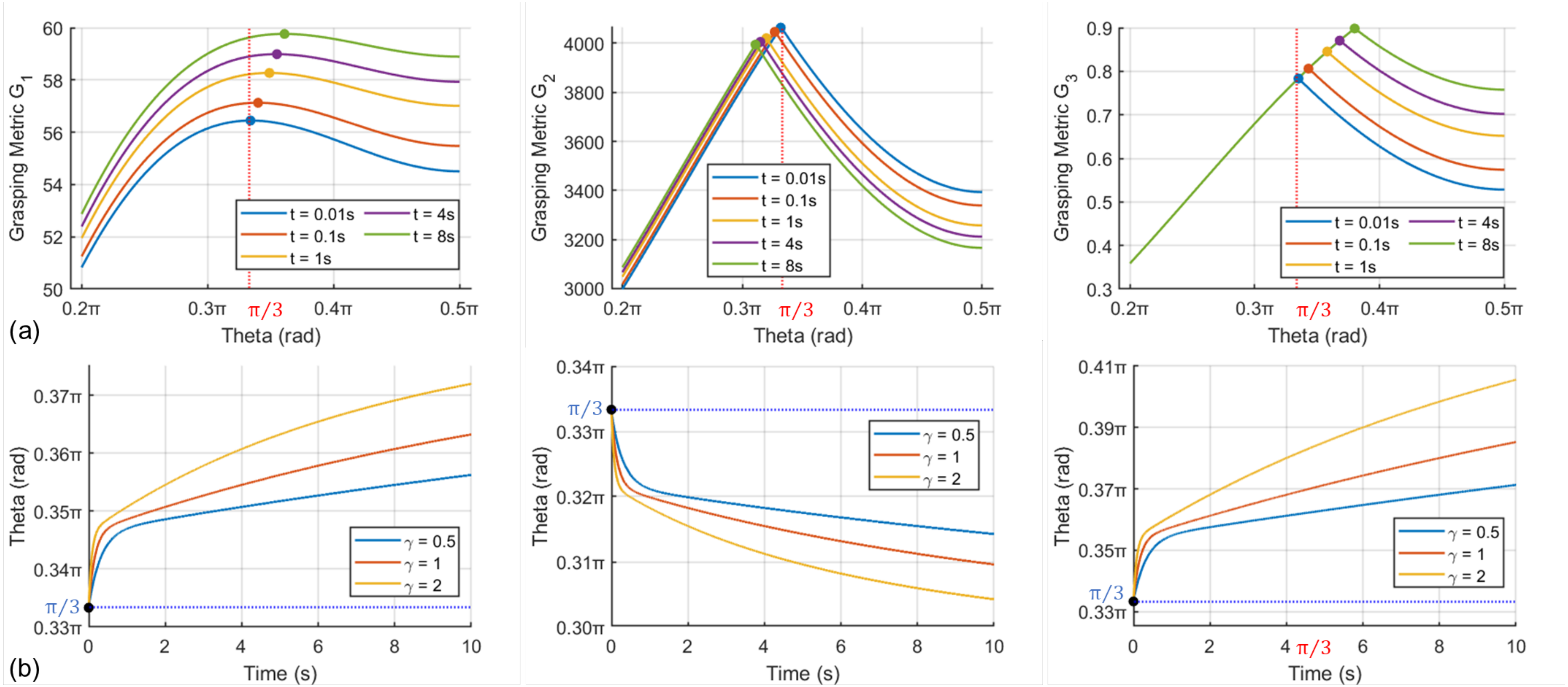

[2] Mingxuan. Li *et al.*, submitted to *IEEE TASE*, Jun. 2025

Material Properties (4)

- **Grasping Quality Evaluation**

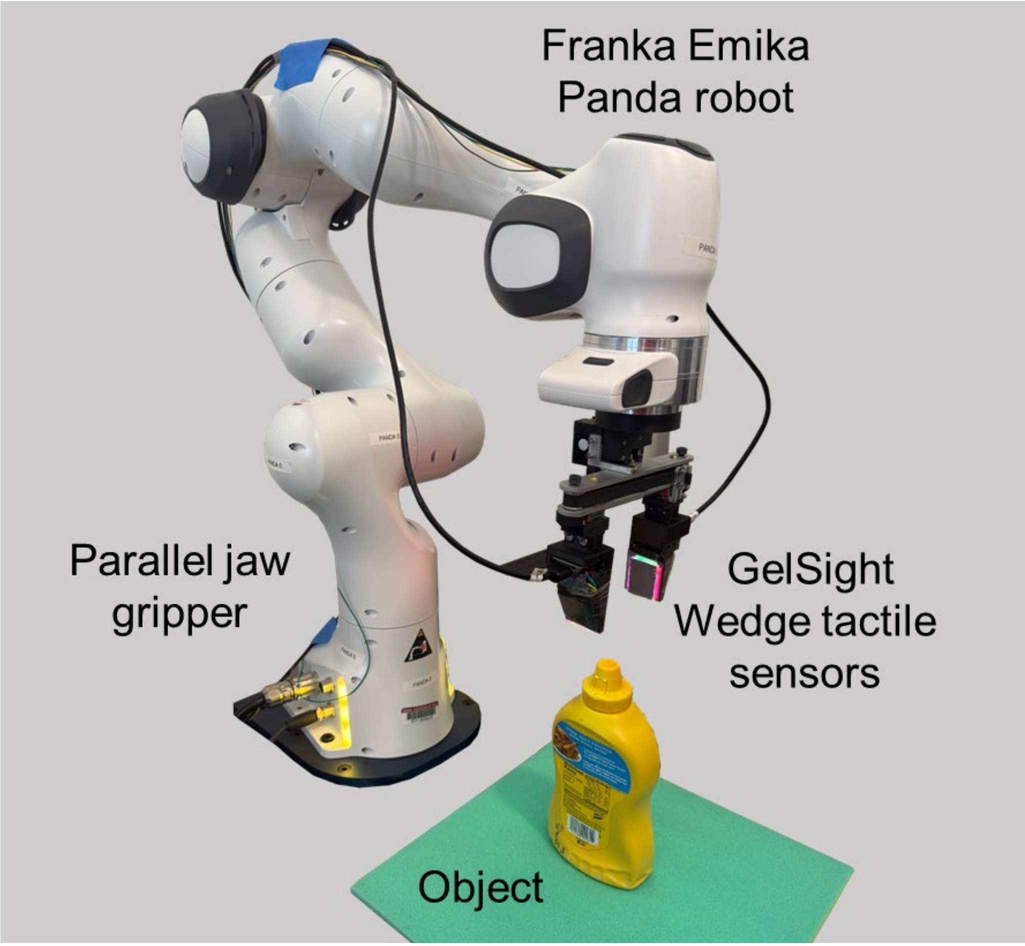

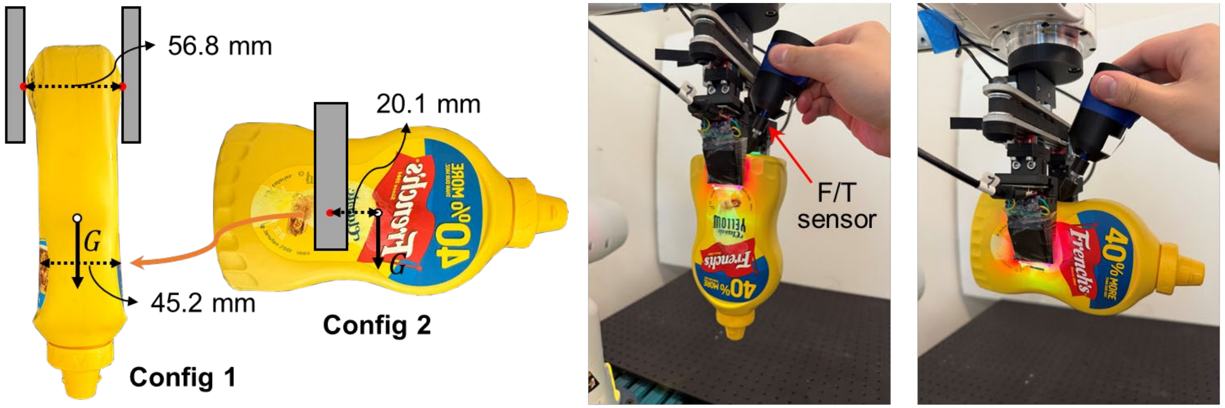

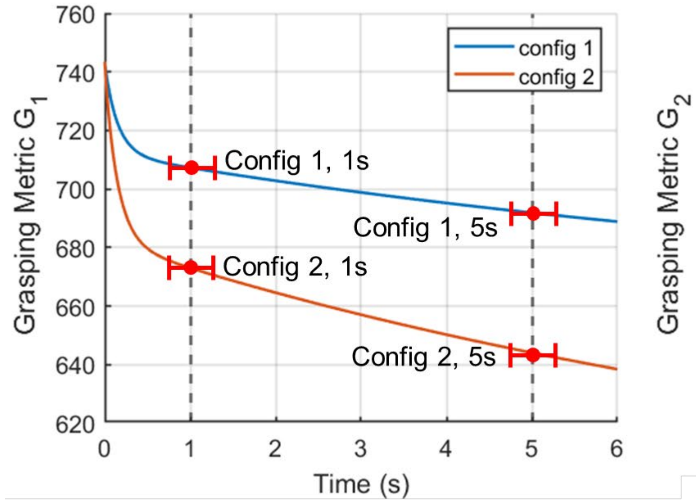

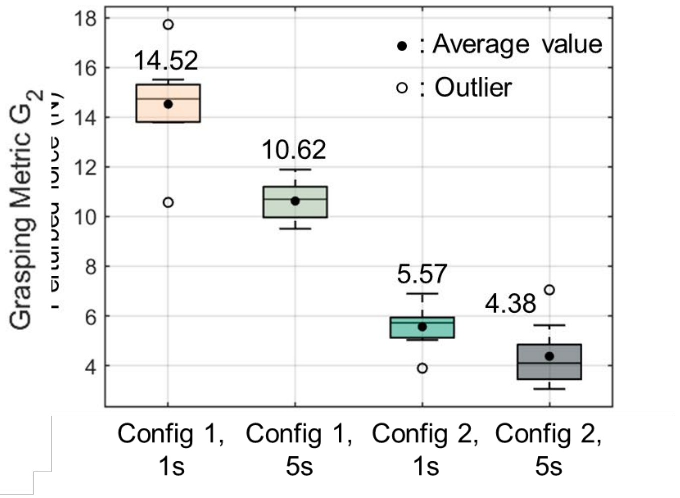

Contribution: Quantitatively evaluation grasp quality

[2] Mingxuan. Li *et al.*, submitted to *IEEE TASE*, Jun. 2025

Grasp Evaluation (1)

● Normal contact mechanical model:

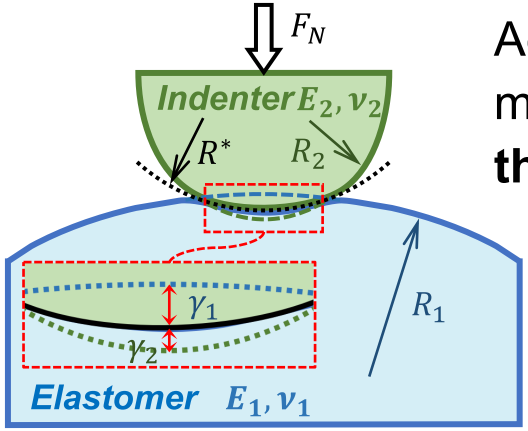

According to **Hertz contact** modified based on **Tatara theory** and **Yoffe theory**:

$$\gamma_2 = H_1 \cdot \gamma_1 + H_2 \cdot \gamma_1^{1.5},$$

$$H_1 = \frac{32}{9\pi} \cdot \frac{1-\nu_2^2}{1-\nu_1^2} \cdot \frac{E_1}{E_2}$$

● Torsional contact mechanical model:

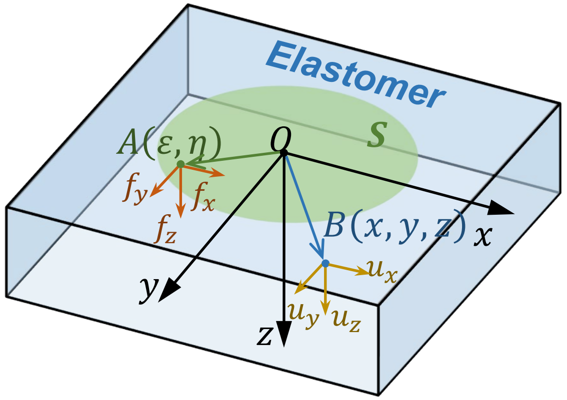

According to **Boussinesq-Cerruti function**, **Jäger theory**, and **rod model**:

$$\theta_2 = H_3 \cdot \theta_1,$$

$$H_3 = 2.014 \cdot \frac{1+\gamma_2}{1+\gamma_1} \cdot \frac{E_1}{E_2}$$

● Mechanical parameter calibration:

Fit the mechanical parameters of the tactile sensor's elastomer based on calibration data:

$$E_1 = \left[0.993 - 0.279 \cdot \frac{H_3}{H_1}(1-\nu_2)\right] \cdot \frac{H_3 E_2}{1+\nu_2},$$

$$\nu_1 = 1 - 0.562 \cdot \frac{H_3}{H_1}(1-\nu_2)$$

● Contact force reconstruction:

Contact   Sensing   **FEM model**[2]

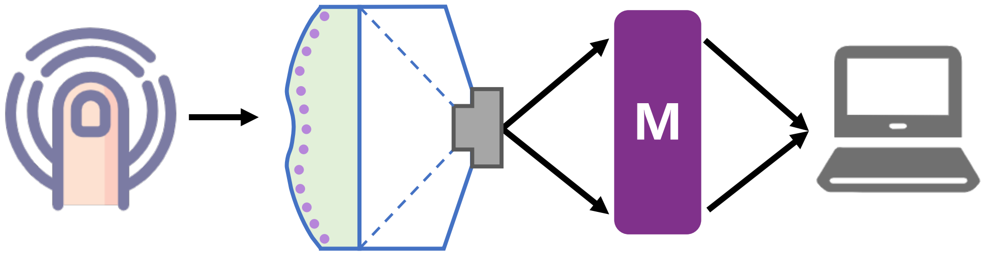

[2] L. Zhang et. al., IEEE RA-L, 2023.

[3] Mingxuan. Li *et al.*, ***IEEE RA-L***, Jul. 2024

[4] Mingxuan. Li et al., in preparation

Grasp Evaluation (2)

- **Limit Surface:**

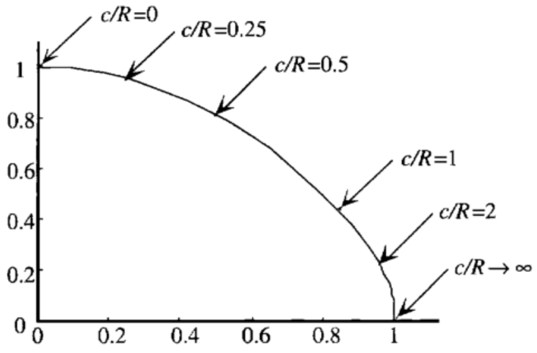

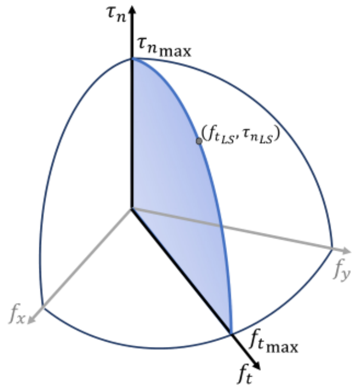

✓ **Semi analytical numerical calculation:**

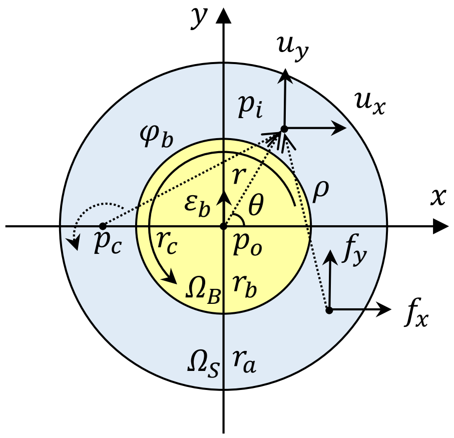

$$F_t = 4\Delta^2 \sum_{k=1}^{N} f_y^k = 4\Delta^2[\varphi_b(C_1 - C_2 r_c) + C_3]$$

$$M_n = 4\Delta^2 \sum_{k=1}^{N} [-f_x^k y + f_y^k x] = 4\Delta^2[\varphi_b(D_1 - D_2 r_c) + D_3]$$

$$C_i(\beta) = \begin{cases} \mathbf{1}_{N_B\times N_B}{}^T \cdot \boldsymbol{H}_{2i}, i \in \{1,2\} \\ \mathbf{1}_{N_B\times N_B}{}^T \cdot \boldsymbol{H}_{2i} + \dfrac{\pi G r_a}{2\Delta^2} \mathbf{1}_{N_S\times N_S}{}^T \cdot \boldsymbol{b}_y^S, i \in \{3\} \end{cases}$$

$$D_i(\beta) = \begin{cases} (\boldsymbol{x}_B)^T \cdot \boldsymbol{H}_{2i} - (\boldsymbol{y}_B)^T \cdot \boldsymbol{H}_{1i} (\boldsymbol{x}_S)^T, i \in \{1,2\} \\ (\boldsymbol{x}_B)^T \cdot \boldsymbol{H}_{2i} - (\boldsymbol{y}_B)^T \cdot \boldsymbol{H}_{1i} + \\ \dfrac{\pi G r_a}{2\Delta^2} [(\boldsymbol{x}_S)^T \cdot \boldsymbol{b}_y^S - (\boldsymbol{y}_S)^T \cdot \boldsymbol{b}_x^S], i \in \{1,2\} \end{cases}$$

- **Transitional Limit Surface:**

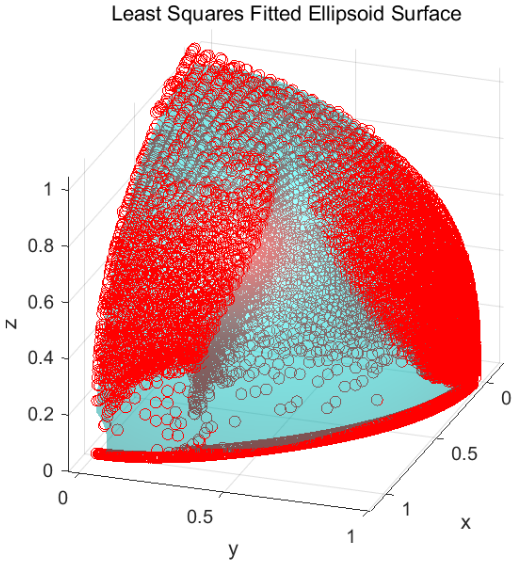

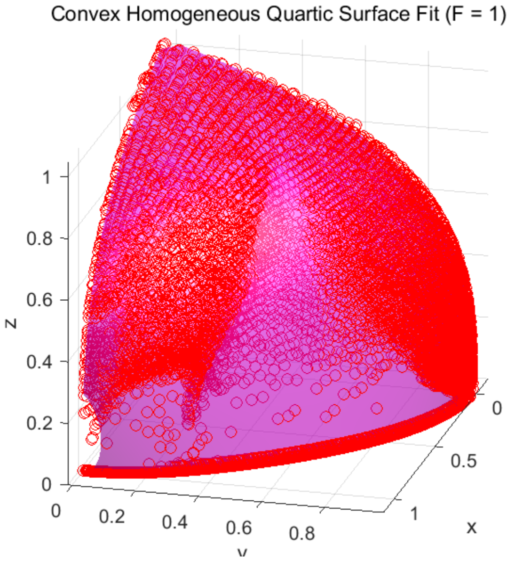

$$\tilde{F}_t^{\delta}(\tilde{r}_c) = \sum_{i=1}^{n} \omega_{f_i}^{\delta} \left(\frac{2}{1 + e^{\alpha_{f_i}^{\delta}(\tilde{r}_c - \varsigma_{f_i}^{\delta})}} - 1 \right)$$

$$\tilde{M}_n^{\delta}(\tilde{r}_c) = \sum_{i=1}^{n} \omega_{m_i}^{\delta} e^{-\frac{(\tilde{r}_c - \varsigma_{m_i}^{\delta})^2}{2(\alpha_{m_i}^{\delta})^2}}$$

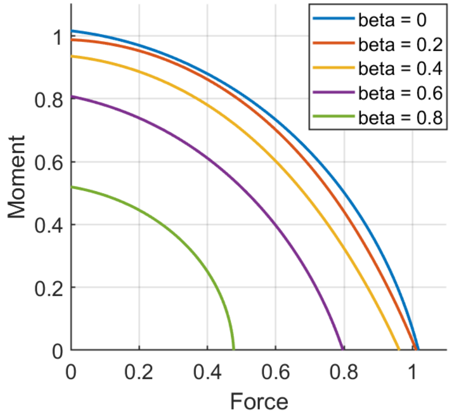

✓ **Contribution:** Quantitative description contact stability

[3] Mingxuan. Li *et al.*, ***IEEE RA-L***, Jul. 2024
[4] Mingxuan. Li et al., in preparation

Overview

1. Background and Motivation
2. Contact Modelling
3. **Contact Representation**
4. Contact Reconstruction
5. Contact-Rich Tasks

Selection of Sensor Type

Array-Type Sensor

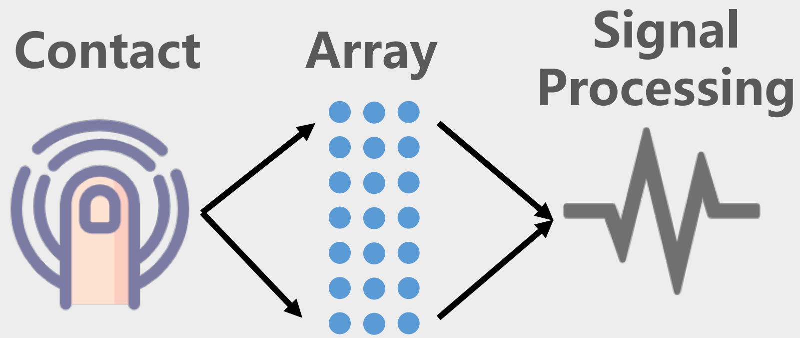

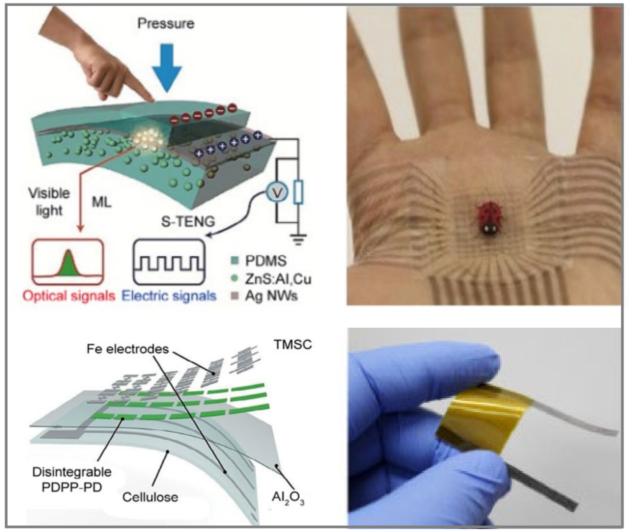

- ✓ Limited functionality in tactile sensor
- ✓ Lack of perception density

Model-Type Sensor

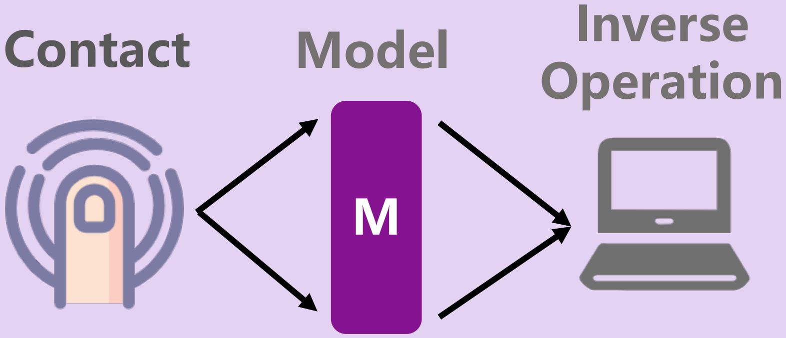

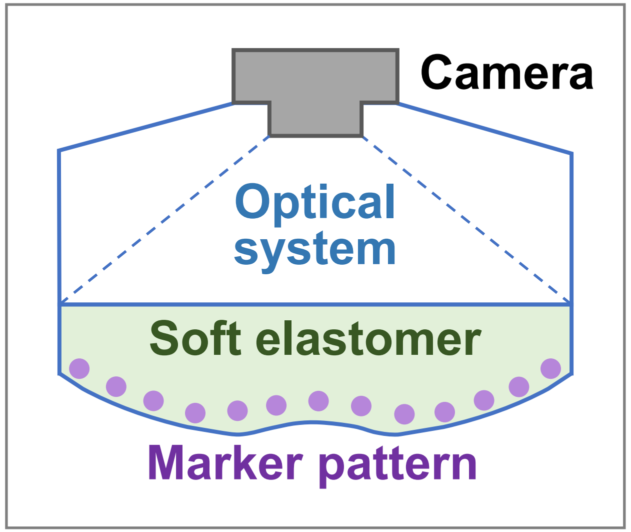

- ✓ Capable of multimodal tactile information measurement
- ✓ Possesses super-resolution fineness

Vision-Based Tactile Sensor (VBTS)

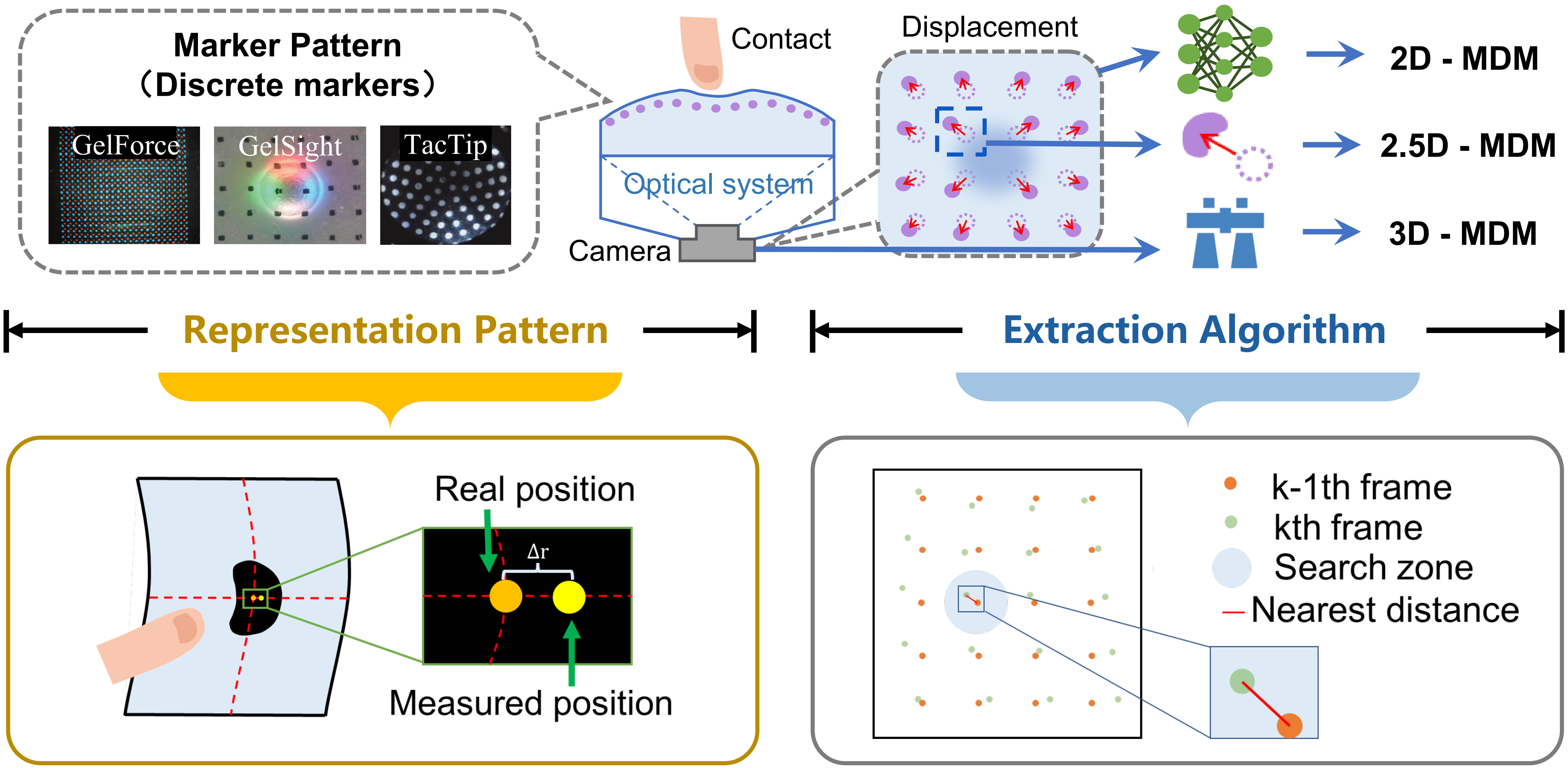

[5] Mingxuan. Li *et al.*, ***IEEE Sensors Journal*** **(review article),** Apr. 2023

Contact Representation

Raw Information

- ✓ Static representation: Reflect the current contact state

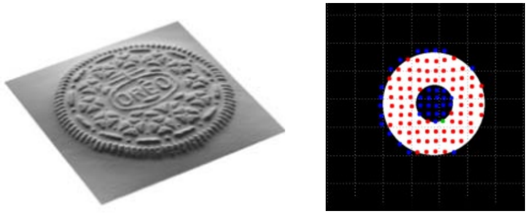

- ✓ Dynamic representation: Reflect the changing process

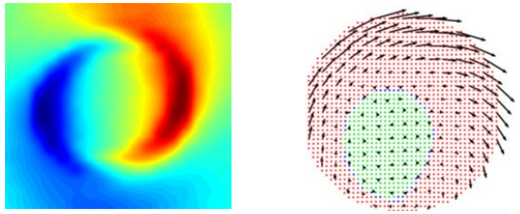

Contact → **Deconstruct Spatio-Temporal Correlations**

State Description:
Temporal Topological Relationships

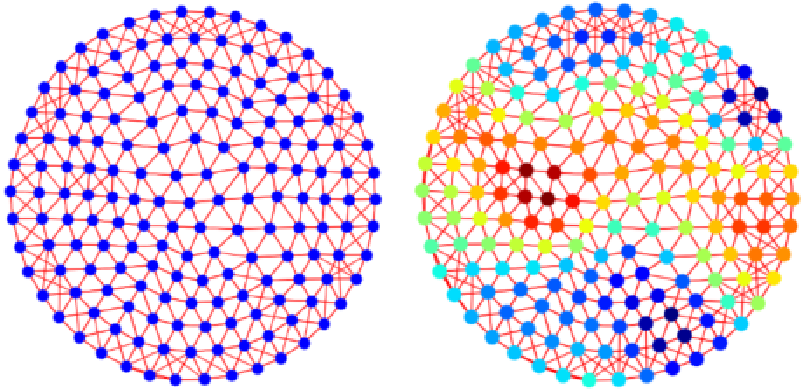

Process Description:
Spatial Topological Relationships

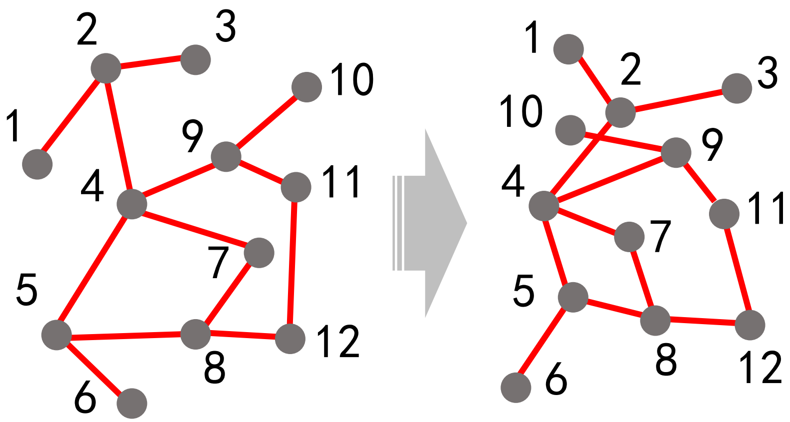

[6] Mingxuan. Li *et al.*, ***IEEE TIM***, Aug. 2022

[7] Mingxuan. Li *et al.*, ***IEEE RA-L***, Sep. 2023

Representation Pattern

Continuous Marker Pattern (CMP)

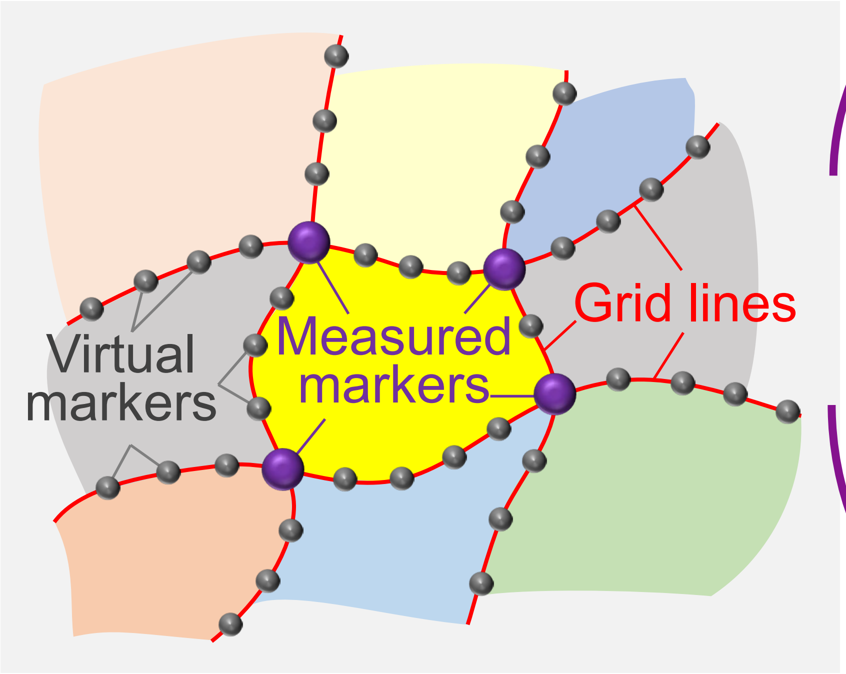

Example 1: Square-CMP

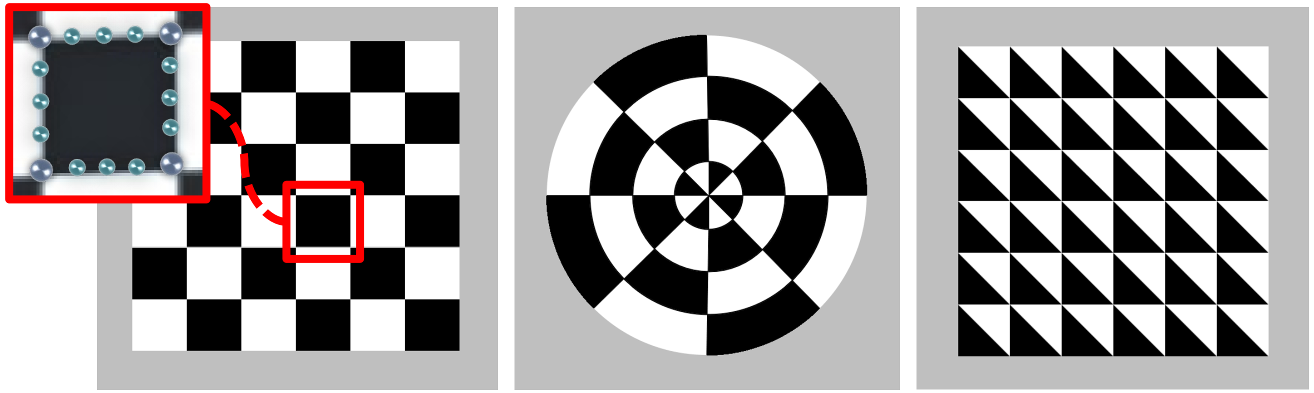

Example 2: Multicolor-CMP

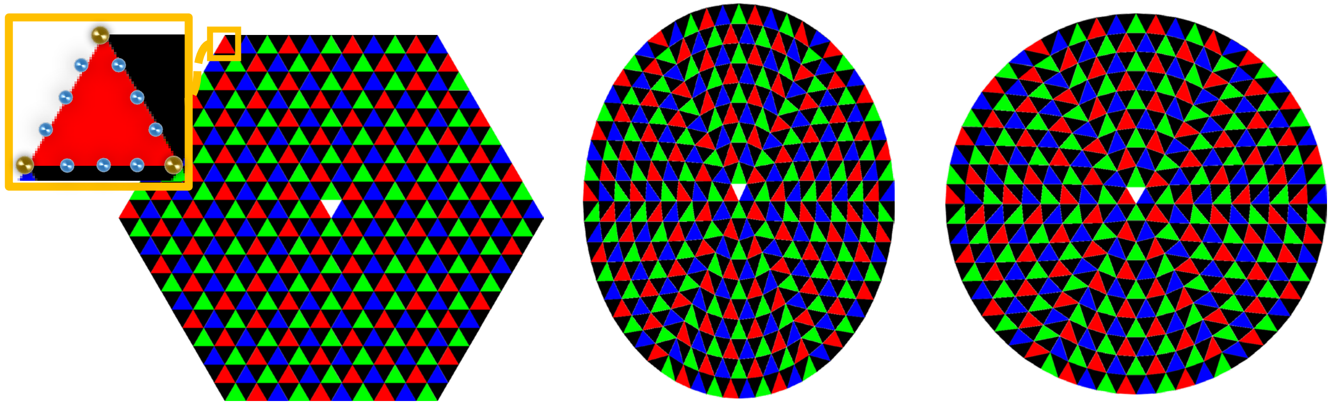

[6] Mingxuan. Li *et al.*, ***IEEE TIM***, Aug. 2022

[7] Mingxuan. Li *et al.*, ***IEEE RA-L***, Sep. 2023

Extraction Algorithm

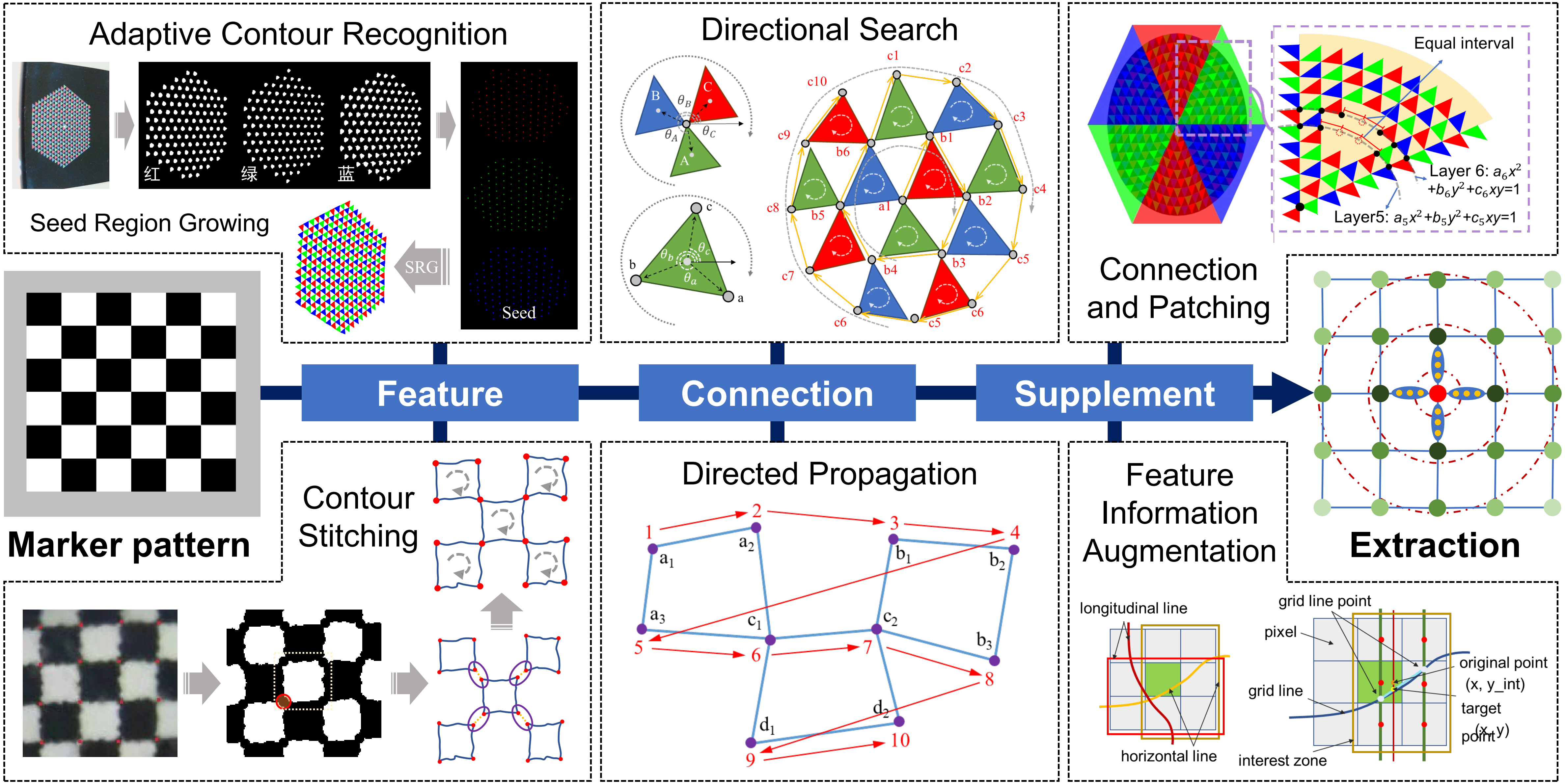

[6] Mingxuan. Li *et al.*, ***IEEE TIM***, Aug. 2022 [7] Mingxuan. Li *et al.*, ***IEEE RA-L***, Sep. 2023

Simulation Evaluation

Test object

Deformation

Displacement

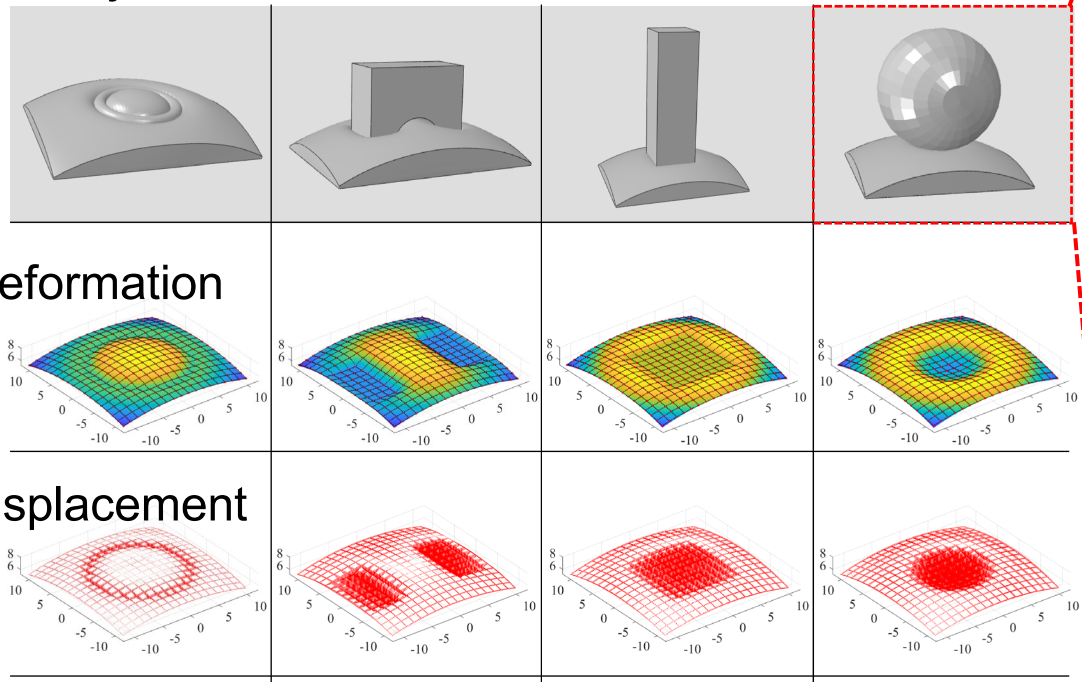

Error

0.018mm	0.020mm	**0.021**mm	0.019mm

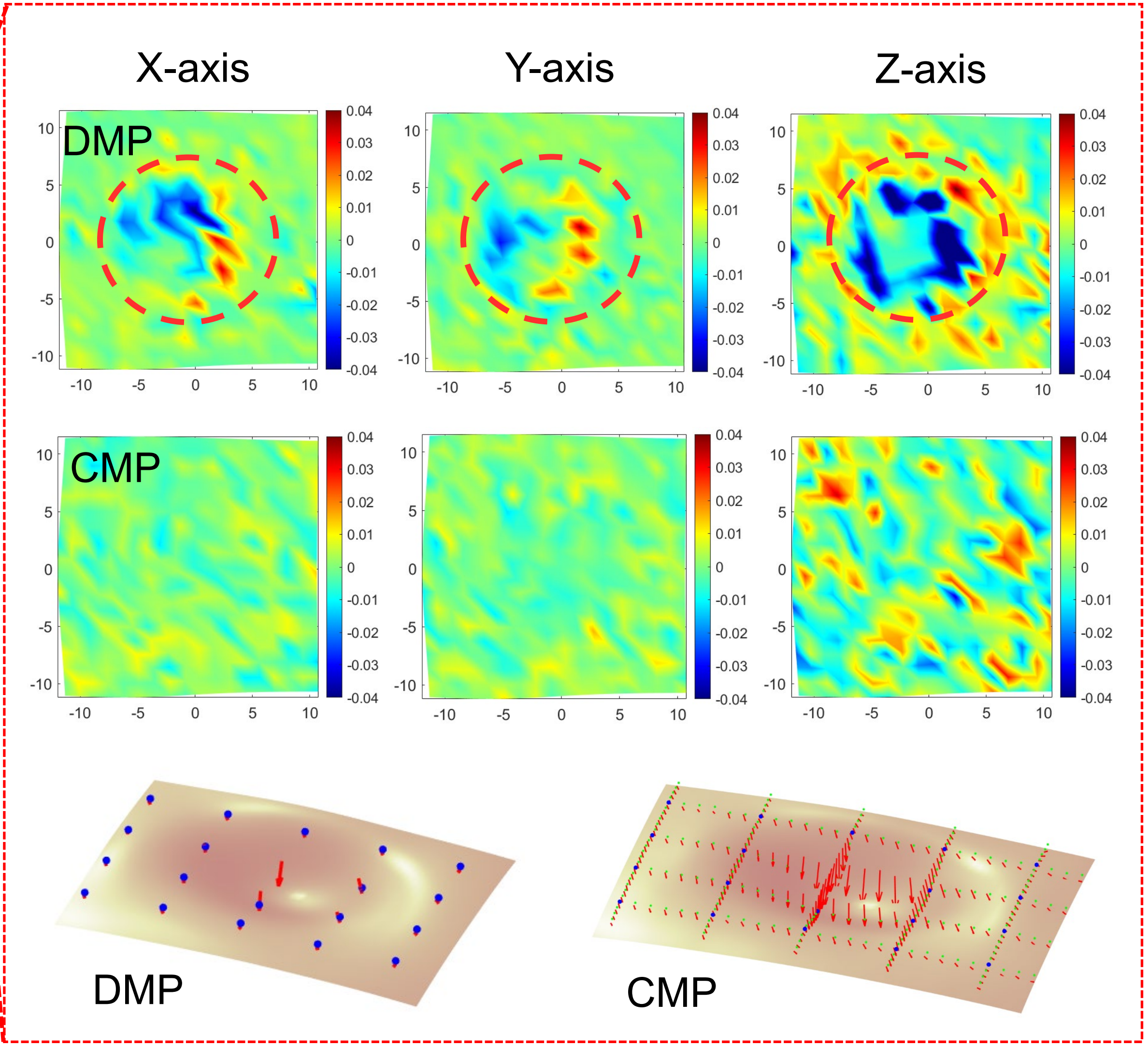

[6] Mingxuan. Li *et al.*, ***IEEE TIM***, Aug. 2022

[7] Mingxuan. Li *et al.*, ***IEEE RA-L***, Sep. 2023

Sensor Design

- **Virtual Binocular Vision:**

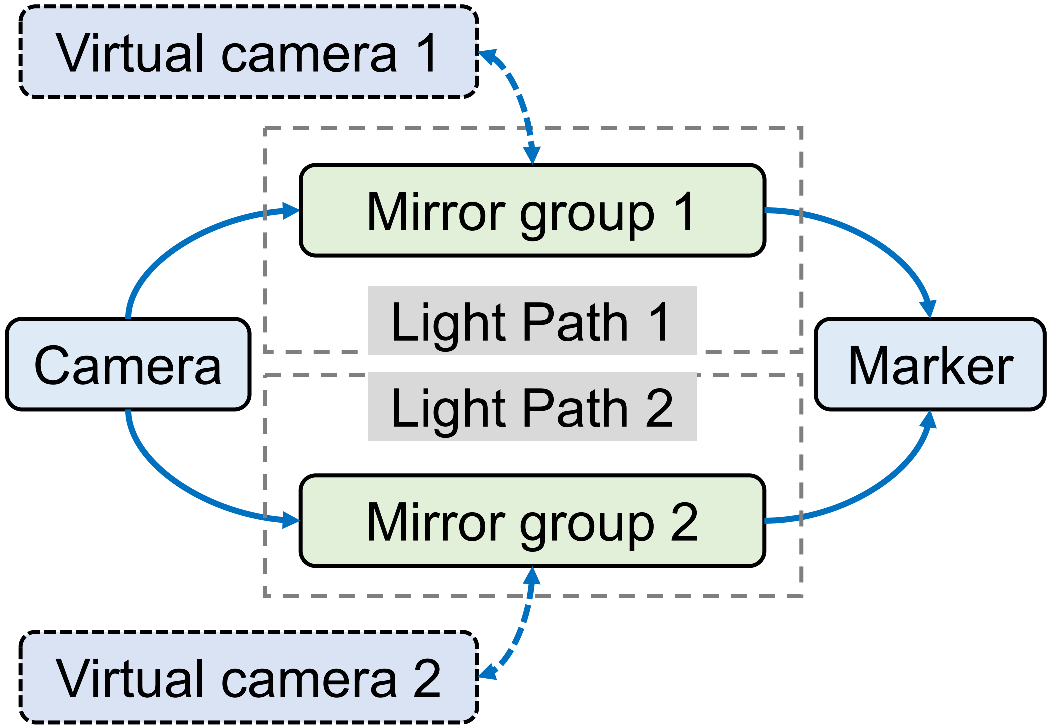

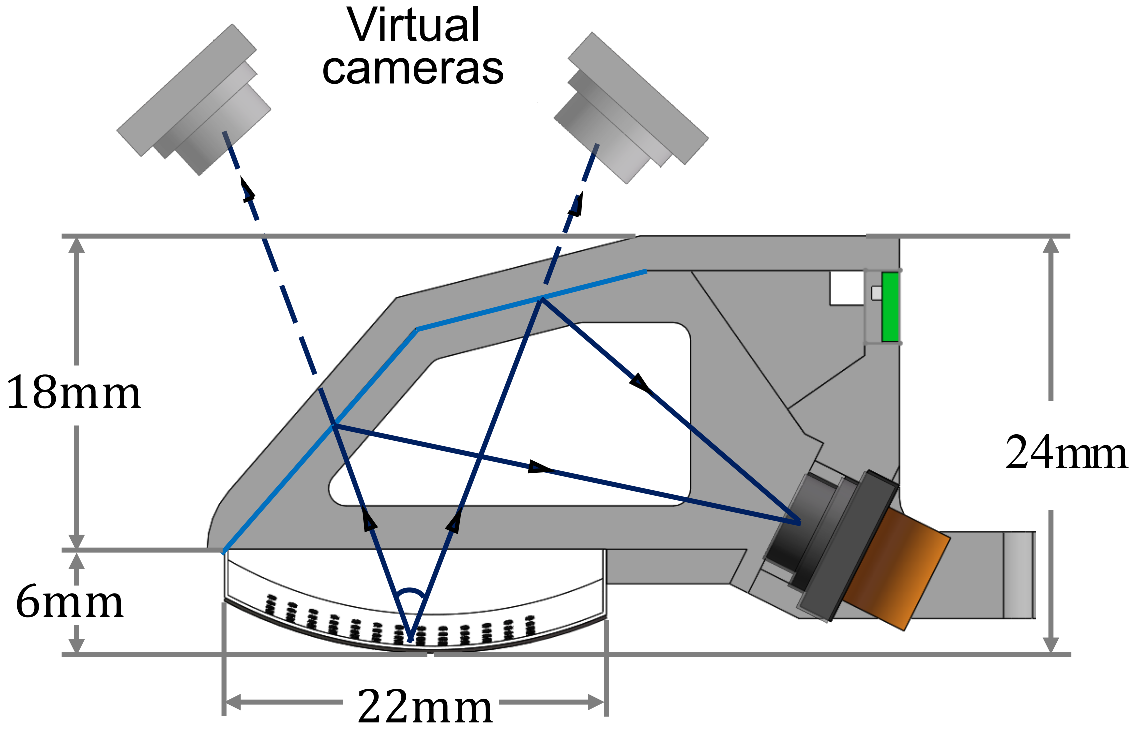

Lunwei Zhang, Yue Wang, & Yao Jiang. (2022). Tac3D: A Novel Vision-based Tactile Sensor for Measuring Forces Distribution and Estimating Friction Coefficient Distribution.

✓ **Only one camera** is needed to achieve **stereoscopic vision** (for synchronization and compactness)

[6] Mingxuan. Li *et al.*, ***IEEE TIM***, Aug. 2022

Experiment Evaluation

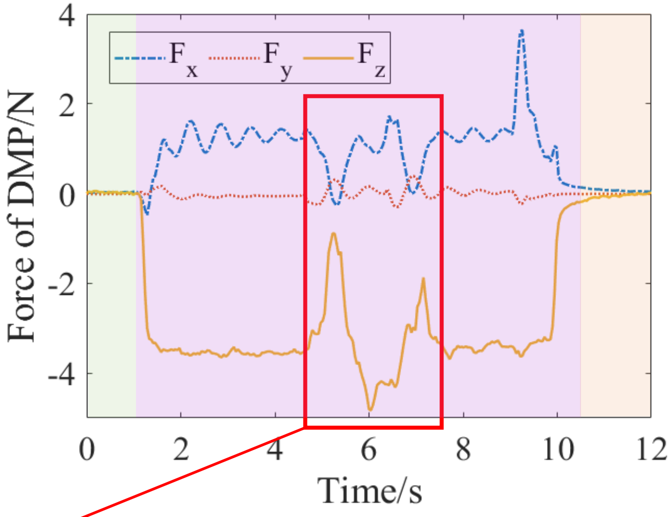

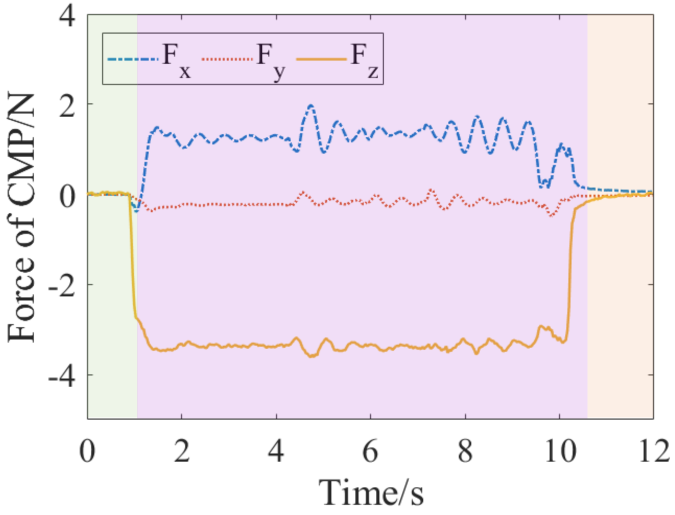

Match Failure

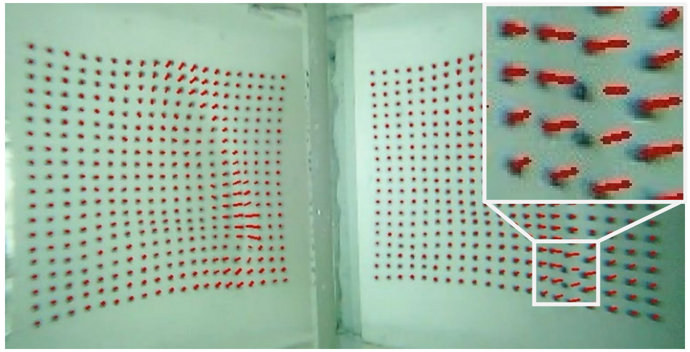

DMP

(d)

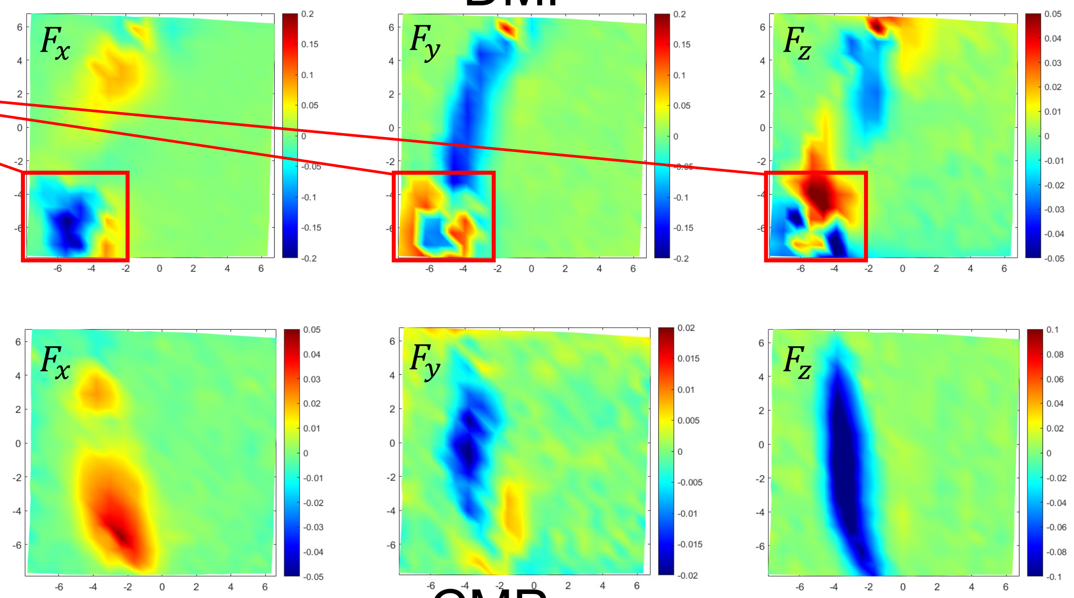

CMP

[6] Mingxuan. Li *et al.*, ***IEEE TIM***, Aug. 2022

[7] Mingxuan. Li *et al.*, ***IEEE RA-L***, Sep. 2023

Overview

1. Background and Motivation
2. Contact Modelling
3. Contact Representation
4. **Contact Reconstruction**
5. Contact-Rich Tasks

Deformation Reconstruction

Contact Deformation:

Requirement of Precision:

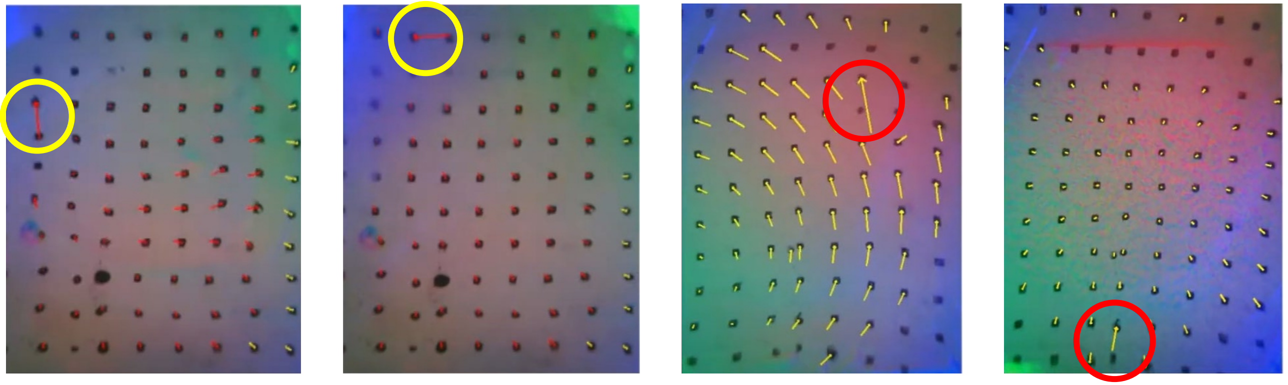

Requirement of Reliability:

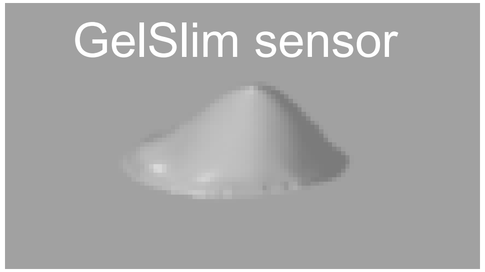

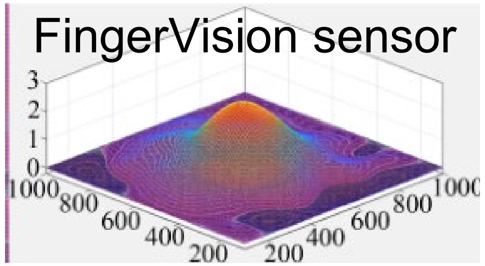

Feature Model Analysis

- **Examples of corner and line features:**

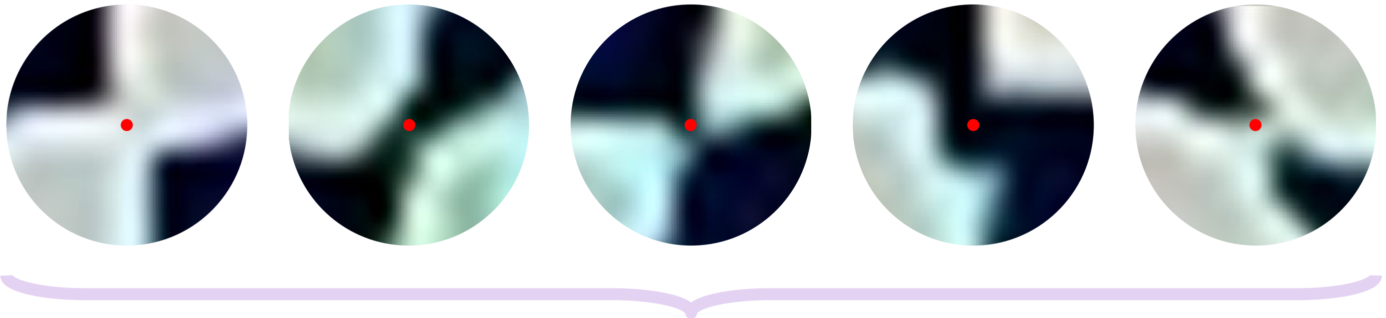

✓ **Geometric distortion** occurs under dynamic contact deformation

✓ Fine representation relies on **real-time and reliable detection** of marker features

- **Feature model of continuous marker pattern:**

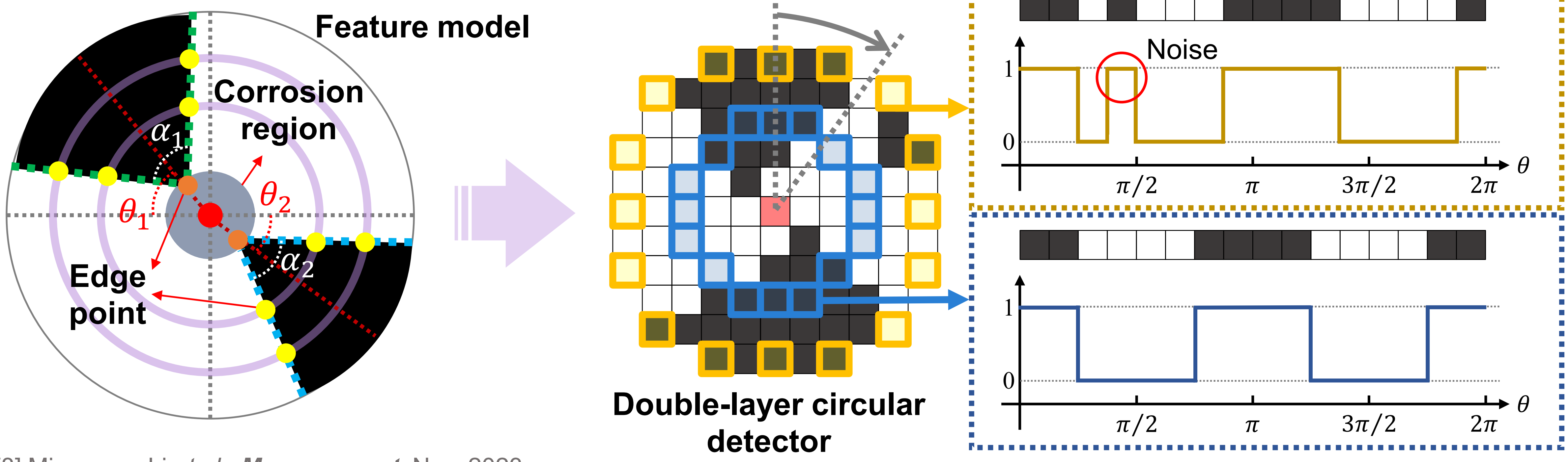

[8] Mingxuan. Li *et al.*, ***Measurement***, Nov. 2023

Feature Quantization: Intra-Layer Criterion (1)

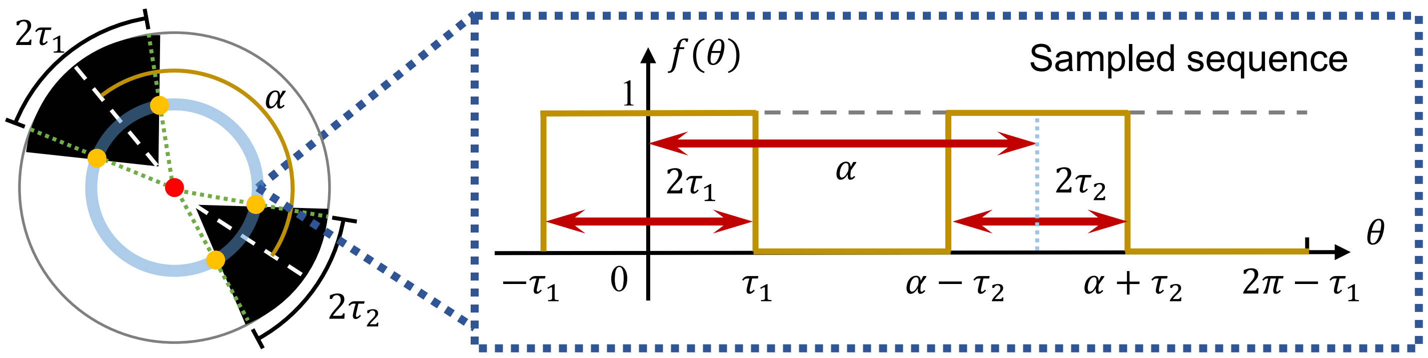

Function: $f(\theta)=u(\theta+\tau_1)-u(\theta-\tau_1)$
$+u(\theta+\tau_2-\alpha)-u(\theta-\tau_2-\alpha)$

Amplitude-frequency characteristic:

$$F(j\omega)=\int_{-\infty}^{+\infty} f(\theta)\cdot e^{-j\omega\theta}$$
$$=\tau_1\cdot Sa(\omega\tau_1)+\tau_2\cdot Sa(\omega\tau_2)\cdot e^{-j\omega\alpha}$$

Amplitude intensity variation at different frequencies:

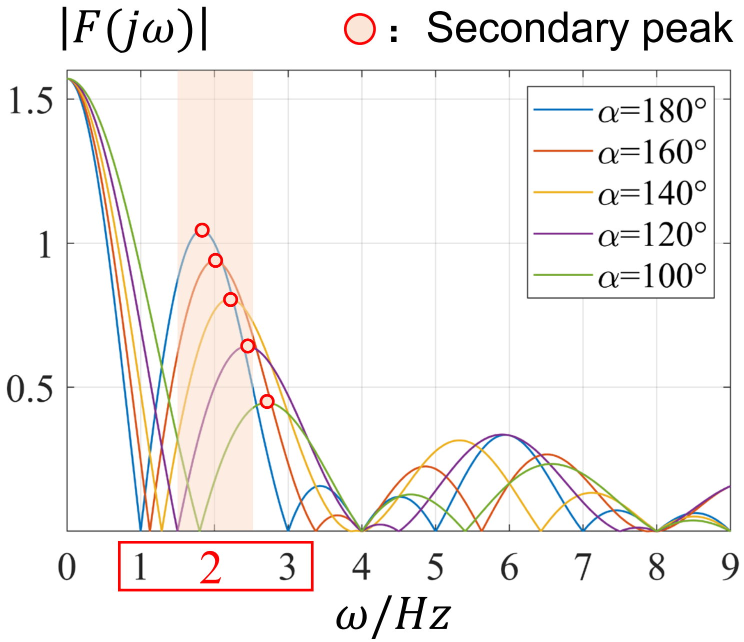

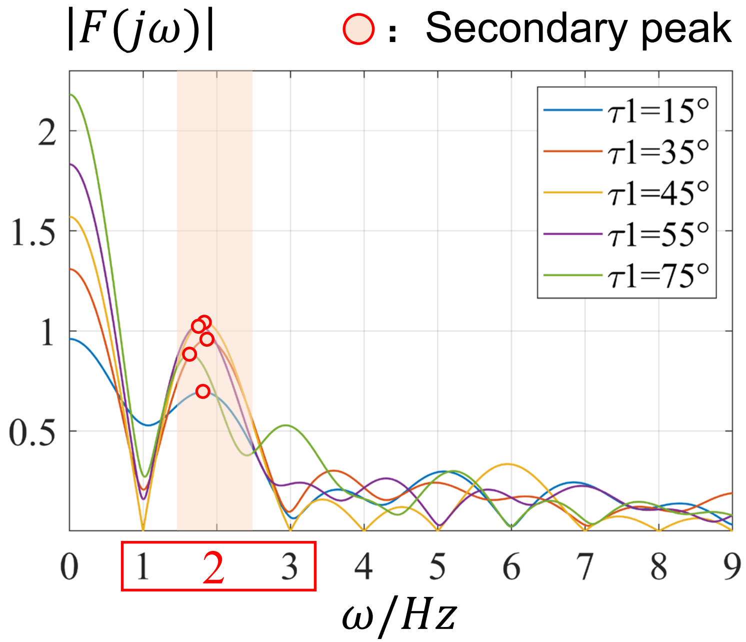

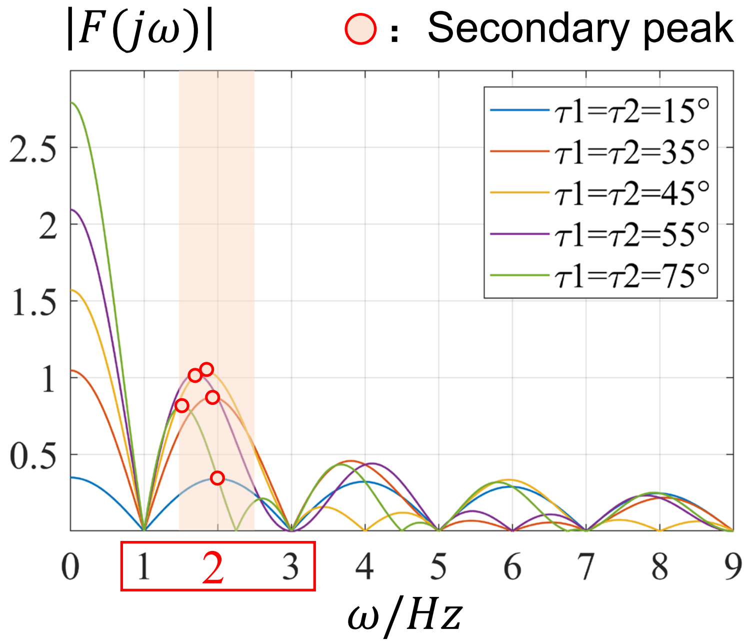

[8] Mingxuan. Li *et al.*, ***Measurement***, Nov. 2023

Feature Quantization: Intra-Layer Criterion (2)

- **Intra-layer Response Features:** $\Delta_{f_{12}} = |\boldsymbol{F}(2j)| - |\boldsymbol{F}(1j)|$, $\Delta_{f_{23}} = |\boldsymbol{F}(2j)| - |\boldsymbol{F}(3j)|$

Special case 1: $\tau_1 = \tau_2 = \tau$

$$\Delta_{f_{12}}{}^{-1} = \left|\frac{F(1j)}{F(2j)}\right| = \left|\frac{2\sin(\tau)\cos\left(\frac{1}{2}\alpha\right)}{\sin(2\tau)\cos(\alpha)}\right|$$

$$\Delta_{f_{23}}{}^{-1} = \left|\frac{F(3j)}{F(2j)}\right| = \left|\frac{2\sin(\tau)\cos\left(\frac{1}{2}\alpha\right)}{3\sin(2\tau)\cos(\alpha)}\right|$$

Conclusion： $\Delta_{f_{12}}$ and $\Delta_{f_{23}}$ preserve the true features with large distortion and filter out the false positives in **white zones**.

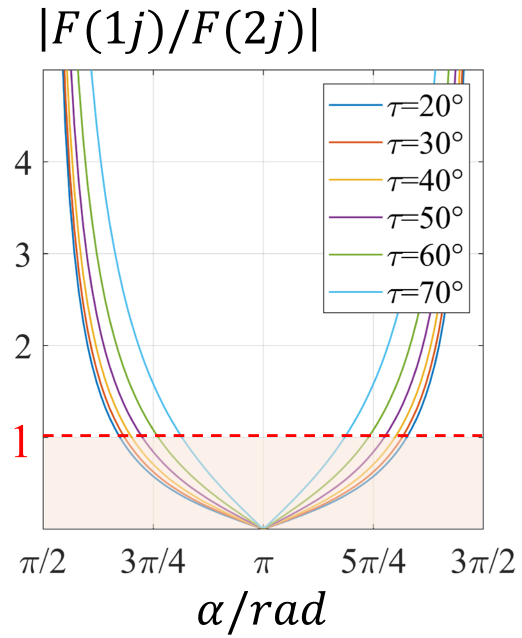

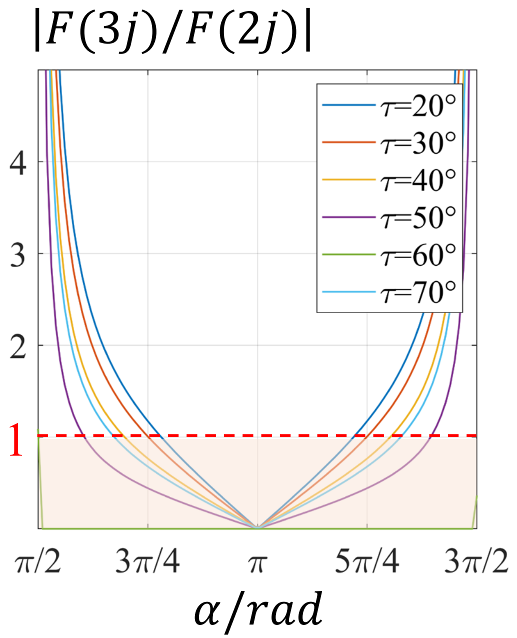

Special case 2: $\alpha = \pi$

$$\Delta_{f_{12}}{}^{-1} = \left|\frac{F(1j)}{F(2j)}\right| = \left|\frac{\sin\left(\frac{1}{2}\delta\right)}{\sin\left(\frac{1}{2}T\right)\cos(\delta)}\right|$$

$$\Delta_{f_{23}}{}^{-1} = \left|\frac{F(3j)}{F(2j)}\right| = \left|\frac{2\cos\left(\frac{3}{2}T\right)\sin\left(\frac{3}{2}\delta\right)}{3\sin(T)\cos(\delta)}\right|$$

Conclusion： $\Delta_{f_{12}}$ and $\Delta_{f_{23}}$ preserve the true features with large distortion and filter out the false positives in **black zones**.

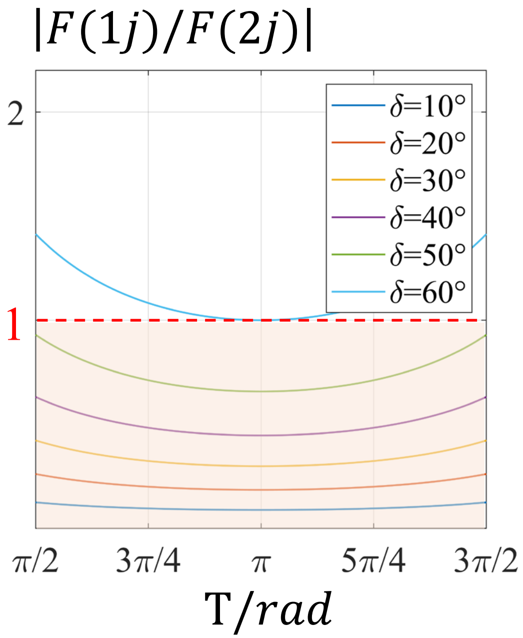

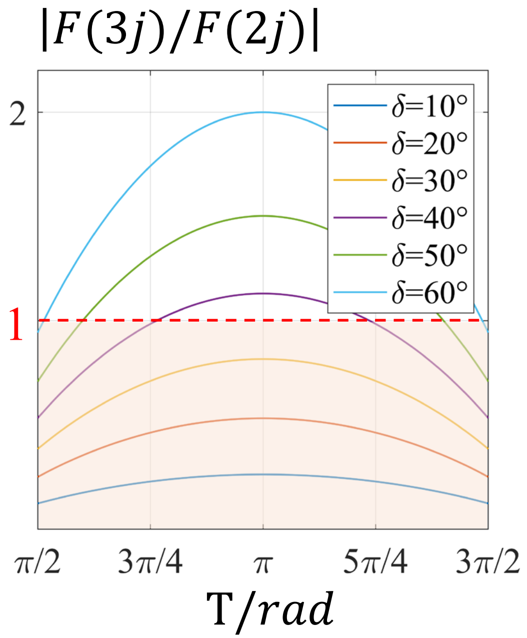

[8] Mingxuan. Li *et al.*, ***Measurement***, Nov. 2023

Feature Quantization: Inter-Layer Criterion

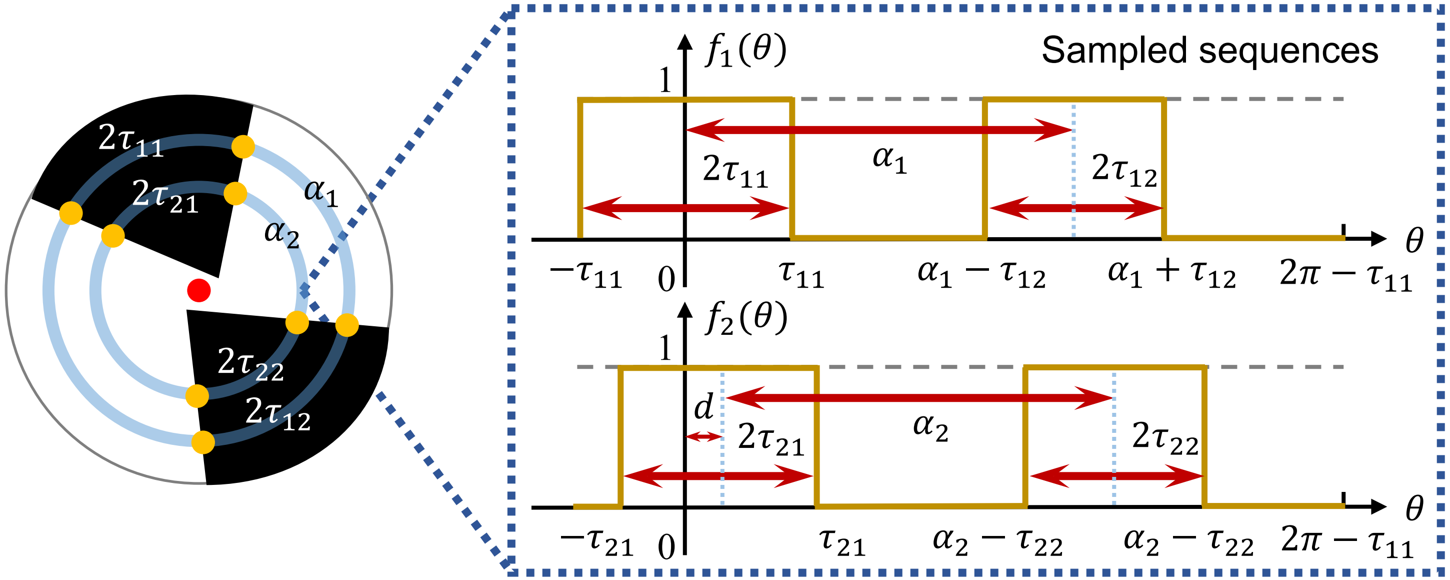

Cross-correlation function:

$$R_{1,2}(\varphi) = \int_{-\infty}^{+\infty} f_1^*(\theta)\cdot f_2^*(\theta-\varphi)d\theta$$

- **Inter-layer Response Features:**

$\Delta_A = R_{1,2}(\varphi_{max})$ Cross-correlation coefficient

$\Delta_\varphi = \left|\frac{\varphi_{max,l}+\varphi_{max,r}}{2}\right|$ Maximum values interval

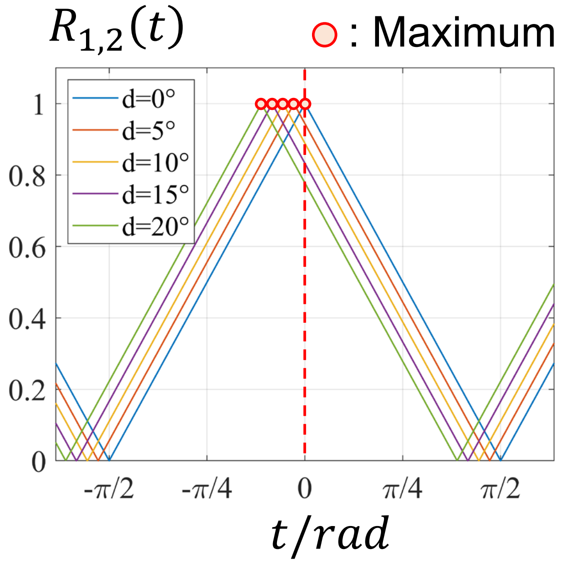

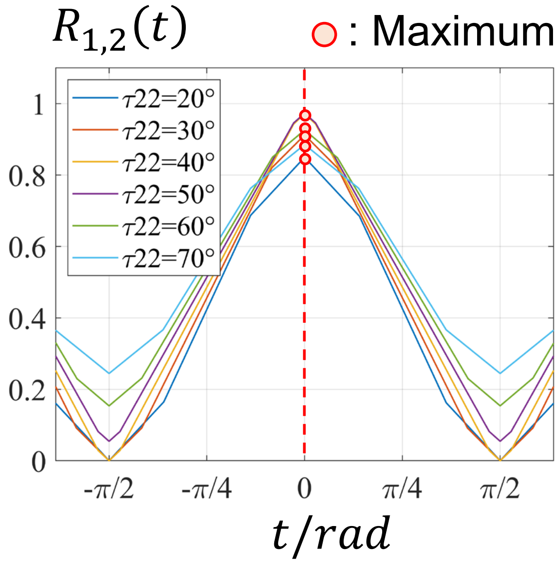

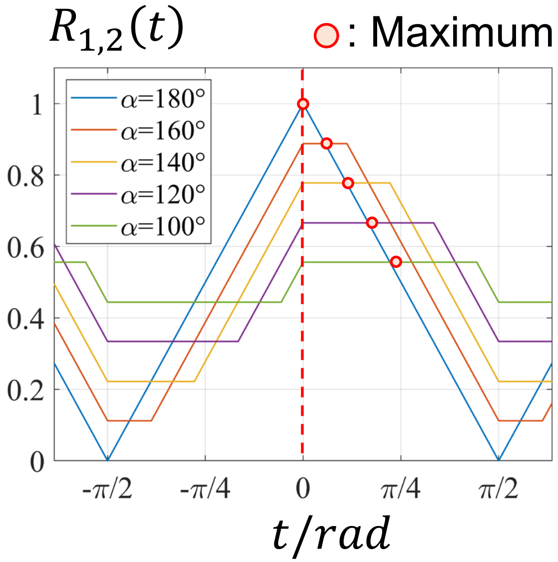

Conclusion： Δ_A and Δ_φ describe the symmetry and similarity between two sampled signal, and can filter out the false positives **from noise** ($\Delta_A > 0.75$ and $\Delta_\varphi < 20°$).

[8] Mingxuan. Li *et al.*, ***Measurement***, Nov. 2023

Evaluation of Feature Detection

- **Quantitative Comparison:**

False Negative *False Positive*

Ball


Torus
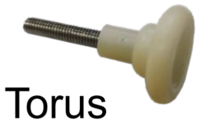

Cube
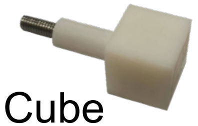

Rib
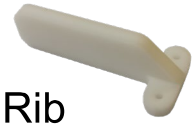

- **Qualitative Comparison:**

Origin image: **Proposed:** ChESS:

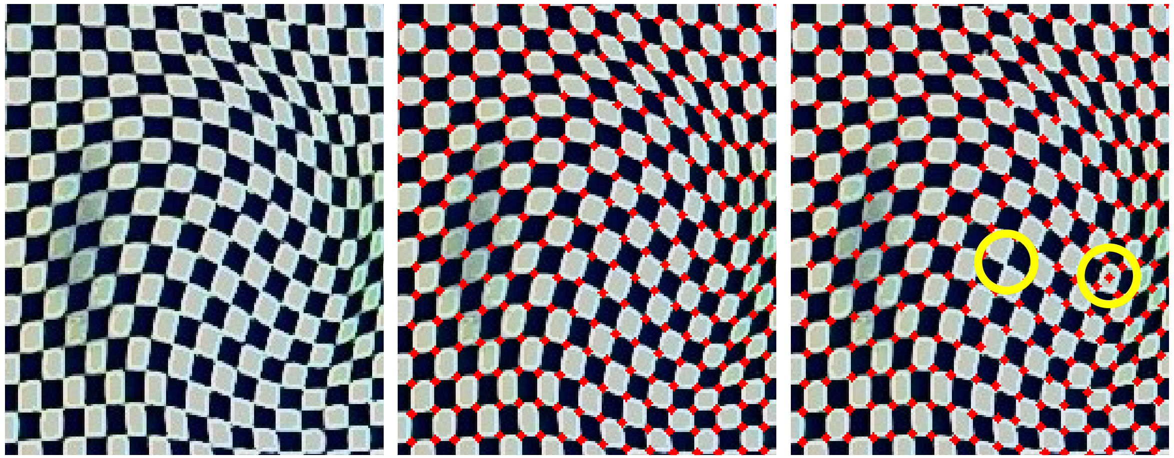

Harris: Shi-Tomasi's: Zhang's:

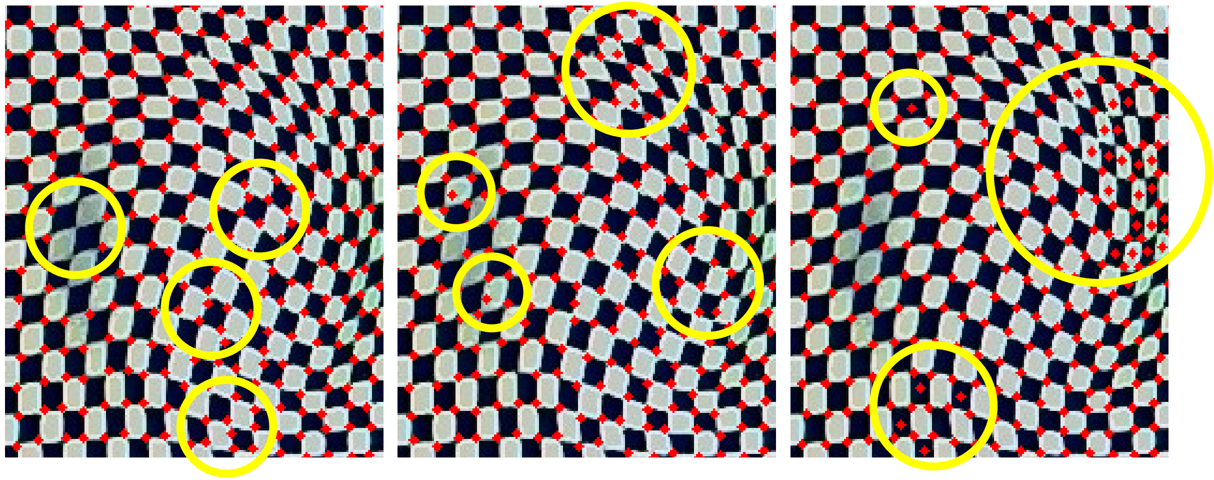

[8] Mingxuan. Li *et al.*, ***Measurement***, Nov. 2023

Evaluation of Deformation Reconstruction

3-D Deformation Reconstruction: Execution Speed 120Hz, Success Rate 97.5%

- **Static Reconstruction:**

Sharp contact:

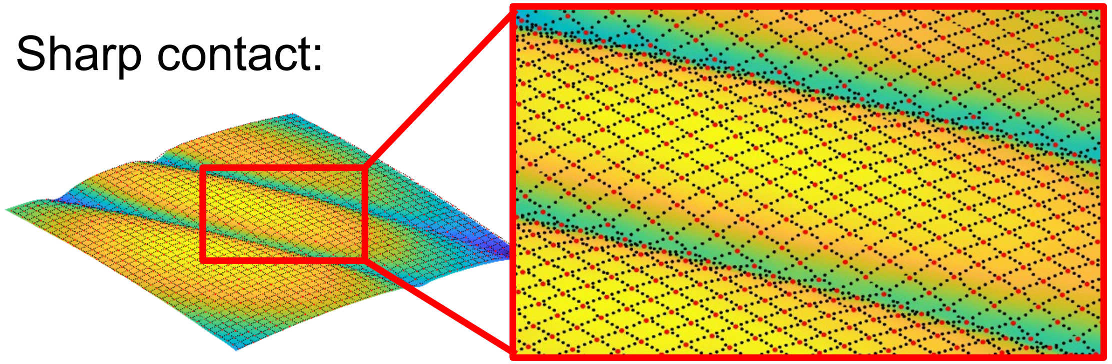

Smooth contact:

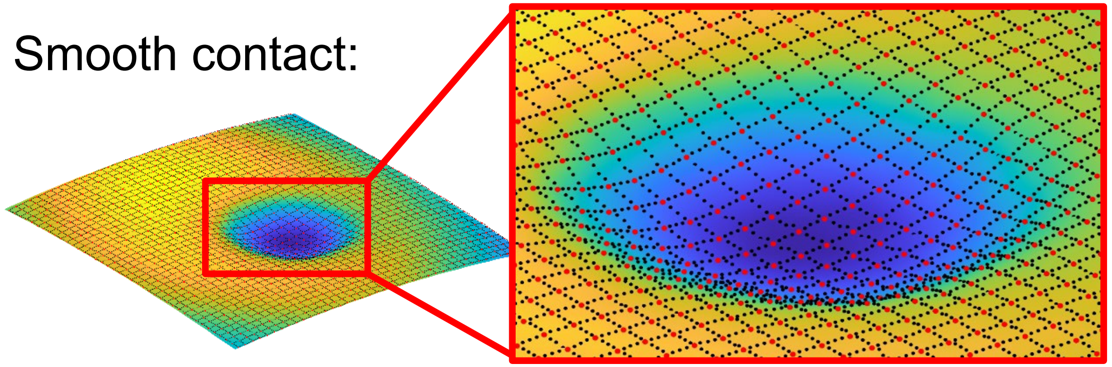

- **Dynamic Tracking:**

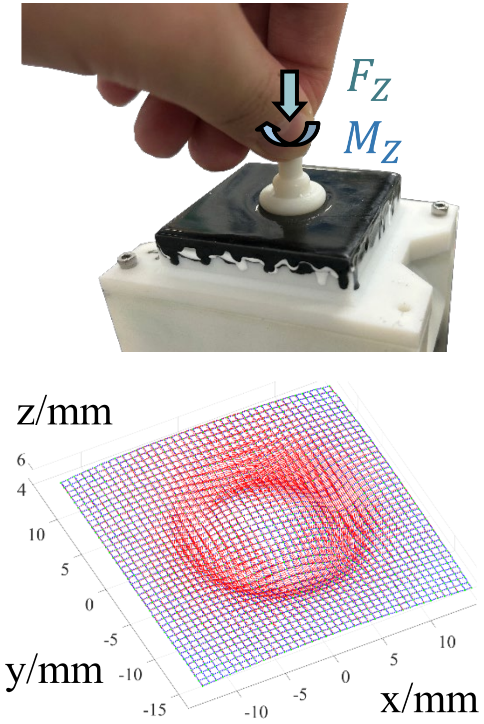

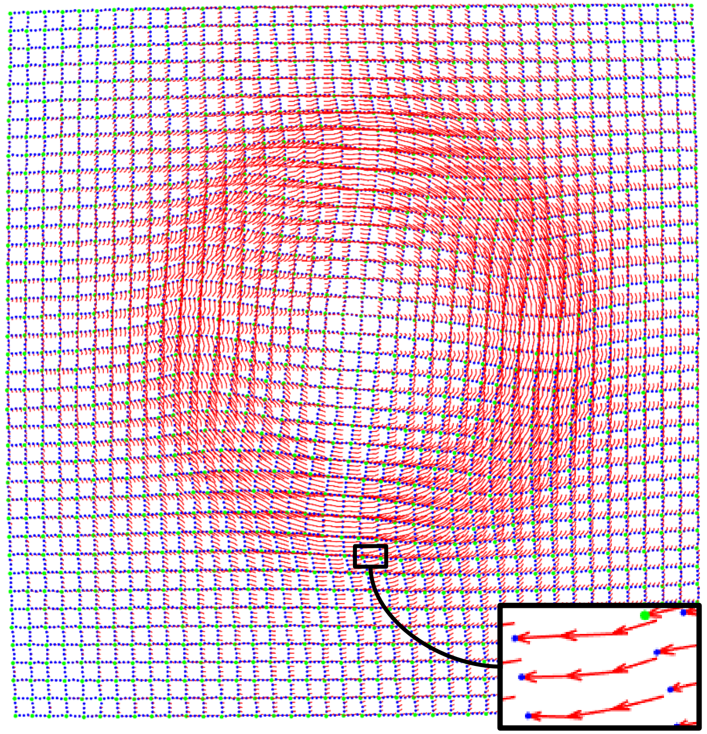

Conclusion:

✓ The proposed method achieves the **high-density representation** (10.7 effective markers per square millimeter) with advantages in terms of **real-time performance and robustness**.

[8] Mingxuan. Li *et al.*, ***Measurement***, Nov. 2023

Force Reconstruction

Fabrication error、Material aging…

Physical-based force estimation: Requiring reliable **mechanical parameters** (Young's modulus *E* and Poisson's ratio *v*) of the contact elastomer in vision-based tactile sensors.

- **In-situ calibration method**: Measuring the relationship between **normal contact force** and **indentation depth**.
- **Limitations:**
  - ✓ **Expensive** (robot arm, gripper, and ATI F/T sensors);
  - ✓ **Require additional accessories** (e.g., DAQ boards);
  - ✓ **Difficult to operate** outside laboratory environments.

[1] C. Zhao et. al., 2023 ICRA.

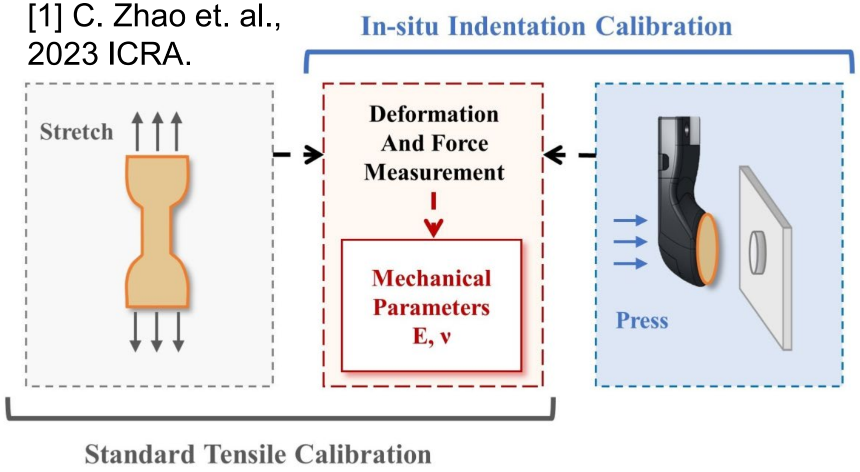

Main Challenge: How to achieve **low-cost and easy-to-use** mechanical calibration without using expensive equipment (tensile platform or robot arm).

Simple and Low-Cost Calibration

Purpose: Constructing the **contact deformation relationship** between the **standard elastic calibration indenter** and the sensor's elastomer.

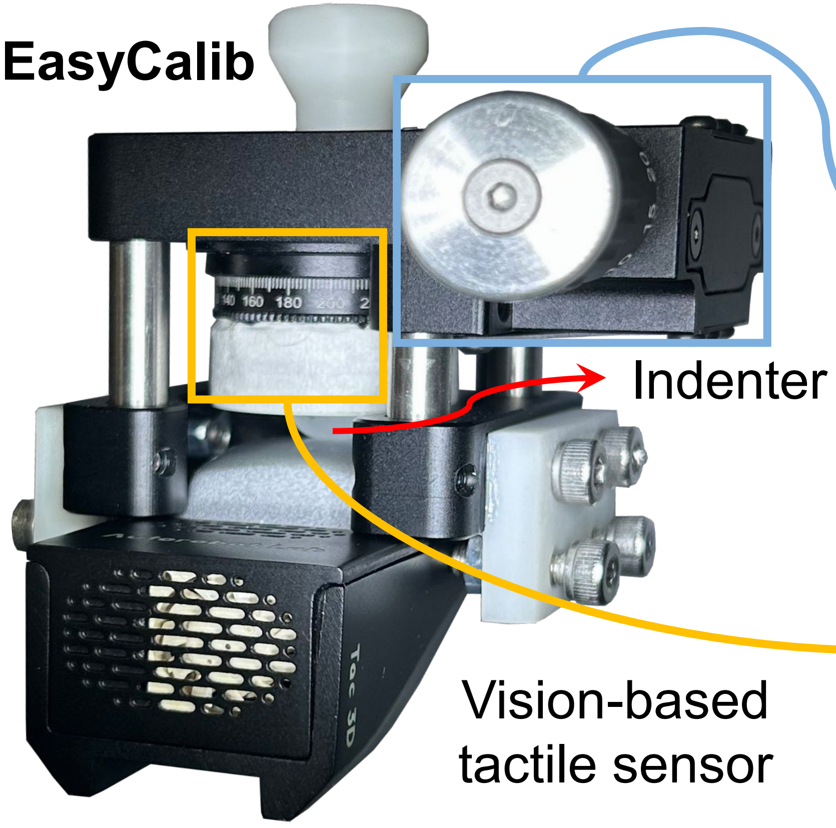

Normal Contact

The relationship between normal displacements $\boldsymbol{\gamma_1}$ and $\boldsymbol{\gamma_2}$

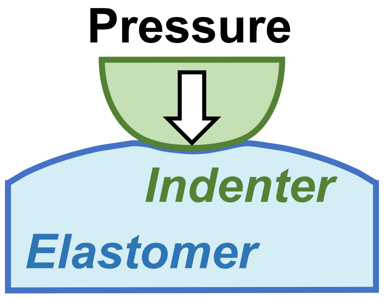

Torsional Contact

The relationship between the rotational angles $\boldsymbol{\theta_1}$ and $\boldsymbol{\theta_2}$

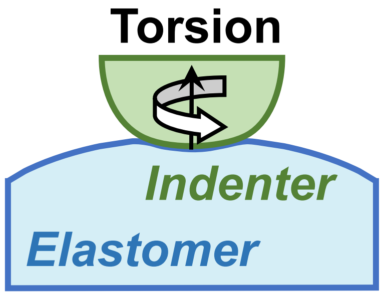

Contact deformation relationship:

$$\boldsymbol{g}_1(E_1, \nu_1, \gamma_1, \theta_1) = \boldsymbol{g}_2(E_2, \nu_2, \gamma_2, \theta_2)$$

Calculating E_1 and ν_1

[3] Mingxuan. Li *et al.*, ***IEEE RA-L***, Jul. 2024

Simulation Validation

- **Simulation in Abaqus:**

Change parameters and verify two contact theories.

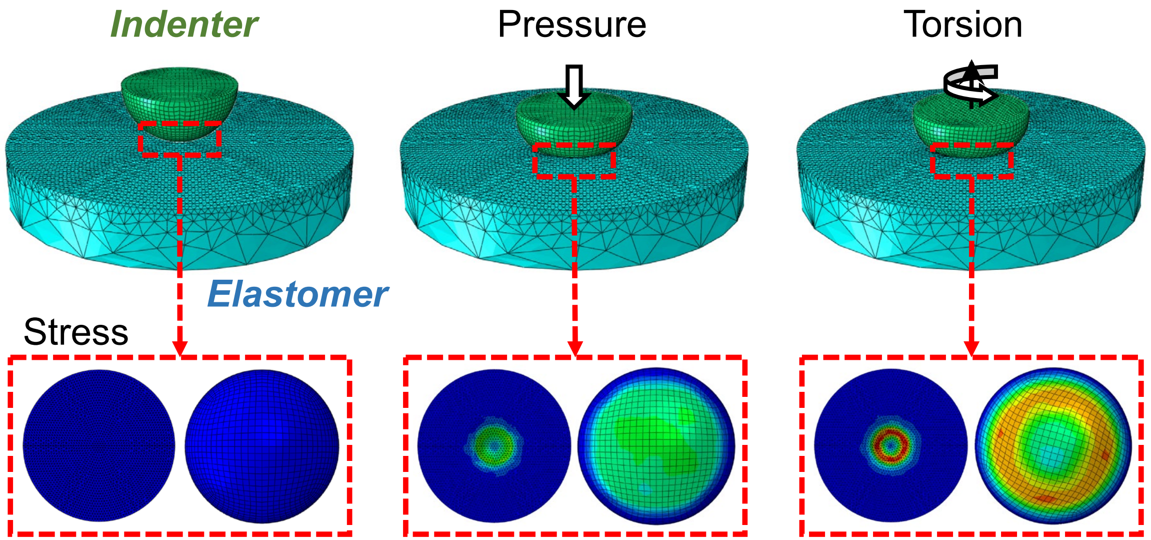

- **Conclusion:**

✓ The best result is obtained when $\boldsymbol{E_2 = 2E_1 \sim 3E_1}$, $\boldsymbol{\nu_2 = 0.4}$;

✓ In most cases, **the simulation and theory exhibit good consistency**.

- **Normal contact:**

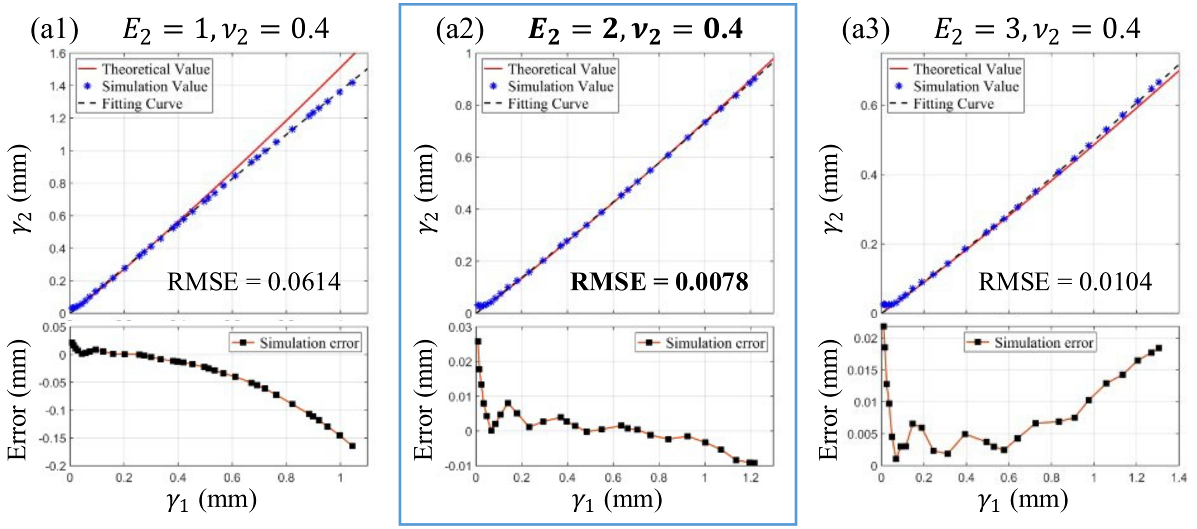

- **Torsional contact:**

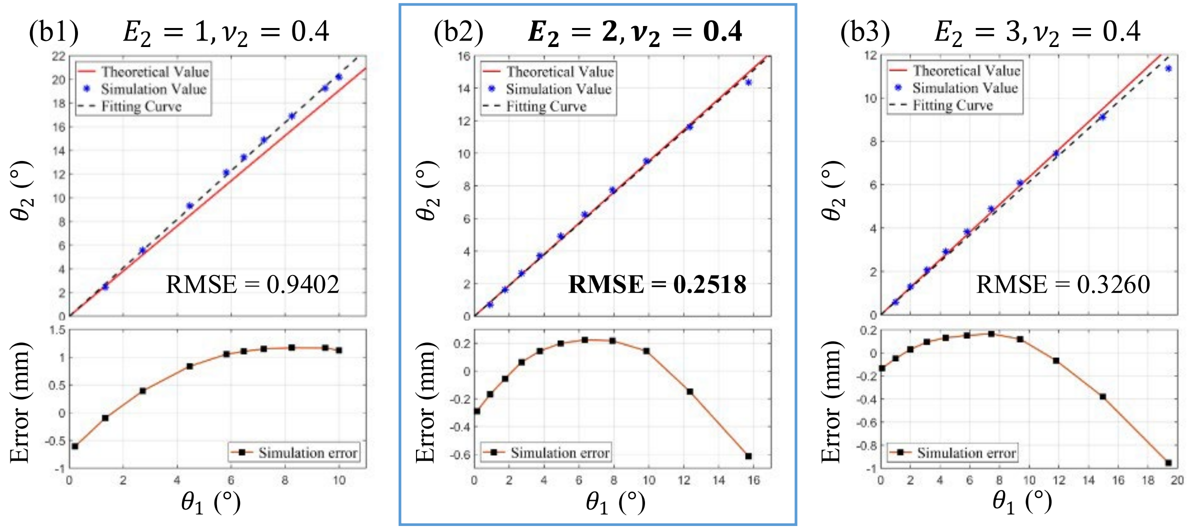

[3] Mingxuan. Li *et al.*, ***IEEE RA-L***, Jul. 2024

Design of EasyCalib

● Structure of EasyCalib:

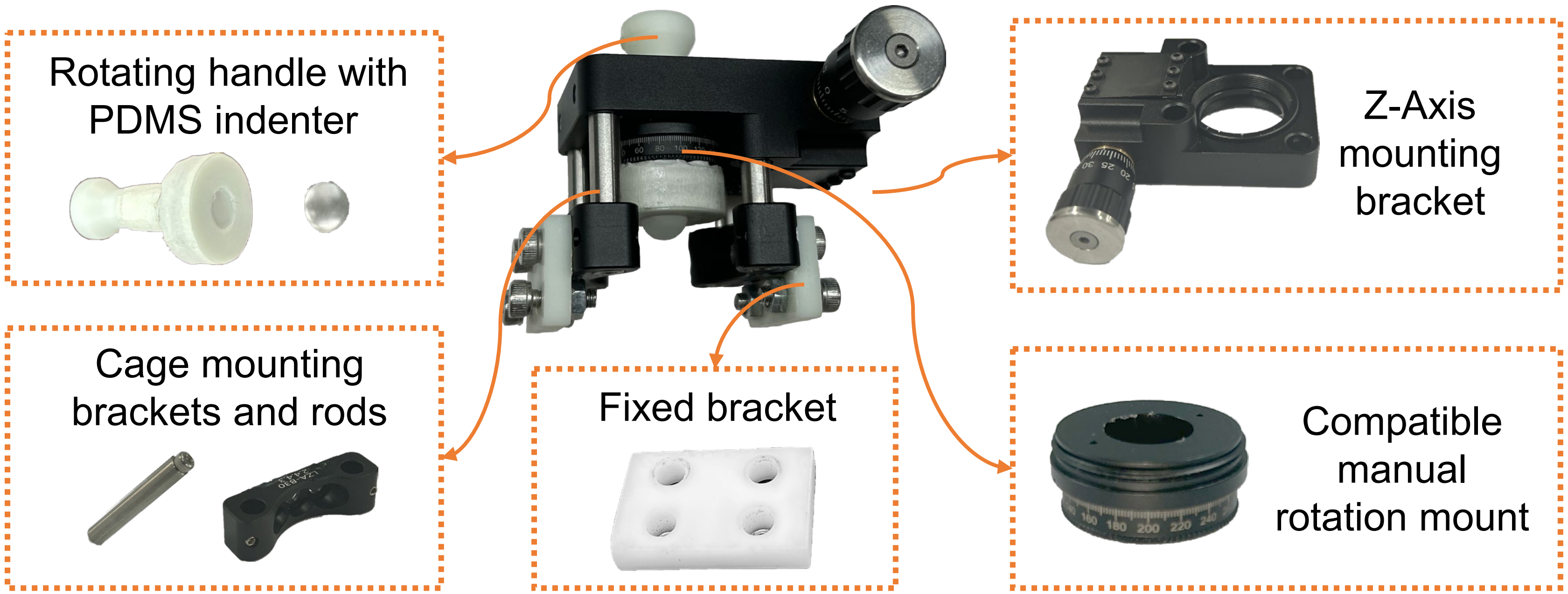

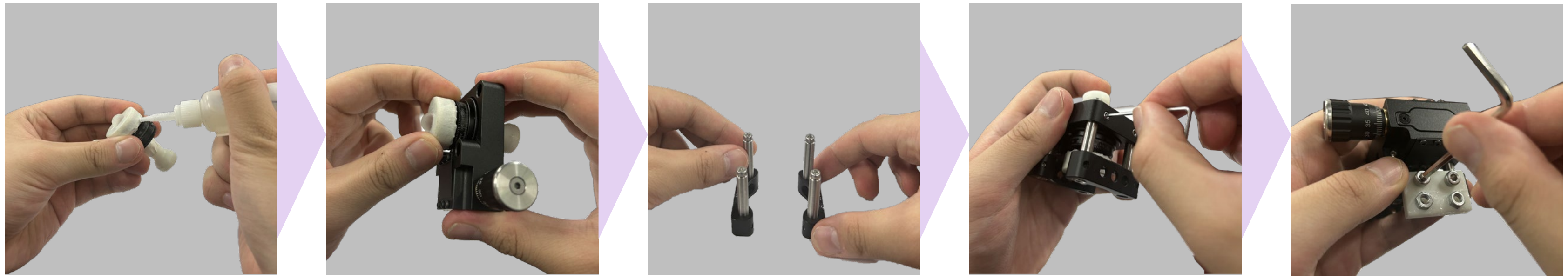

● Usage of EasyCalib:

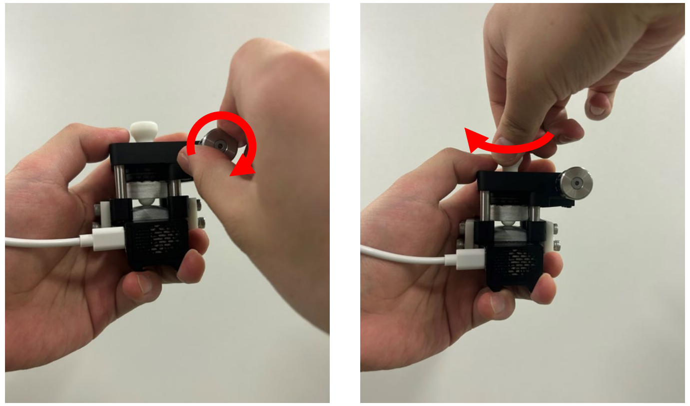

- ✓ Adjust the differential head to obtain the curve from γ_1 to γ_2, and fit $\boldsymbol{H_1}$;
- ✓ Adjust the rotating handle to obtain the curve between θ_1 and θ_2, and fit $\boldsymbol{H}_3$;
- ✓ Calculate $\boldsymbol{E_1}$ and $\boldsymbol{\nu_1}$ based on $\boldsymbol{H_1}$ and $\boldsymbol{H}_3$.

[3] Mingxuan. Li *et al.*, ***IEEE RA-L***, Jul. 2024

In-situ Calibration Evaluation

- **Experimental process:** Calibrate the elastic indenter of EasyCalib through the experiment platform, and then use EasyCalib to measure the parameters of the Tac3D tactile sensor.

- **Experiment platform:**

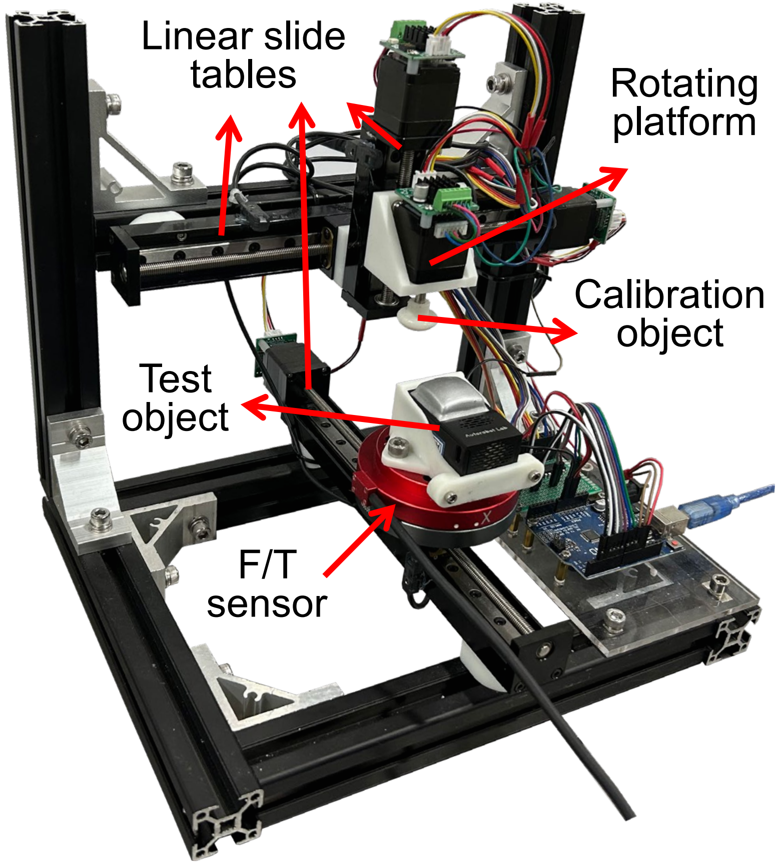

- **Results of Calibration:**

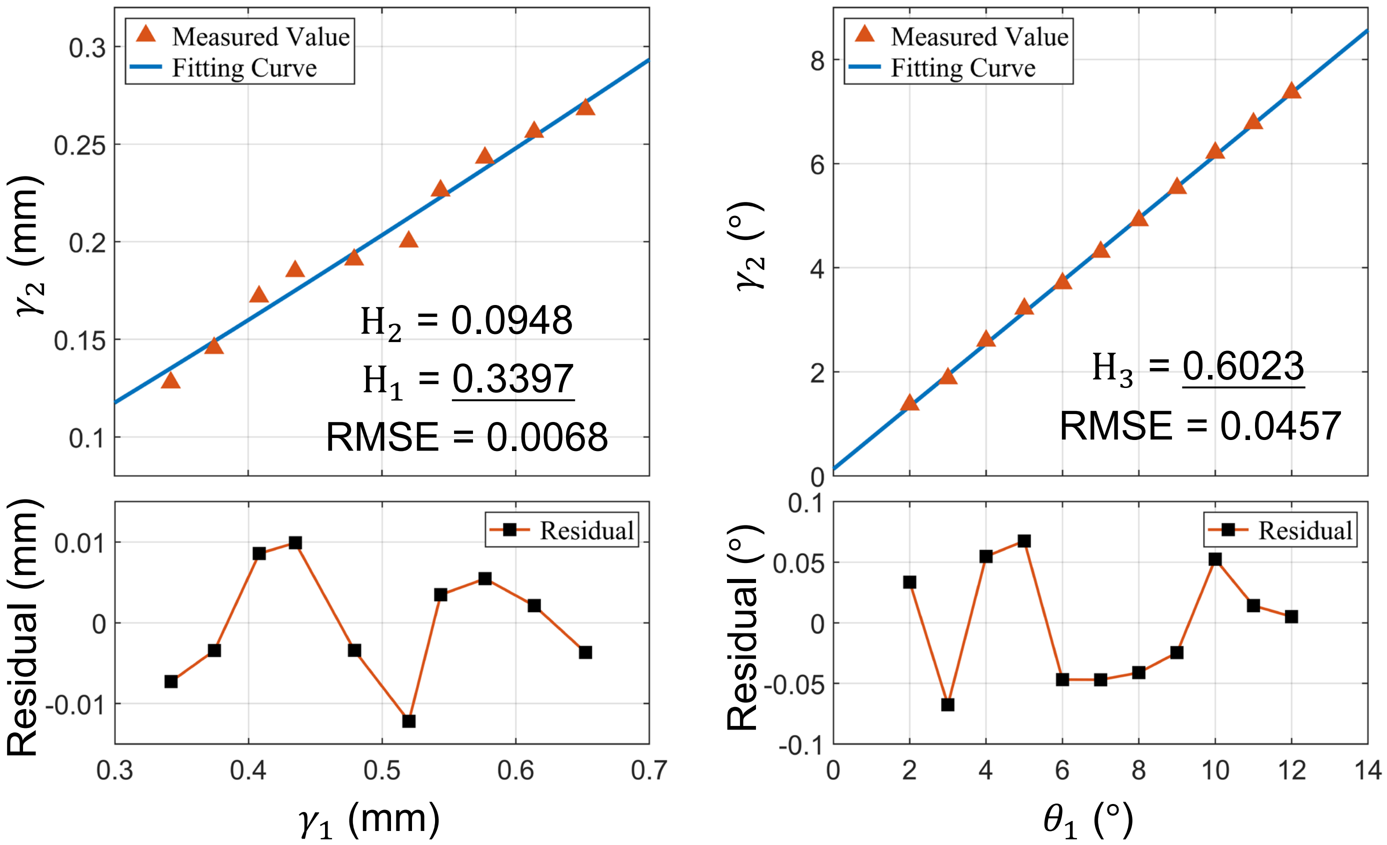

[3] Mingxuan. Li *et al.*, ***IEEE RA-L***, Jul. 2024

Force Reconstruction Evaluation

- **Force reconstruction evaluation:**

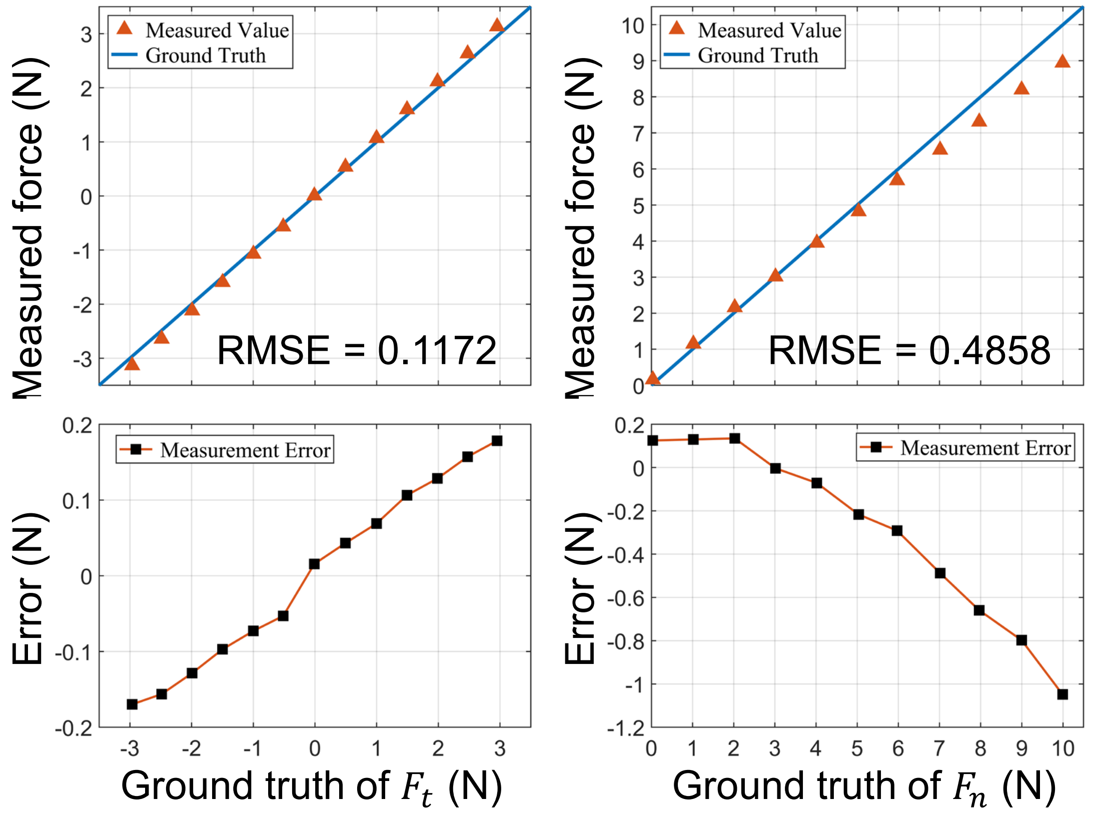

- **Force Distribution:**

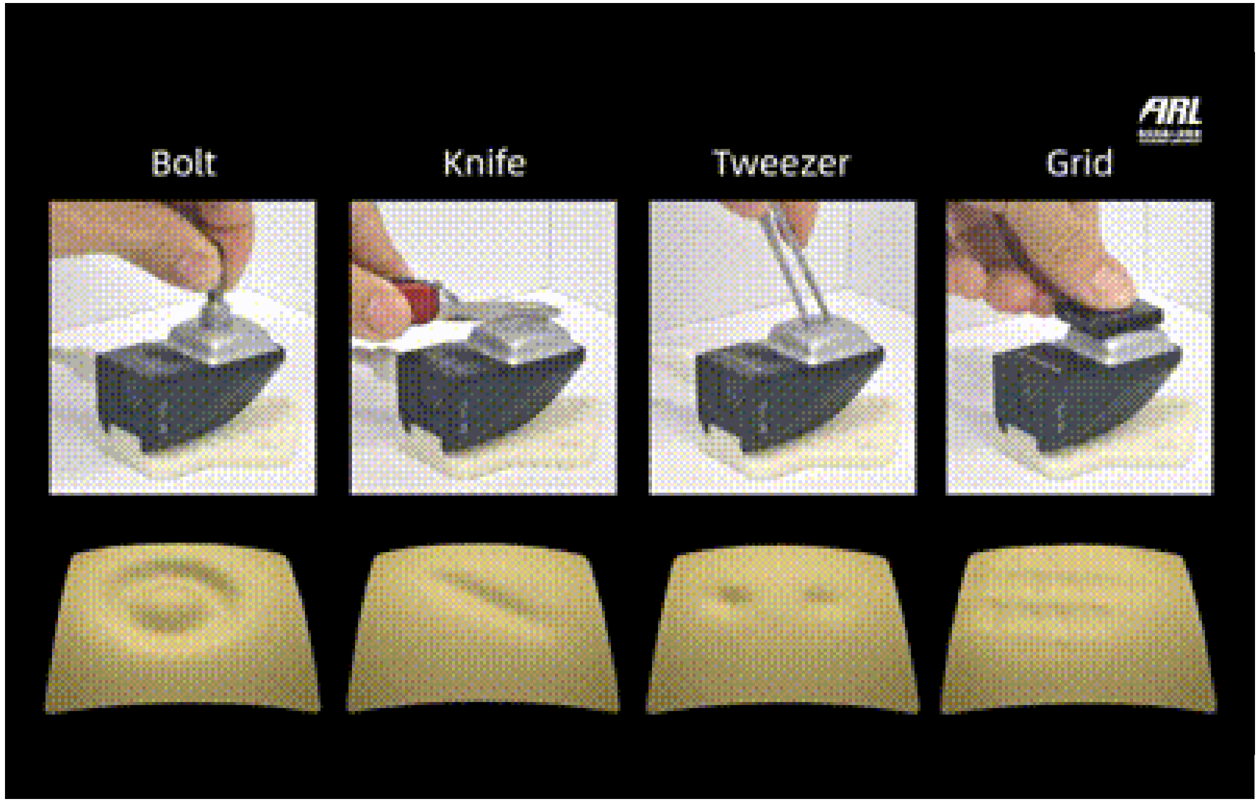

- **Conclusion: Effective force reconstruction** can be realized based on the mechanical parameter calibration [ranges: 1~10 N (normal force) and -3~3 N (tangential force)].

[3] Mingxuan. Li *et al.*, ***IEEE RA-L***, Jul. 2024

Overview

1. Background and Motivation
2. Contact Modelling
3. Contact Representation
4. Contact Reconstruction
5. **Contact-Rich Tasks**

Task 1: In-hand Object Pivoting

- ✓ Utilizing **additional resources** in the environment (gravity and extrinsic contact...) to assist with manipulation
- ✓ The object **rotates around an axis** defined by the contact between the robot hand and itself

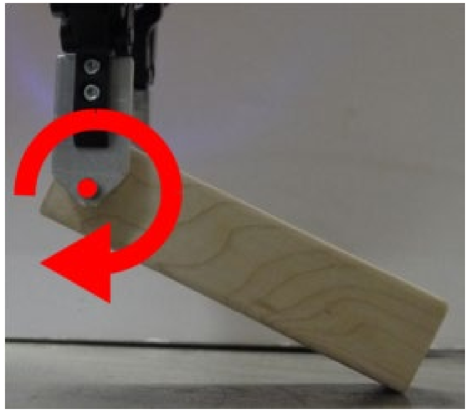

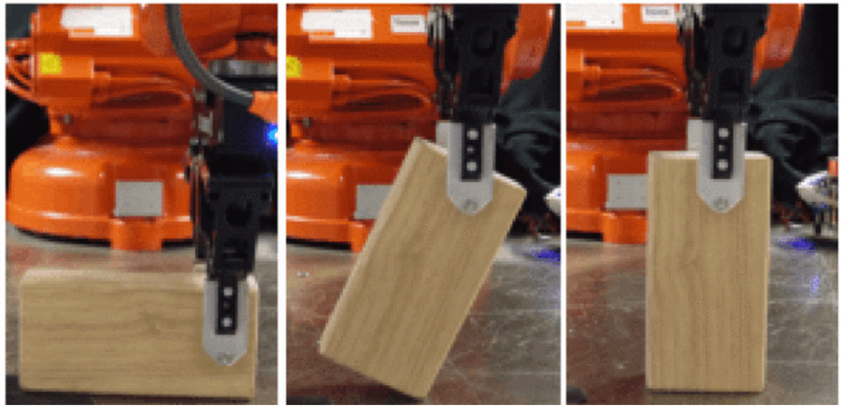

For Manipulation:

- ✓ Re-locating objects to specific rotation angles

Guarantee of robotic dexterity and stability: Pose Estimation during in-hand pivoting

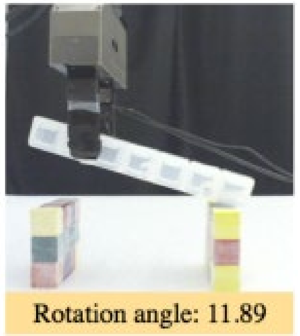

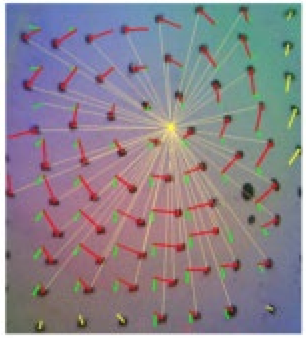

For Grasping:

- ✓ Detecting rotational slip to predict falling events

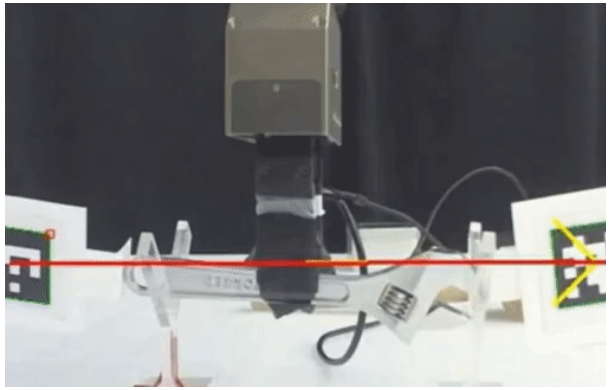

Reviewing Pose Estimation

- **Rotation relative to the contact surface:**

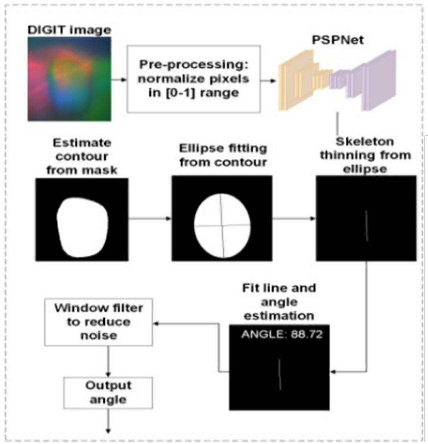

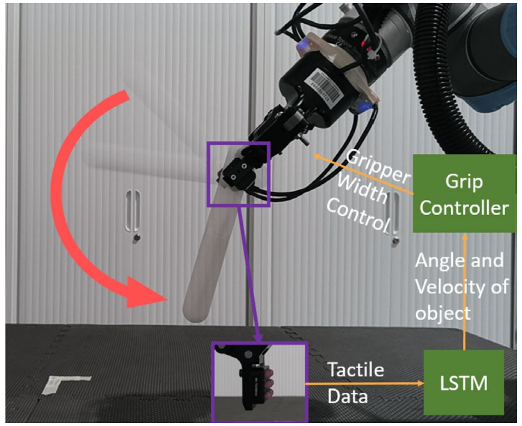

Regard as Macro Slip

- **Rotation of the contact surface per se:**

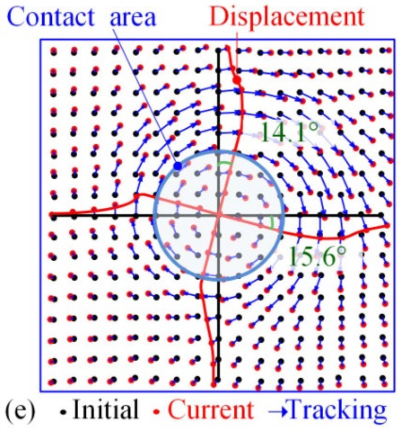

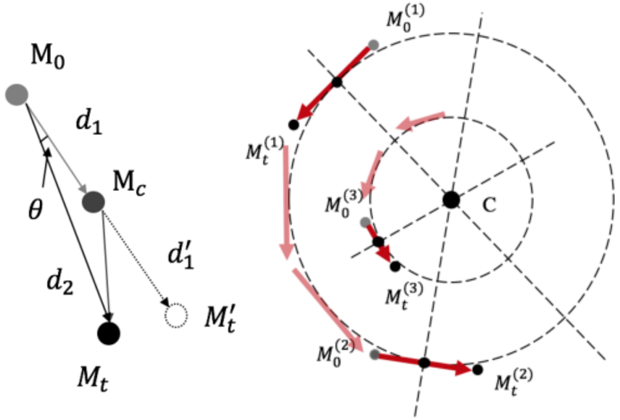

Regard as No Slip

Common problem:
Failure to consider a **transition state** during the pivoting:
Incipient Slip

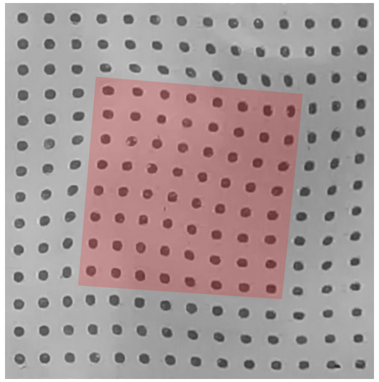
Full stick

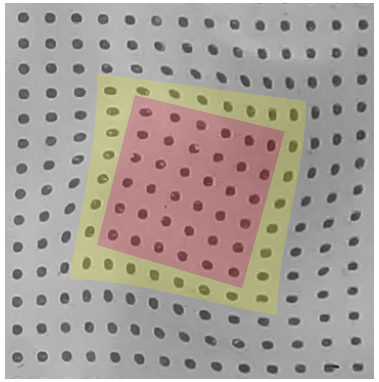
Incipient slip

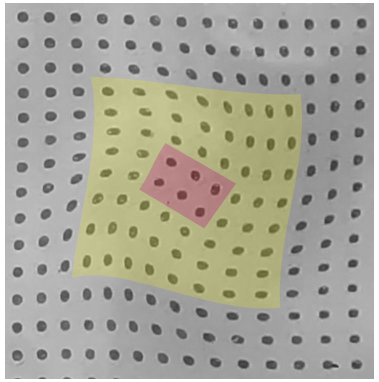
Near macro slip

: Stick region

: Slip region

A Demonstration of On-Line Measurement

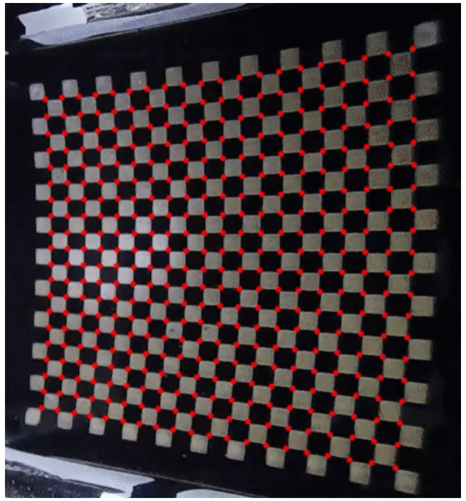

Right view of Tac3D image

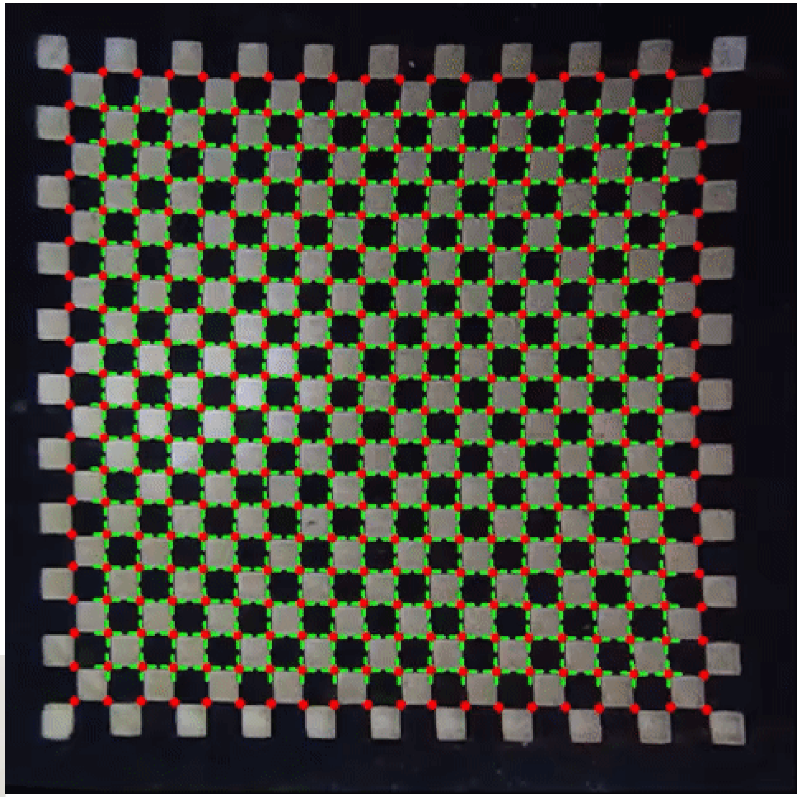

Left view of Tac3D image

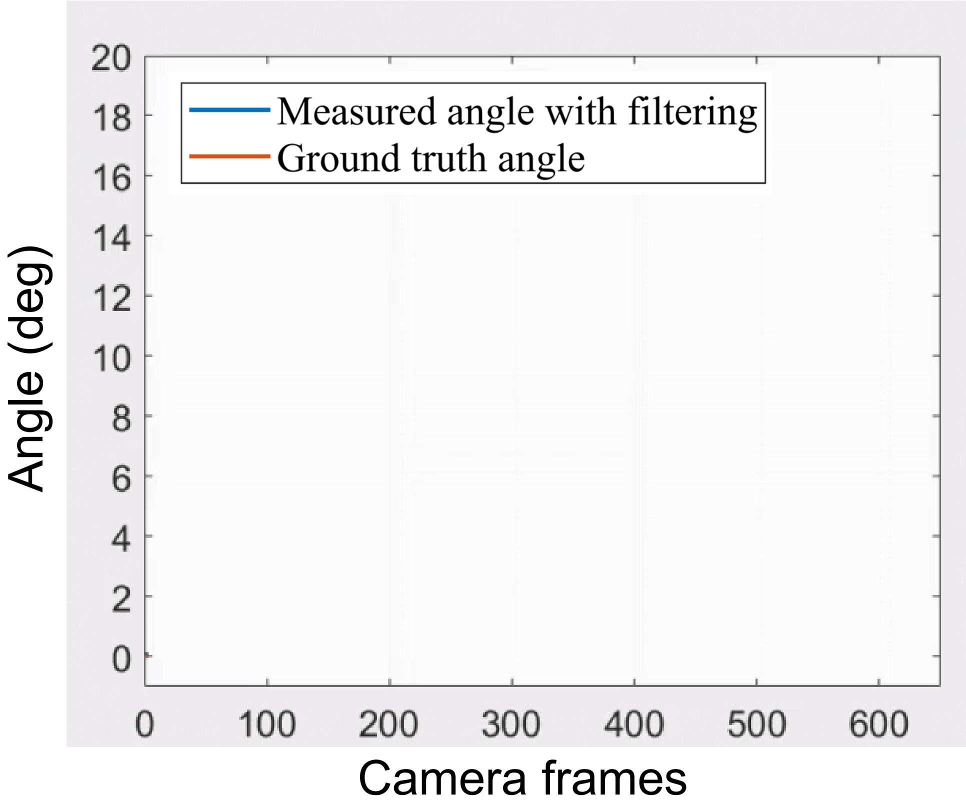

Measured angle vs Ground truth

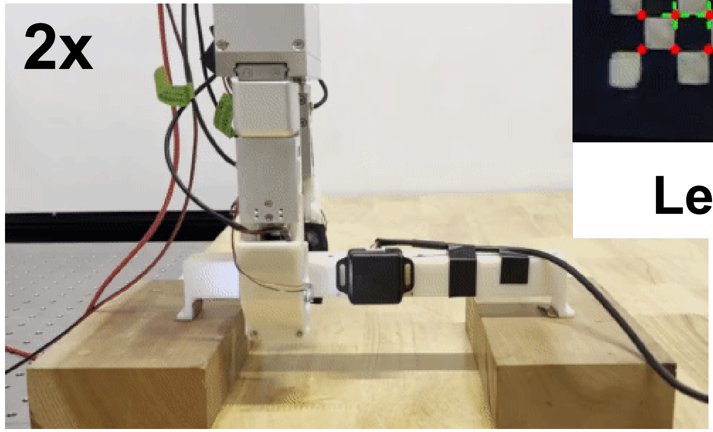

Side View

- ✓ The ground truth is provided by the **angular sensor**.
- ✓ The determination of stick region and rotation angle are achieved using the line features provided by **continuous marker patterns**.

[9] Mingxuan. Li *et al.*, ***2024 ICRA***, Sep. 2024

Evaluation of On-Line Rotation Measurement

- **Quantitative Evaluation:**

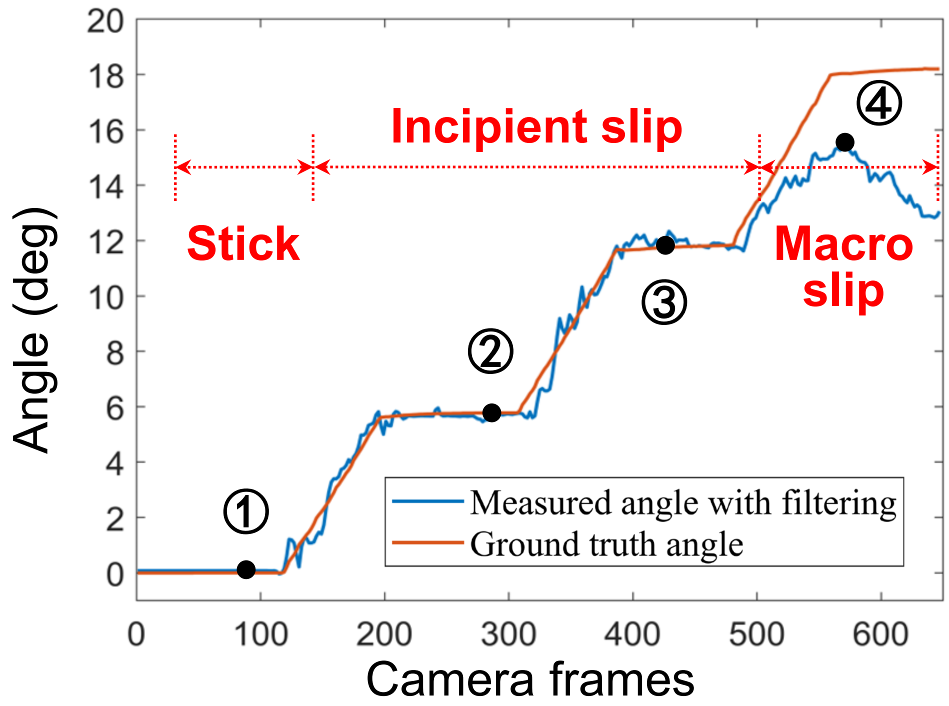

Measured angle vs Ground truth

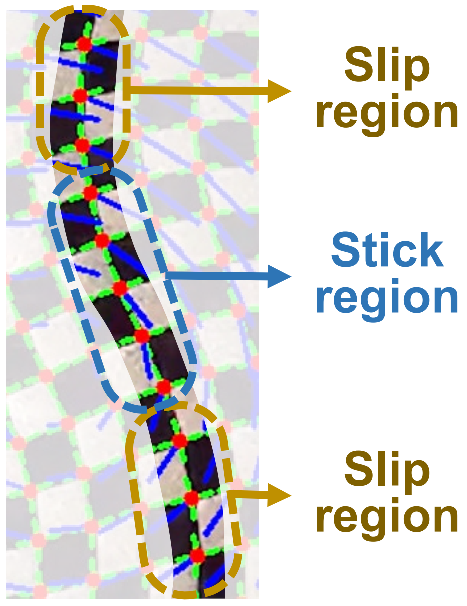

- **Qualitative Evaluation:**

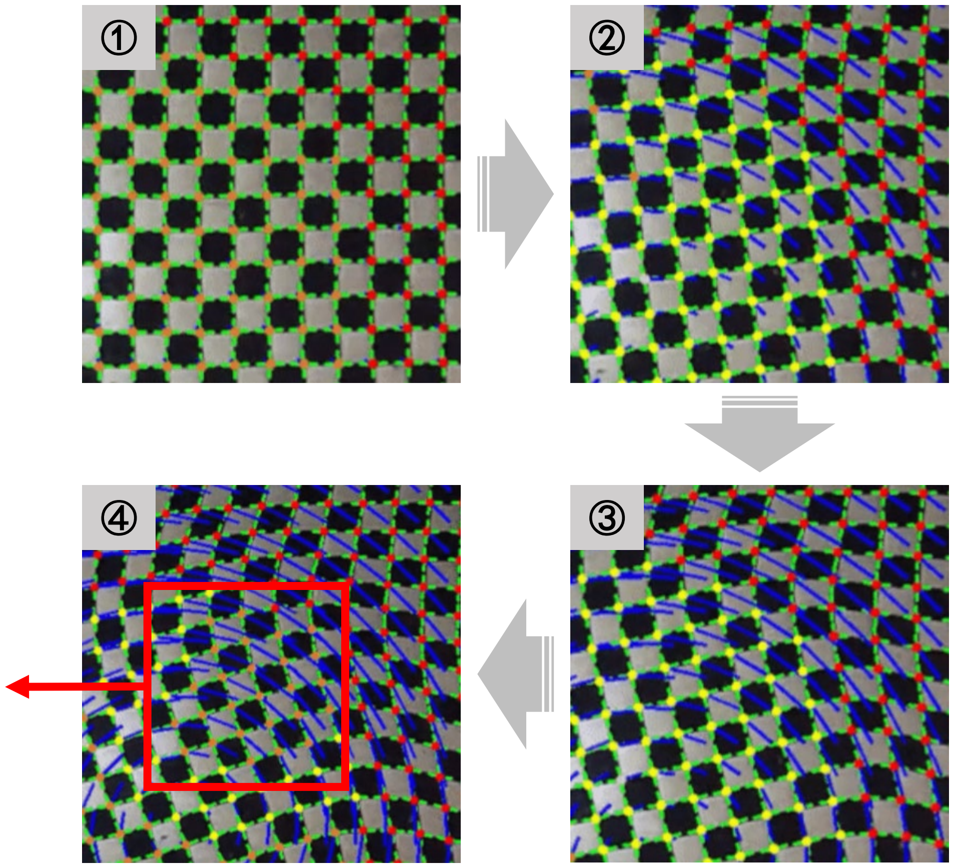

Conclusion:

- ✓ The proposed method can **identify the stick and slip points** during the incipient slip process.
- ✓ The **error amplifies** when the rotation increases until the contact state transitions to **macro slip**.

[9] Mingxuan. Li *et al.*, ***2024 ICRA***, Sep. 2024

Gripping and Lifting Tasks on Robot

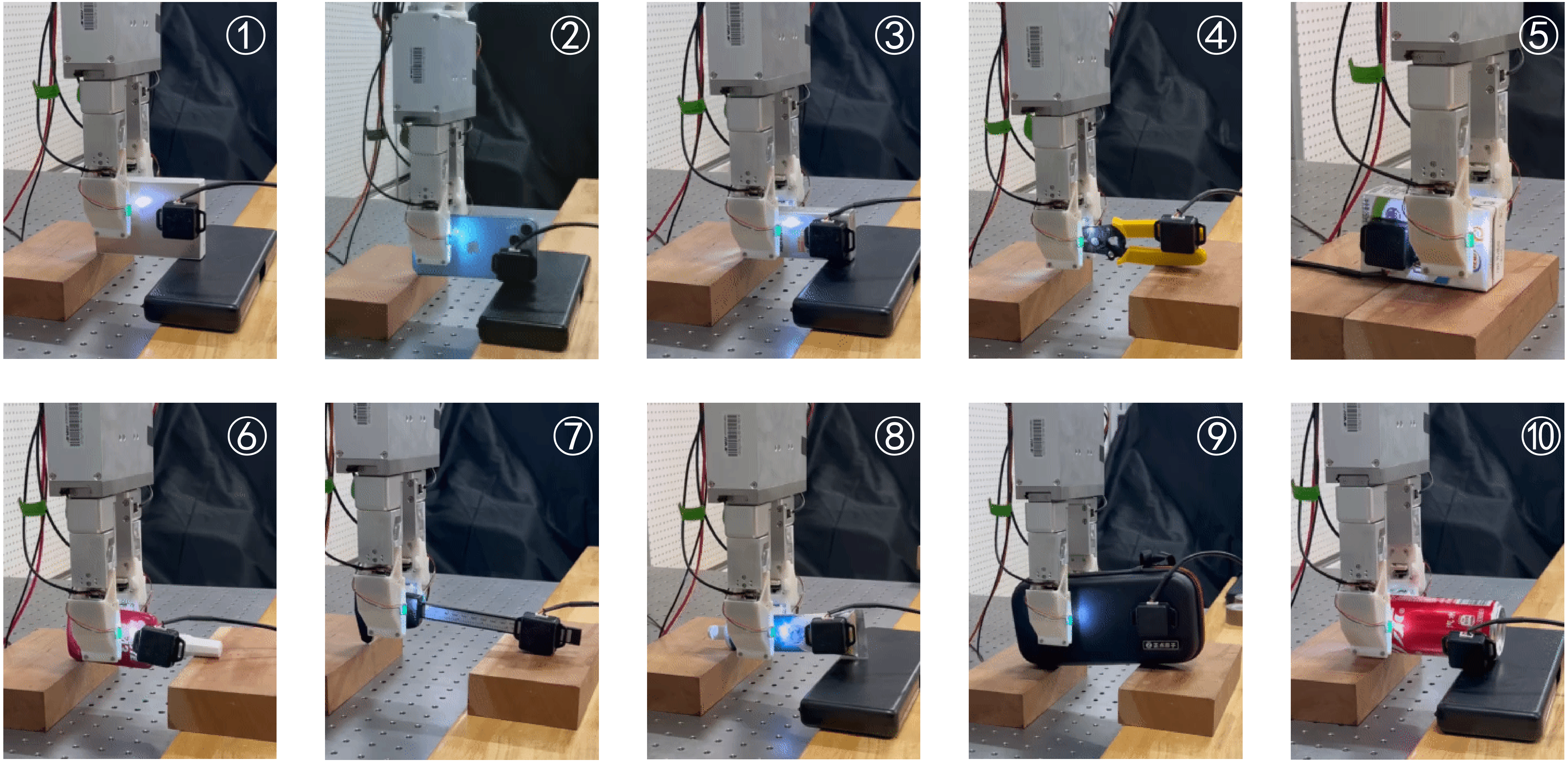

[9] Mingxuan. Li *et al.*, ***2024 ICRA***, Sep. 2024

Evaluation of Adaptability to Different Objects

- **Household Objects**

□ : Contact position

- **Measurement Error Evaluation**

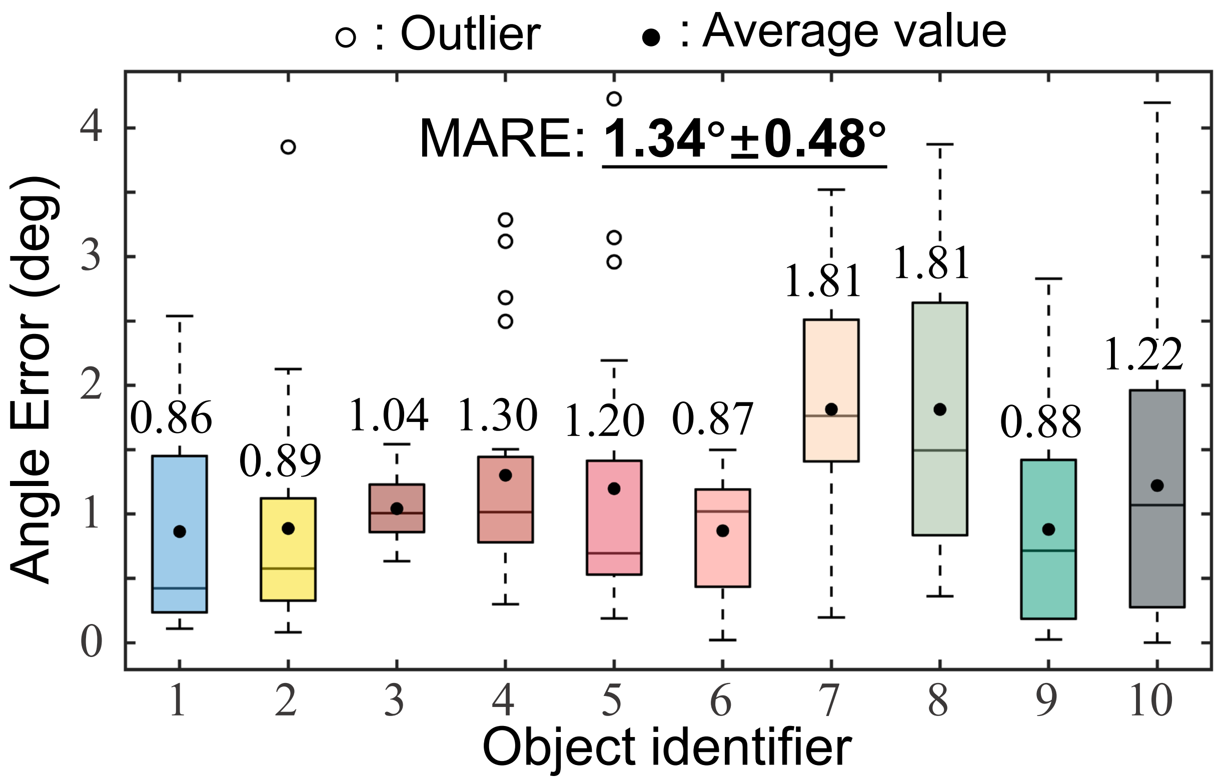

Measured angle vs Ground truth

Conclusion:

- ✓ The proposed method is suitable for **typical household objects** of different materials, shapes, and masses **without any prior information**.
- ✓ It achieves a **dynamic MARE of $1.34° \pm 0.48°$ (SOTA)** [Baseline: MARE of $\mathbf{1.85° \pm 0.96°}$].

[9] Mingxuan. Li *et al.*, ***2024 ICRA***, Sep. 2024

Task 2: In-Hand Object Pivoting

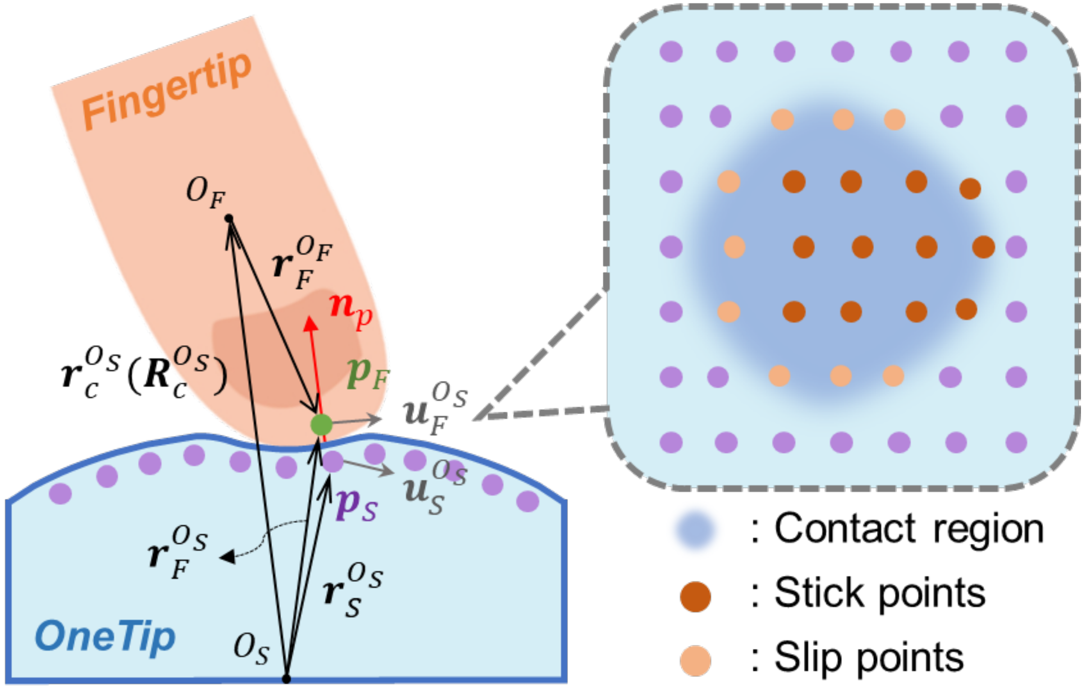

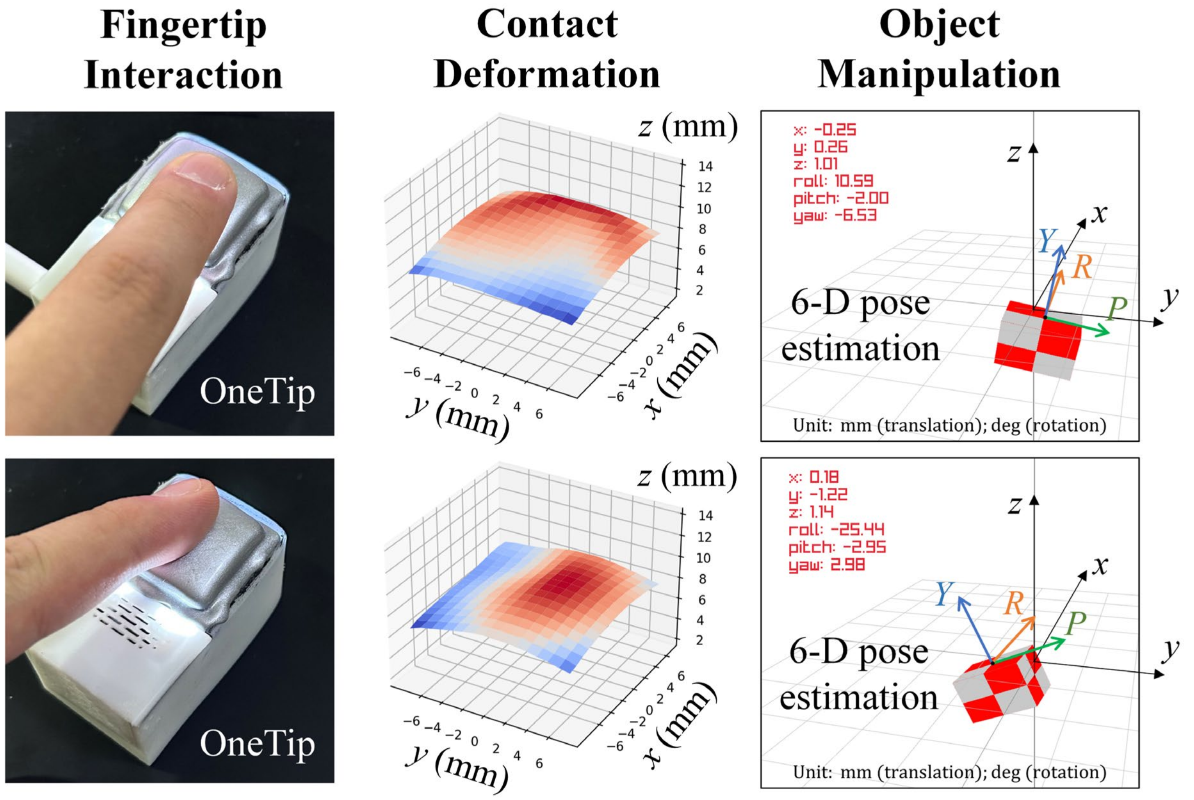

- ✓ **Fingertip Pose Estimation:** **Incipient slip detection** method that can be applied for **soft object**
- ✓ **OneTip:** A non-rigid **tactile interface** for single-fingertip human-computer interaction with 6 DOFs

[10] Mingxuan. Li *et al.*, ***Sensors and Actuators: A. Physical***, Sep. 2024

Task 3: Gentle Grasping Control

Grasping

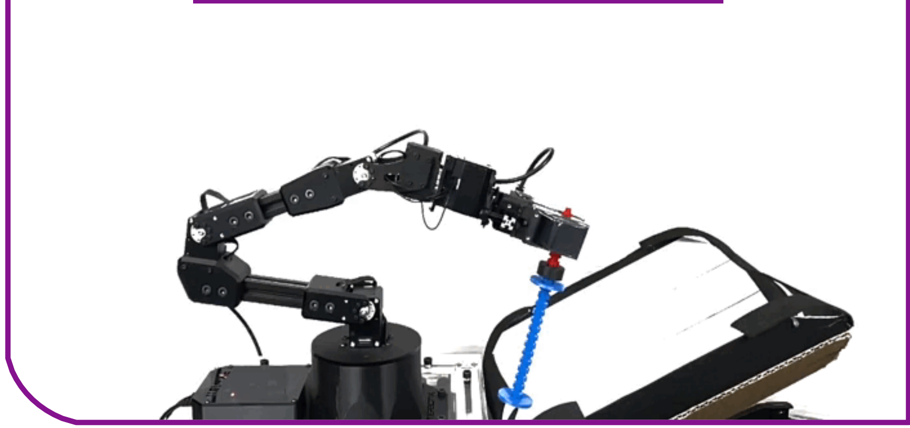

Manipulation

Requirement: Grasping objects **stably and safely** **(Gentle Grasping)**

Nature Review: Human can quickly adjust grasping force in a short period of time through tactile sensing

- (1) The force should **not be too small** to avoid object slip (above the minimum force);
- (2) The force should **not be too large** to prevent damage (typically no more than 60%).

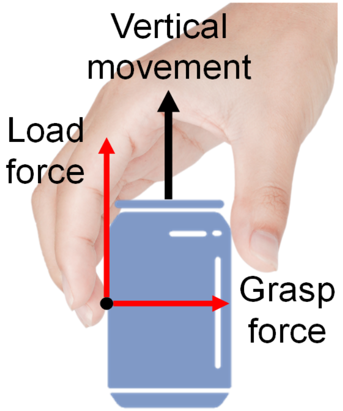

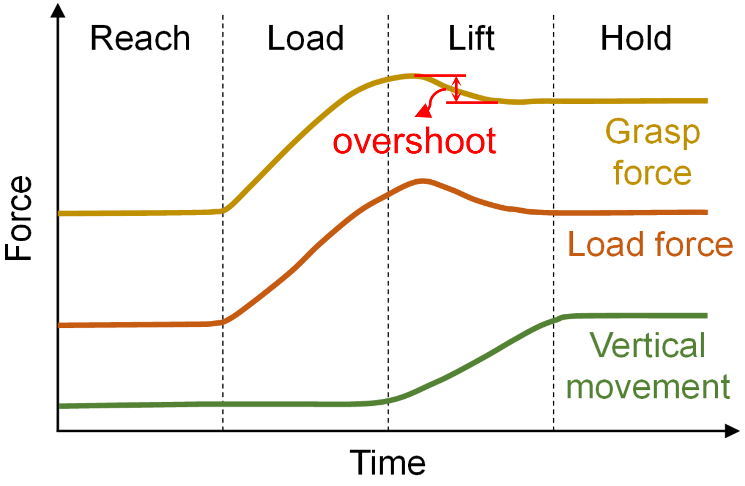

Safety Margin of Incipient Slip

- **Micro-element resultant forces and grasp force**

$$F_{MER,n} = \int_S \|\boldsymbol{f}_n^i\| \cdot dA = \int_S \|(\boldsymbol{f}^i \cdot \boldsymbol{n}^i) \cdot \boldsymbol{n}^i\| \cdot dA$$

$$F_{MER,t} = \int_S \|\boldsymbol{f}_t^i\| \cdot dA = \int_S \|\boldsymbol{f}^i - (\boldsymbol{f}^i \cdot \boldsymbol{n}^i) \cdot \boldsymbol{n}^i\| \cdot dA$$

$$F_g = \int_S (\boldsymbol{f}^i \cdot \hat{\boldsymbol{z}}) \cdot dA = (\boldsymbol{F}_n + \boldsymbol{F}_t) \cdot \hat{\boldsymbol{z}}$$

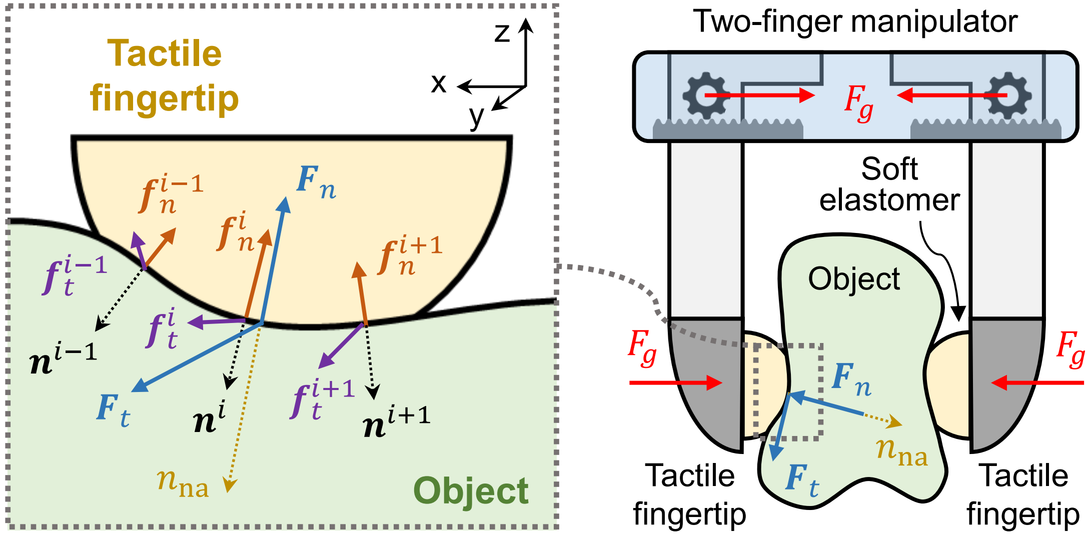

- **Dynamical estimation with historical information**

$$\beta = \begin{cases} \beta_{\max}, & \text{if } t \geq t_m \\ \beta_{\min} + \dfrac{\beta_{\max} - \beta_{\min}}{1 + \exp(-k \cdot (t - t_{\text{bias}}))}, & \text{if } t < t_m \end{cases}$$

$$F_{\text{Target},n}^{k+1} = \beta\mu^{-1} \cdot \max\left(F_{MRE,t}^k, F_m^{k-1}\right)$$

$$F_g^{k+1} = \begin{cases} F_g^k, & \text{if } \ F_{MER,n}^{k-1} = F_{MER,n}^k \\ F_g^k + \left(F_g^k - F_g^{k-1}\right) \cdot \dfrac{F_{\text{Target},n}^{k+1} - F_{MER,n}^k}{F_{MER,n}^k - F_{MER,n}^{k-1}} \\ \text{if } \ F_{MER,n}^{k-1} \neq F_{MER,n}^k \end{cases}$$

- **Time-dependent function of safety margin**

✓ Initially, the grasping force is relatively small, and the tangential force increases rapidly, requiring a **larger safety margin**;

✓ As the grasping force gradually approaches the final target value and the tangential force increase rate decreases, a **smaller safety margin** is needed to prevent overshooting.

[11] Mingxuan. Li *et al.*, ***IEEE RA-L***, Jan. 2025

Force-Control Demonstration Generation

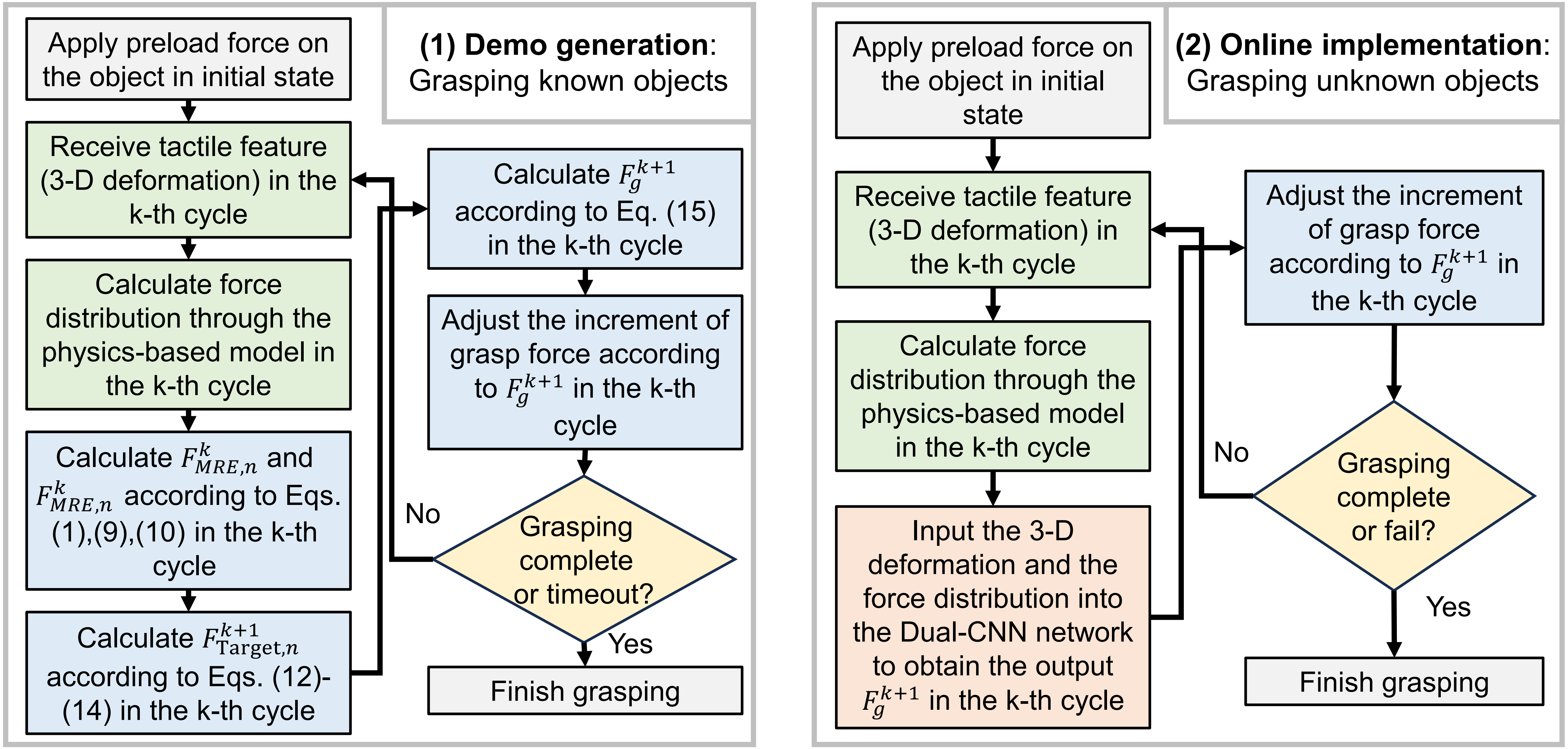

[11] Mingxuan. Li *et al.*, ***IEEE RA-L***, Jan. 2025

Robot Experiment Platform

Experiment platform:

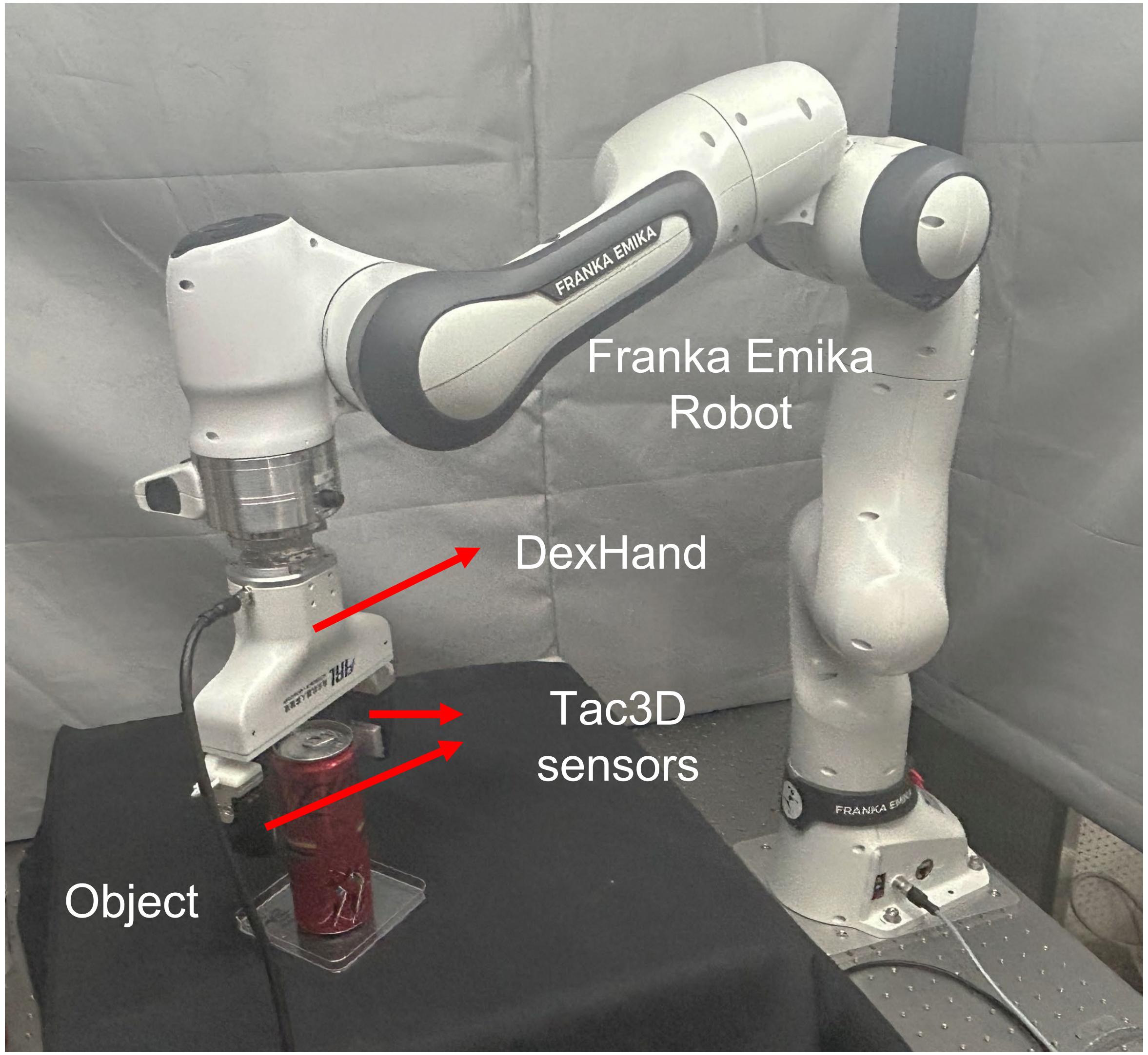

Test object and friction coefficient:

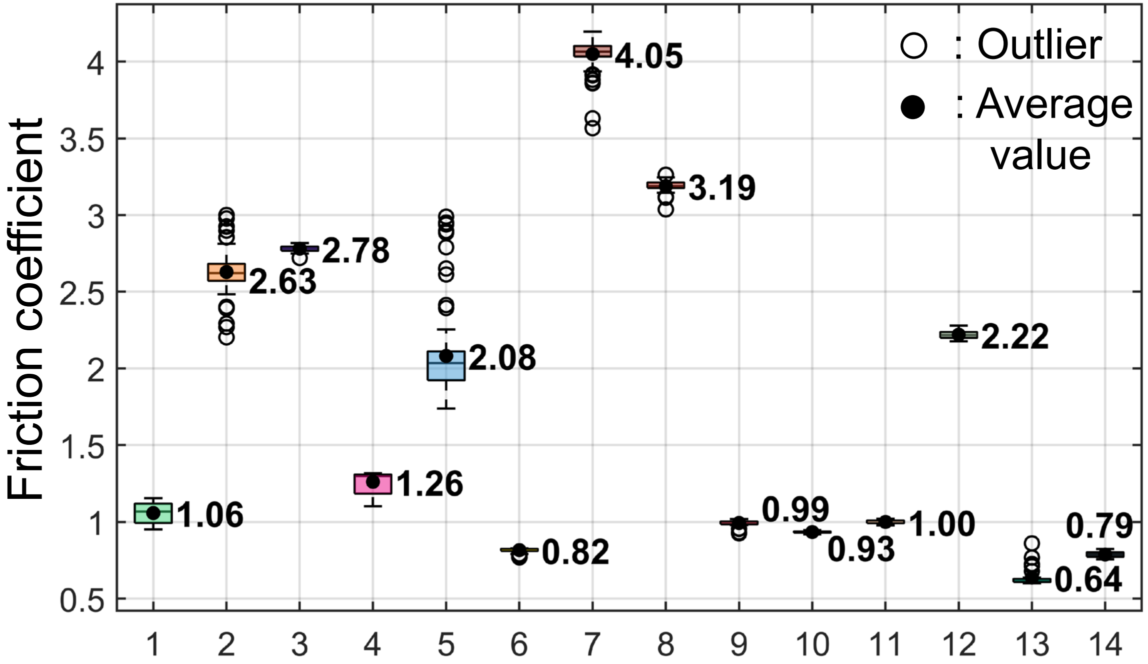

[11] Mingxuan. Li *et al.*, ***IEEE RA-L***, Jan. 2025

Offline Evaluation

Grasping different unknown objects **for four stages like human** (reach, load, lift, hold)

Ablation study results:

Models	MSE test loss / N^2
CNN (trained with deformation only)	0.0236
Dual-CNN (3×3 kernels)	0.0037
Dual-CNN (5×5 kernels)	0.0036
Dual-CNN (decrease one layer)	0.0039
Dual-CNN (increase one layer)	0.0054

Conclusion: Force reconstruction module improve the **accuracy of target force prediction**

Accuracy Score: **0.6933**

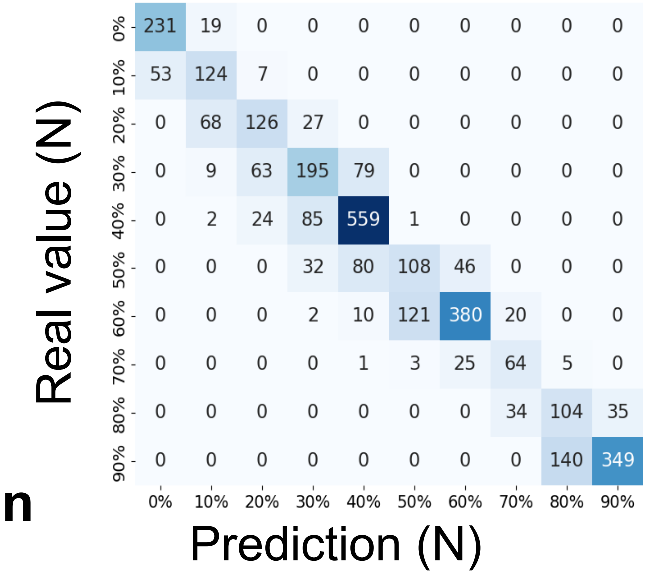

Accuracy Score: **0.2573**

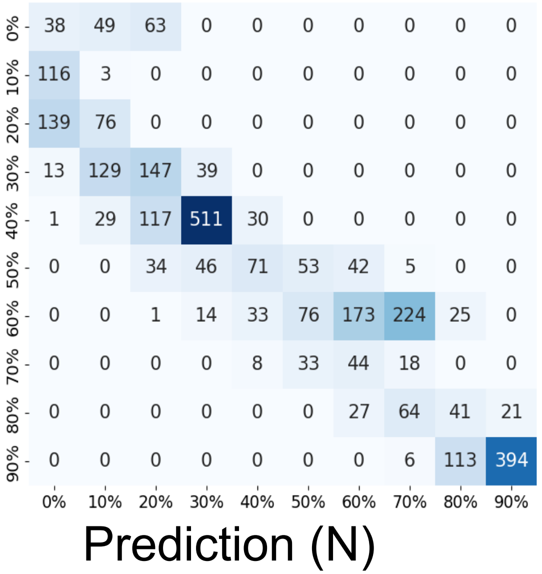

[11] Mingxuan. Li *et al.*, ***IEEE RA-L***, Jan. 2025

Online Evaluation

Evaluation of load-force/grasp-force status:

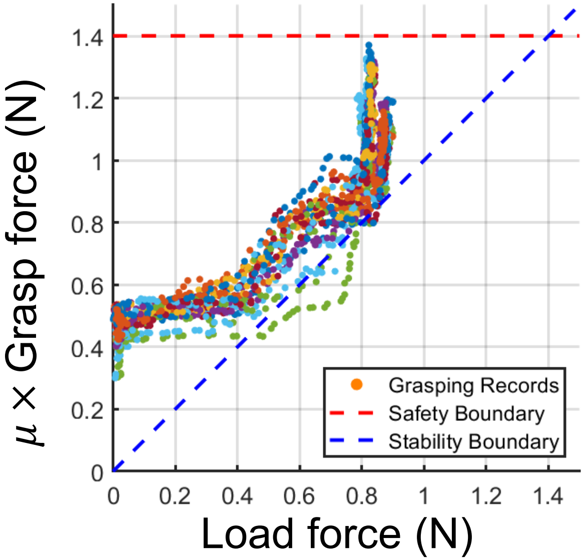

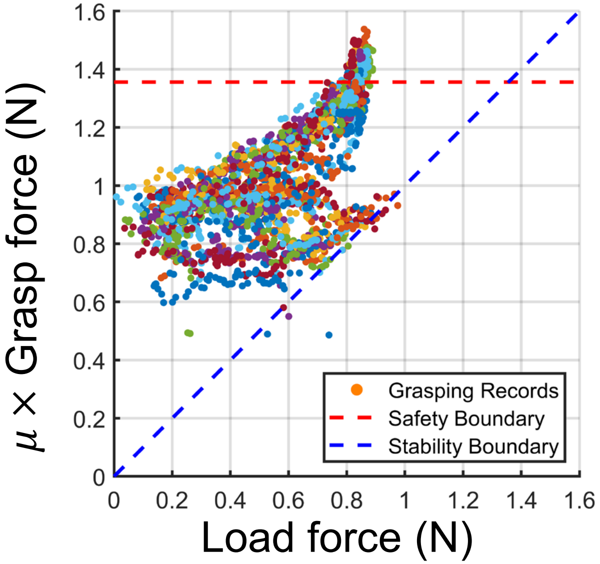

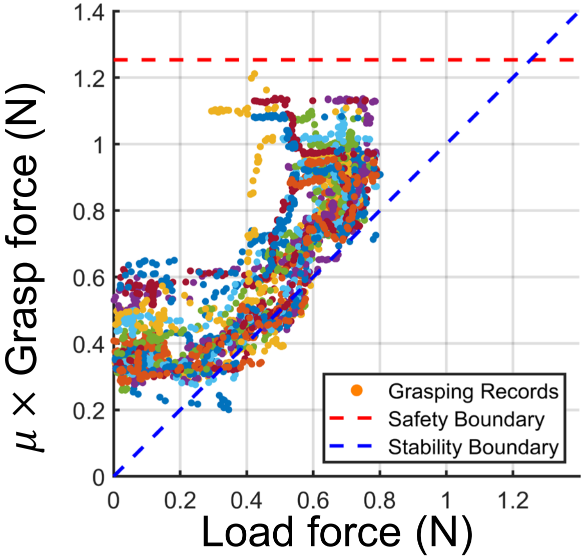

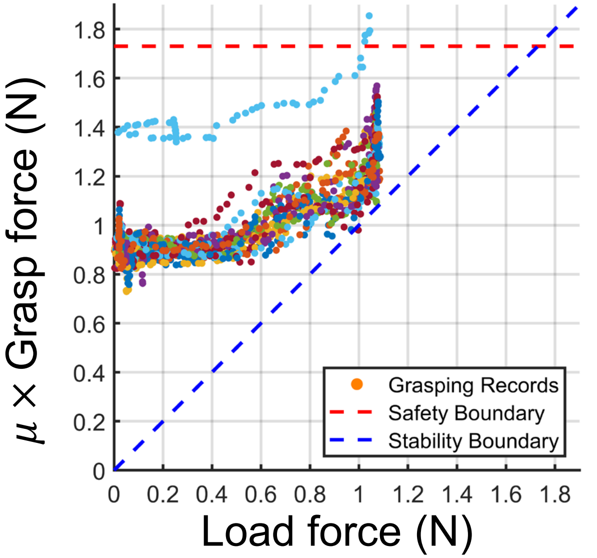

[11] Mingxuan. Li *et al.*, **IEEE RA-L**, Jan. 2025

Comparison of Grasping Force Control

Grasping based on the <u>proposed method</u>

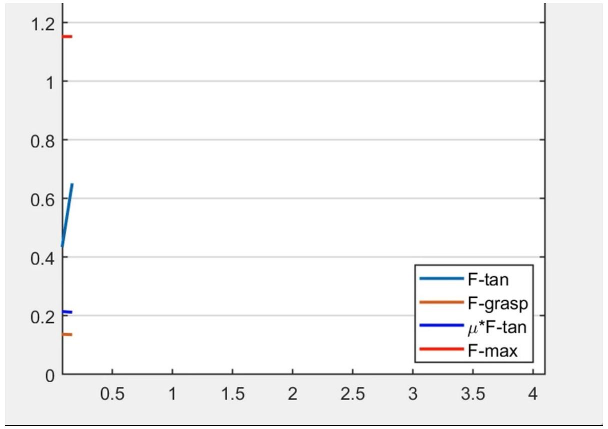

Grasping based on online friction coefficient measurement

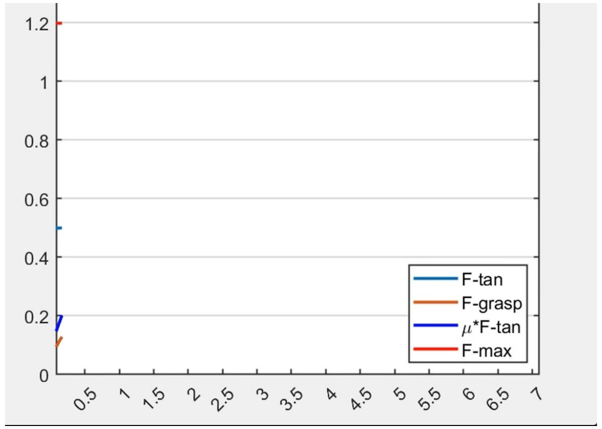

Grasping based on a slip detection model

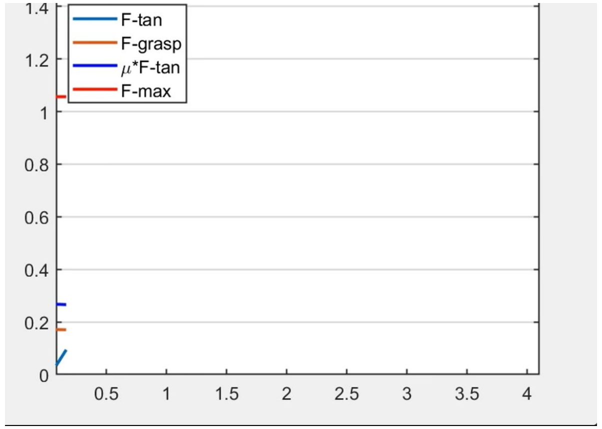

[1] Mingxuan. Li *et al.*, in revision to *IEEE TRO*
[11] Mingxuan. Li *et al.*, ***<u>IEEE RA-L</u>*****,** Jan. 2025

Various Manipulation Tasks

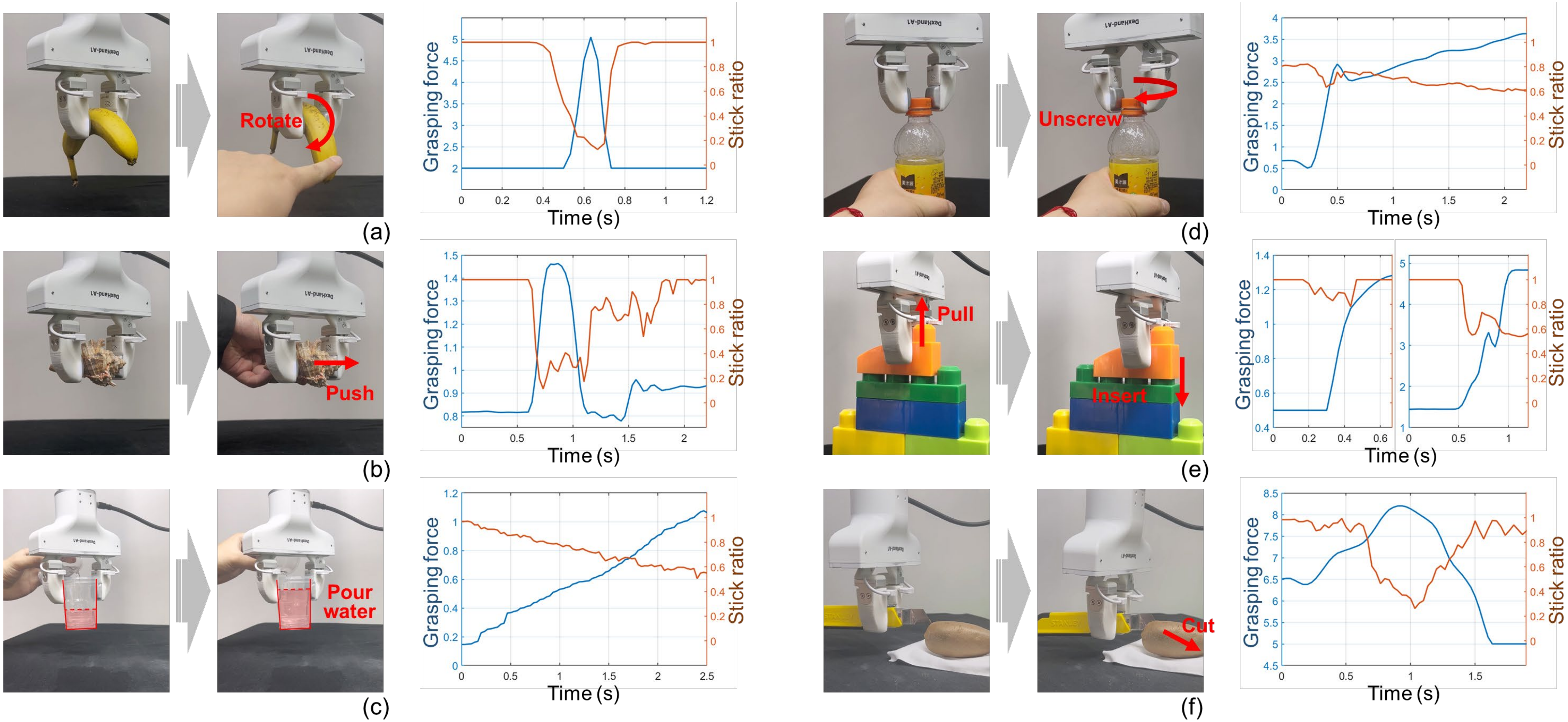

[1] Mingxuan. Li *et al.*, in revision to *IEEE TRO*

[11] Mingxuan. Li *et al.*, ***IEEE RA-L***, Jan. 2025

Thank You Very Much